AD-A151 702 CRACK CLOSURE CHARACTERISTICS CONSIDERING CENTER CRACKED AND COMPACT TENS..(U) AIR FORCE INST OF TECH WRIGHT-PATTERSON AFB OH SCHOOL OF ENGI.. C L HENKEL 1/2

UNCLASSIFIED DEC 84 AFIT/GAE/AA/84D-9 F/G 20/11 NL

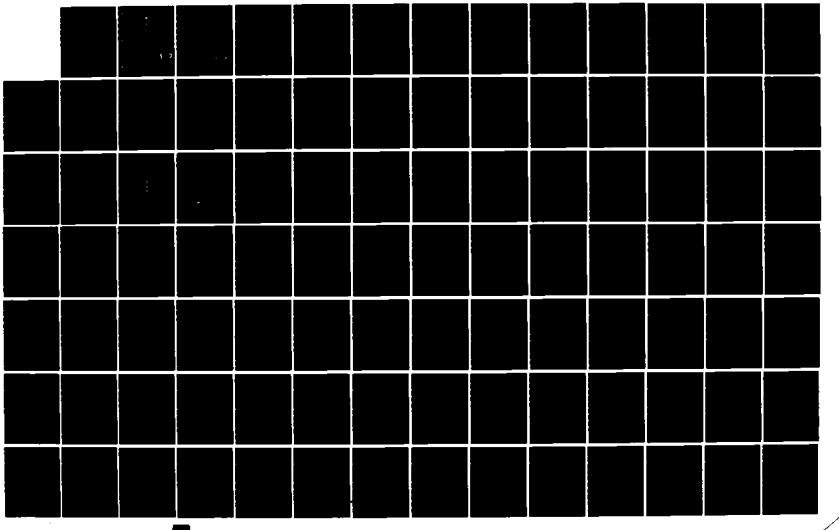

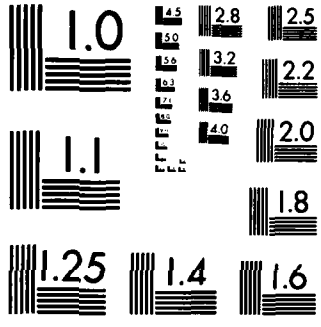

(1)

CRACK CLOSURE CHARACTERISTICS CONSIDERING CENTER CRACKED AND COMPACT TENSION SPECIMENS

THESIS

Casey L. Henkel
Captain, USAF

AFIT/GAE/AA/84D-9

DEPARTMENT OF THE AIR FORCE
AIR UNIVERSITY
AIR FORCE INSTITUTE OF TECHNOLOGY

Wright-Patterson Air Force Base, Ohio

AFIT/GAE/AA/84D-9

CRACK CLOSURE CHARACTERISTICS CONSIDERING CENTER CRACKED AND COMPACT TENSION SPECIMENS

THESIS

Casey L. Henkel
Captain, USAF

AFIT/GAE/AA/84D-9

Approved for public release; distribution unlimited.

AFIT/GAE/AA/84D-9

CRACK CLOSURE CHARACTERISTIC CONSIDERING CENTER CRACKED AND COMPACT TENSION SPECIMENS

THESIS

Presented to the Faculty of the School of Engineering
of the Air Force Institute of Technology
Air University
In Partial Fulfillment of the
Requirements for the Degree of
Master of Science in Aeronautical Engineering

Casey L. Henkel, B. S.
Captain, USAF

December 1984

Acknowledgements

I am thankful that Dr. A. N. Palazotto was my advisor in this study. His guidance was the single most important factor in the success of this thesis. Thanks also go to Dr. T. Nicholas of the AFWAL Materials Laboratory for his helpful ideas and for sponsoring this study.

My wife, Debra, and my three daughters, Ashley, Lauren, and Jordan deserve a lot of credit too. They are as thankful as I am that this project has been successfully completed.

Casey L. Henkel

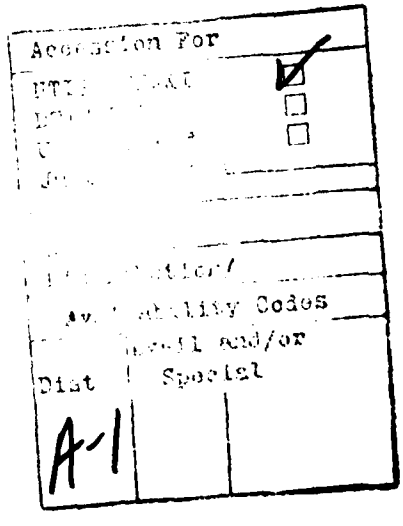

Table of Contents

List of Symbols

$(\dot{})$	Time Rate of Change ( )
a	Crack Length in Compact Tension Specimen
C	Compliance
B	Compact Tension Specimen Depth
D_2^p	Second Invarient of Plastic Strain Rate
D_o	Bodner Material Constant
E	Elastic Modulus
G	Shear Modulus
H, λ	Proportionality Constants
i,j	Indices
J_2, J_3	Second and Third Invarient of Deviatoric Stress Tensor
K_I	Stress Intensity Factor
k	Hardening Parameter
m	Bodner Material Constant
n	Bodner Material Constant
p	Applied Load
r	Bodner Material Constant
R	Load Ratio Min Load/Max Load
S_{ij}	Deviatoric Stress
U_d	Distortion Strain Energy
W_p	Plastic Strain Energy Density
Z	Bodner Model Internal State Variable
Z_o, Z_1, Z_2	Bodner Material Constant

List of Symbols

ε	Total Uniaxial Strain
ε_{ij}	Components of Total Strain
ε_{ij}^{e}	Elastic Components of Total Strain
ε_{ij}^{p}	Plastic Components of Total Strain
σ	Uniaxial Stress
σ_{ij}	Components of Stress
σ_{ys}	Uniaxial Material Yield Stress
$\dot{Z}_{rec}$	Rate of Work Hardening Recovery
Hz	Frequency of Cycles Per Second

List of Figures

List of Figures

List of Figures

List of Figures

List of Tables

III. Method of Analysis

Computer Program

In order to properly account for the complex response of a metal subjected to high temperature cyclic loading, a specialized finite element program has been used. VISCO, utilizing the Bodner-Partom constitutive law, is a two-dimensional viscoplastic finite element program capable of accurately modeling cyclic loading, cyclic hardening or softening, cyclic relaxation, and cyclic creep [13]. It uses constant strain triangles for both plane strain and plane stress solutions. VISCO was originally developed by Hinnerichs [6, 7, 8], with accuracy verified by Smail [9], Keck [10], and Wilson [11].

The Bodner-Partom viscoplastic constitutive equations in VISCO are economically solved using the Gauss-Seidel indirect solution procedure incorporating an optimum overrelaxation factor to speed convergence [14]. An Euler extrapolation scheme is employed for the numberical time integration of the Bodner equations [6]. The incremental solution process is based on incrementing time directly. Loads, strains, stresses, etc. are thus incremented indirectly and are solved for using the residual force method. The time-step size is checked by comparing results with prescribed constraints. These constraints are the allowable amounts of change in stress, σ_{TOL}, and strain,

Table 2.1

Bodner Coefficients for IN-100 at 1350° F

Material Parameter	Description	Value
E	Elastic modulus	26.3×10^2 KSI (18.133×10^4 MPa)
n	Strain rate exponent	0.7
D_o	Limiting value of strain rate	10^4 sec.
Z_o	Limiting value of hardness	915.0KSI (6304 MPa)
Z_1	Maximum value of hardness	1015.0KSI (6993 MPa)
Z_2	Minimum value of hardness	600.0KSI (4134 MPa)
m	Hardening rate exponent	2.57KSI^{-1} ($.37273 \text{ MPa}^{-1}$)
A	Hardening recovery coefficient	1.9×10^{-3} sec^{-1}
r	Hardening recovery exponent	2.66

(1 KBAR = 100 MPa = 14.504KSI)

Z_2 is the stable non-work hardened value of Z. A and r are material constants for IN-100 at 1350° F [12]. All the Bodner-Partom material constants are listed in Table 2.1. Note, these values are constant only for the specified temperature and material.

It is pointed out that, for fatigue type loading, the load can change sign and effect the normal stress strain relationship. The assumption made here is that the material is isotropic. Consequently, the properties presented for a tension stress strain function are duplicated when the specimen is stressed into the compression range.

strain rate, Z is the measure of material hardening, and exponent n is a rate sensitivity parameter. Only Z depends on the deformation history of the material. Z is assumed to be a function of plastic work, W_p, such that

$$Z = Z_1 + (Z_o - Z_1)\ \mathrm{EXP}(-\frac{mW_p}{Z_o}) \qquad (2.19)$$

Z_1 is the maximum expected value of Z, Z_o is the initial value of Z correspondning to the reference point from which plastic work is measured, and m is a material constant that controls the rate of work hardening. In this thesis, W_p the plastic work done relative to some initial state, is the only variable in Equation (2.19) [6]. At low temperature

$$W_p = \int S_{ij}\ \dot{\varepsilon}_{ij}^{\,p} dt \qquad (2.20)$$

However, this analysis, based on high temperature conditions, requires a thermal recovery term which effectively reduces the increase of material hardening due to plastic deformation:

$$W_p = \int S_{ij}\ \dot{\varepsilon}_{ij}^{\,p} dt + \int \frac{\dot{Z}_{rec}\, dt}{m(Z_1 - Z)} \qquad (2.21)$$

where

$$\dot{Z}_{rec} = -A(\frac{Z - Z_2}{Z_1})^r\ Z_1 \qquad (2.22)$$

Bodner-Partom Constitutive Law

The Bodner-Partom constitutive law is based on dislocation dynamics which suggests a continuous flow relationship exists between stress and viscoplastic strain starting at the onset of loading [5]. As such, the Bodner-Partom equations are able to represent the principal features of cyclic loading behavior, including recovery upon stress reversal, cyclic hardening or softening, cyclic relaxation and cyclic creep [6, 13]. The formulation of the equations is arrived at by squaring the Prandtl-Reuss relation (2.13)

$$\dot{\varepsilon}_{ij}^{p} \dot{\varepsilon}_{ij}^{p} = \lambda^2 S_{ij} S_{ij} \tag{2.14}$$

now substitute into this equation the following

$$J_2 = \frac{1}{2} S_{ij} S_{ij} \tag{2.15}$$

$$D_2^{p} = \frac{1}{2} \dot{\varepsilon}_{ij}^{p} \dot{\varepsilon}_{ij}^{p} \tag{2.16}$$

yields

$$D_2^{p} = \lambda^2 J_2 \tag{2.17}$$

where D_2^{p} is defined as the second invariant of plastic strain rate. Bodner and Partom expressed D_2^{p} as

$$D_2^{p} = D_o^{2} \text{ EXP } [-(\frac{Z^2}{3J_2})^{n} (\frac{n+1}{n})] \tag{2.18}$$

This expression is based on extensive experimental data and has been modified to fit results found by several researchers [12]. D_o is the limiting value of plastic

$$U_d = \frac{1}{2G} J_2 \tag{2.9}$$

G is the shear modulus. Under the Von Mises distortion energy theory, yielding begins when the distortion energy in the multiaxial case equals the distortion energy at yielding in the uniaxial case. In terms of principle stress,

$$J_2 = \frac{1}{6} [(\sigma_1-\sigma_2)^2 + (\sigma_2-\sigma_3)^2 + (\sigma_3-\sigma_1)^2] \tag{2.10}$$

at the yield point in uniaxial tension, J_2 reduces to

$$J_2 = \frac{1}{3} \sigma_{ys}^2 \tag{2.11}$$

where σ_{ys} is the uniaxial yield stress. Thus, yielding occurs when

$$\frac{1}{2} [(\sigma_1-\sigma_2)^2 + (\sigma_2-\sigma_3)^2 + (\sigma_3-\sigma_1)^2] = \sigma_{ys}^2 \tag{2.12}$$

Now we have a criterion to predict when yielding begins; however, we still need a way to relate viscoplastic strain to stress in a manner that conveys the flow nature of the problem. This requirement is satisfied by the Prandtl-Reuss equations in rate form [15].

$$\dot{\varepsilon}_{ij}^{p} = \lambda S_{ij} \tag{2.13}$$

where $\dot{\varepsilon}_{ij}^{p}$ are the components of the deviatoric viscoplastic strain tensor, and S_{ij} are the components of the deviatoric stress tensor and λ is a positive proportionality constant. Eqn. (2.13) will be used in subsequent development.

deformation begins, but the Von Mises distortion energy theory is considered best for isotropic materials subjected to yielding [5]. Due to the condition of isotropy, the yield criterion is a function of three stress invariants only:

$$I_1 = \sigma_{ii} \tag{2.3}$$

$$I_2 = \frac{1}{2}\ \sigma_{ij}\ \sigma_{ij} \tag{2.4}$$

$$I_3 = \frac{1}{3}\ \sigma_{ij}\ \sigma_{jk}\ \sigma_{ki} \tag{2.5}$$

Experimental studies have shown that plastic deformation of materials is essentially independent of hydrostatic pressure which can be shown to be (1/3) σ_{KK} [16]. Removing hydrostatic pressure from the three stress invariants leaves the two deviatoric stress invariants:

$$J_2 = \frac{1}{2}\, S_{ij}\, S_{ij} \tag{2.6}$$

$$J_3 = \frac{1}{3}\, S_{ij}\, S_{jk}\, S_{ki} \tag{2.7}$$

where

$$S_{ij} = \sigma_{ij} - \frac{1}{3}\ \delta_{ij}\, \sigma_{kk} \tag{2.8}$$

S_{ij} represents the deviatoric stress tensor.

Von Mises suggested that yielding occurs when J_2 reaches a critical value [5]. His theory related J_2 to distortion energy, U_d.

physical properties of a coldworked metal. Recovery reduces the effect of strain hardening, the process whereby the stress required to produce further plastic deformation is increased because of prior plastic strain. Creep is the time dependent strain that occurs even when stresses well below the yield stress exists. If a specimen is deformed and then held in a fixed position, the stresses will gradually decrease due to the creep process; this is called relaxation [5].

A model that includes purely elastic as well as viscoplastic behavior is called elasto-viscoplastic [16]. Total strain in this model separates elastic (reversable) strain from viscoplastic (irreversible) strain:

$$\varepsilon_{ij} = \varepsilon_{ij}^{e} + \varepsilon_{ij}^{p} \tag{2.1}$$

By taking the time derivative of equation (2.1), an expression for the total strain rate is obtained.

$$\dot{\varepsilon}_{ij} = \dot{\varepsilon}_{ij}^{e} + \dot{\varepsilon}_{ij}^{p} \tag{2.2}$$

The elastic strain rate, $\dot{\varepsilon}_{ij}^{e}$, is related to the stress rate simply through the time derivative of Hookes law. Unfortunately, viscoplastic strain rate must be related to stress by some other means.

Conventional plastic deformation begins at yield, and is dependent on the yield criterion. Many theories are available to define the stress level at which plastic

II. Viscoplastic Theory

Viscoplasticity combines two inelastic strain groups, conventional plasticity and time-dependent deformation. The conventional theory of plasticity is characterized by an irreversible strain which is not time dependent and which can only be sustained once yield stress has been reached [16]. This theory has been satisfactory since time rate effects are generally not important. However, metals, especially at high temperatures, exhibit significant time dependent deformation which, like conventional plasticity is irreversible. These two permanent strains must be combined in a unified viscoplastic model to adequately study high temperature, time dependent problems.

A discussion of viscoplasticity must include the effects of load rate and temperature. In most metals, high rates of load application result in less plastic flow and higher stress fields than low load rates. This is called rate sensitivity [17]. The magnitude of this effect is relatively minor at room temperature but increases rapidly as temperature increases. This suggests the analogy of viscous flow in a fluid.

Three time-dependent processes also increase in importance as temperature rises: recovery, creep, and relaxation. Recovery is defined as the restoration of the

experimentally determined by Stouffer [12]. The Bodner-Partom viscoplastic flow law has the capability to predict the behavior produced by cyclic effects [13]. This flow law is integrated through time by an Euler extrapolation scheme [14], and the law is incorporated into the finite element program by utilizing the residual force technique [15].

Finite element models of a compact tension specimen used by Wilson [11] and a center crack specimen used by Hinnerichs [6] were investigated in order to compare the effect of different load geometries. Load was input as a sawtoothed stress-time pattern of constant amplitude with zero mean load (load ratio or "R-ratio" of -1.0). For comparison, the compact tension specimen was studied at two cyclic load frequencies, 2.5 Hz. and .167 Hz. Maximum load amplitudes for each case was set to provide a stress intensity factor (K_I) at the crack tip of 35 ksi$\sqrt{in.}$. The study was then repeated at a K_I of 45 ksi$\sqrt{in.}$. Hopefully, this analysis will contribute to the understanding of the failure mechanism in critical high temperature jet engine components and help make a retirement-for-cause program more effective.

cycle predictions could be made for components with subcritical flaws. Only those components with a quantifiable critical flaw size would therefore, need to be retired [5].

Approach

Due to requirements imposed by a retirement-for-cause program for engine components, a significant volume of research has been devoted to high temperature fracture mechanics and the technology appears to be maturing rapidly [1]. The study of material behavior has evolved from high temperature creep analysis [6, 7, 8, 9] to high temperature elasto-VISCO plastic analysis under cyclic loading [10, 11].

This new study compares the effects on material behavior resulting from different cyclic load geometries, frequencies, and amplitudes. The subject material is IN-100, a superplastically forged nickel-based superalloy used in turbine disks for the F-100 jet engine. VISCO, an in-house computer program developed by Hinnerichs [6] was used for this analysis. VISCO is a finite element program which uses constant strain triangular elements and has the capability to run cyclic loads.

The Bodner-Partom flow law subroutine in VISCO was used to model the plastic flow during the load cycling. The Bodner material parameters for IN-100 at 1350_{o} F were

turbine disk containing subcritical flaws, many parts that are currently retired could be kept in service. Parts would be inspected at intervals determined by the ability to reliably detect flaws and provide assurance of adequate safe life, and thus parts would be returned to service until they could no longer pass inspection requirements. The Air Force calls such a program retirement-for-cause and is currently studying its feasibility for many high cost components limited by low cycle fatigue, like F-100 jet engine turbine disks. If we assume a 15-year engine lifetime, a retirement for cause program could result in F-100 engine life cost savings of about $249 million [2]. Actual testing of retired turbine disks has verified that significant cost savings can be safely realized using retirement-for-cause procedures. Note, this testing accepted a wide margin for error due to the relatively unsophisticated fracture mechanics methods available for analyzing components subjected to high temperature and low frequency cycle loading [3].

The life cycle of a turbine disk is a complex one consisting of frequent load cycle variations with ambient temperatures of up to 1350^{o} F. The elevated temperatures introduce time dependent creep phenomenon which interact with varied load spectra to produce complex material behavior [4]. If the material behavior could be determined for the typical life cycle then accurate remaining life

CRACK CLOSURE CHARACTERISTICS CONSIDERING CENTER CRACKED AND COMPACT TENSION SPECIMENS

I. Introduction

Background

The growing use of expensive high performance gas turbine engines in multi-million dollar aircraft has created a problem in the United States Air Force. An accurate failure prediction method is unavailable to retire critical high temperature jet engine components [1].

Normally, aircraft components are periodically inspected for flaws and returned to service if the flaws can not grow to critical size prior to subsequent periodic inspections. However, critical engine components, like turbine engine disks, are removed from service at a time when statistically 1 in 1,000 would be expected to initiate a flaw of some finite length (0.03 in.). From a safety standpoint, this policy works well. However, by definition 99.9 percent of the retired disks still have useful life. Over 80 percent of the disks have at least ten lifetimes remaining and over 50 percent have at least 25 lifetimes remaining [1].

If one could accurately predict the remaining life of a

Abstract

Due to growing use of expensive, high performance gas turbine engines in the United States Air Force, there is a need for improved failure prediction methods for critical high temperature engine components. This new study expands current research in the area of high temperature, low cycle fatigue of IN-100 at 1350^{o} F, the superplastic alloy used in F-100 engine turbine disks.

An in-house, 2-D, finite element program named VISCO employs the Bodner-Partom Constitutive equation to accurately model the principal features of completely reversed cyclic loading. VISCO is used to compare the effects on material behavior by considering a 2.5 Hz. compact tension specimen, a .167 Hz. compact tension specimen, and a 2.5 Hz. center cracked specimen subjected to fully reversed cyclic loading with a stress intensity factor of 35 and 45 ksi $\sqrt{in}$. The comparisons point out the findings of Linear Elastic Fracture Mechanics must be modified under conditions of high temperature viscoplasticity.

ε_{tol}, during a given time step. Stress/strain tolerances effect time stepping as follows:

$$P_\sigma = \frac{\sigma_e^{\,i} - \sigma_e^{\,i-1}}{\sigma_e^{\,i-1}\ \sigma_{TOL}} \tag{3.1}$$

$$P_\varepsilon = \frac{(d\varepsilon_e^{\,p})^i}{\varepsilon^i_{TOTAL}\ \varepsilon_{TOL}} \tag{3.2}$$

where superscript i refers to the timestep, σ_e is effective stress, ε_e is effective plastic strain and ε_{TOL} is defined as

$$\varepsilon_{TOTAL} = (\varepsilon_x^{\,2} + \varepsilon_y^{\,2} + 0.5\ \varepsilon_{xy}^{\,2})^{\frac{1}{2}} \tag{3.3}$$

P_σ and P_ε are parameters evaluated for each element and the largest of the two is set equal to P. The timestep size is then determined from the following equations [8]:

$dt^i = 0.8\ dt^i/P$ if $P > 1$

$dt^i = dt^{i-1}$ if $0.8 \leq P \leq 1$

$dt^i = 1.25\ dt^{i-1}$ if $0.65 \leq P < .8$

$dt^i = 1.5\ dt^{i-1}$ if $P < 0.65$

thus, the timestep interval is increased or decreased for efficient and accurate computations.

To improve understanding of the material behavior of critical high temperature engine components, the full range

of possible fatigue load spectra must be represented. Consequently, a completely reversed (R-ratio = -1.0) sawtoothed load-time pattern is used to drive the finite element models. Frequency, max load, and R-ratio can be individually prescribed for each computer simulation. A typical load spectrum is shown in Figure 3.1.

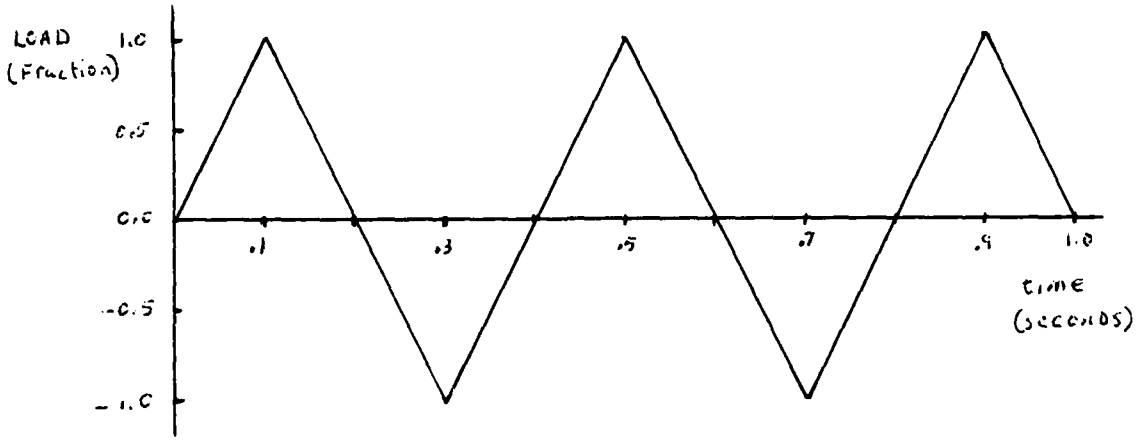

$$\text{R-ratio} = \frac{\text{min load}}{\text{max load}} = -1.0$$

Figure 3.1 Typical Load Cycles 2.5 Hz.

Other than minor modifications listed in Appendix A, VISCO, as used by Wilson [11] was unchanged.

Finite Element Modeling

Two finite element models shown in Figures 3.2 and 3.3, were used in this study: the 382 element compact tension specimen (CTS) and the 355 element center cracked specimen used by Hinnerichs [6]. Due to symmetry only the top half of the CTS was modeled. Adjacent elements differ in size by no more than a factor of 2.

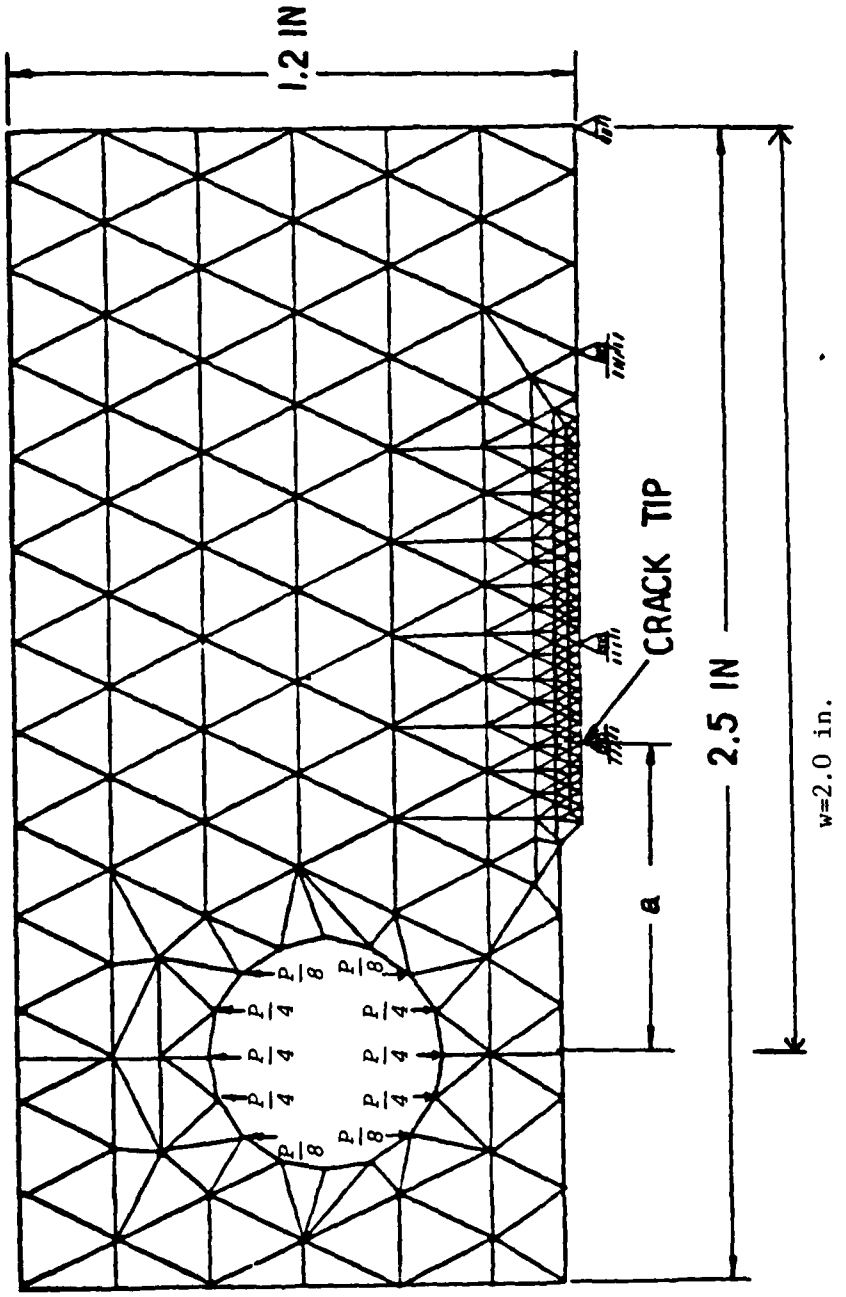

Figure 3.2 382 Element Compact Tension Specimen Mesh

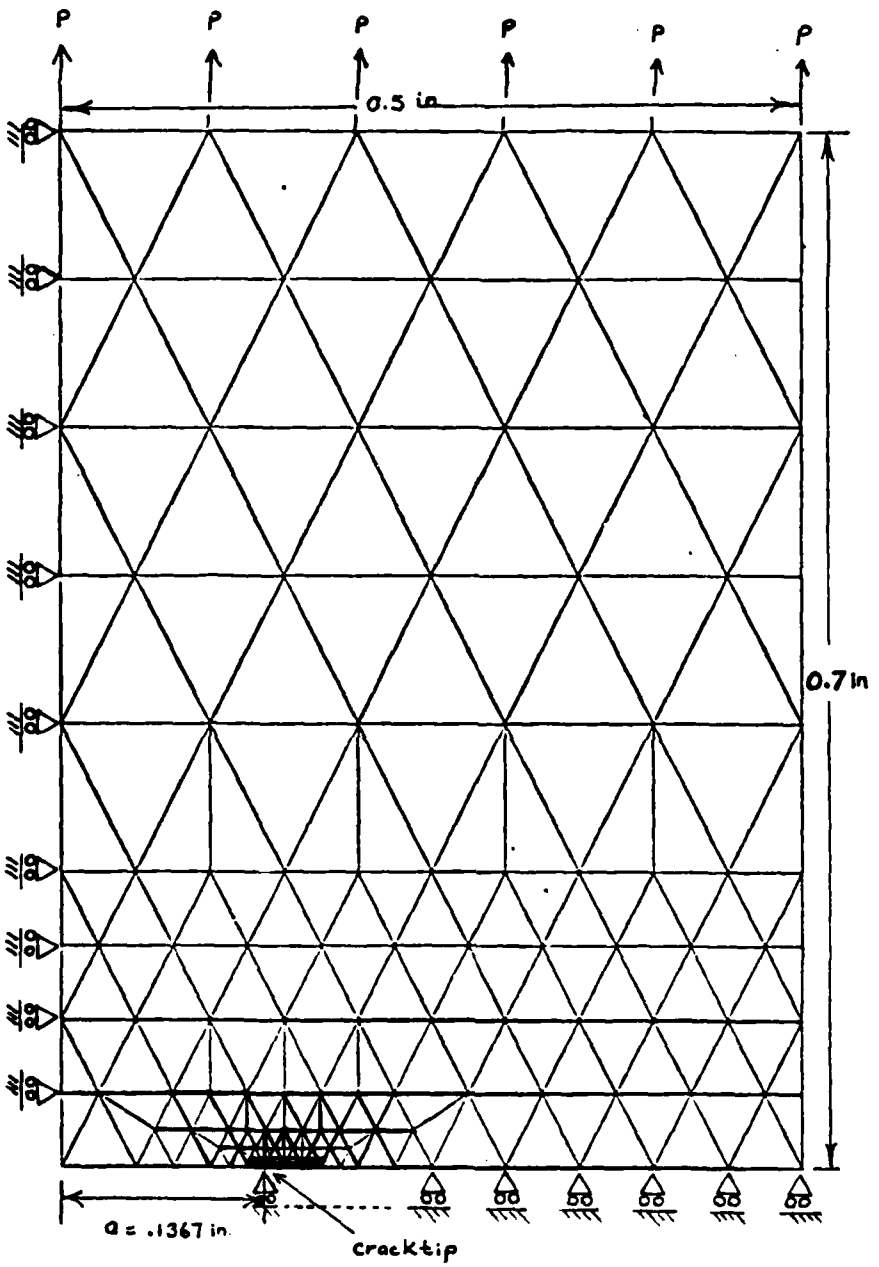

Figure 3.3 355 Element Center Cracked Specimen Mesh

The fine mesh elements near the crack tip have an area of 4.8848×10^{-6} in.^{2}. The crack length and specimen thickness were .6630 in. and .2154 in. respectively. Only the top right quarter of the center-cracked specimen was modeled due to symmetry. Like the CTS, adjacent elements differed in size by no more than a factor of 2. The fine mesh elements near the crack tip were much smaller than the CTS with an area of 3.051757×10^{-7} in.^{2}. The crack length, 2a, is .2734 in. and the plate thickness is .3000 in.

The loads were adjusted on each model to provide the stress intensity factor (K_I) as shown in Table 3.1. K_I for the CTS was found using

$$K_I = \frac{P}{B\sqrt{a}} \left[29.6 \left(\frac{a}{w}\right) - 185.5 \left(\frac{a}{w}\right)^2 + 655.7 \left(\frac{a}{w}\right)^3 - 1017 \left(\frac{a}{w}\right)^4 + 638.9 \left(\frac{a}{w}\right)^5 \right] \tag{3.4}$$

where P is load, B is thickness, a is crack length and w is width, [18]. K_I for the center cracked specimen was found using

$$K_I = \frac{P}{A} \sqrt{\pi a} \left(\sec \frac{\pi a}{w}\right)^{\frac{1}{2}} \tag{3.5}$$

where A is the area over which the load is applied [18]. See Figures 3.4 and 3.5 for dimensions.

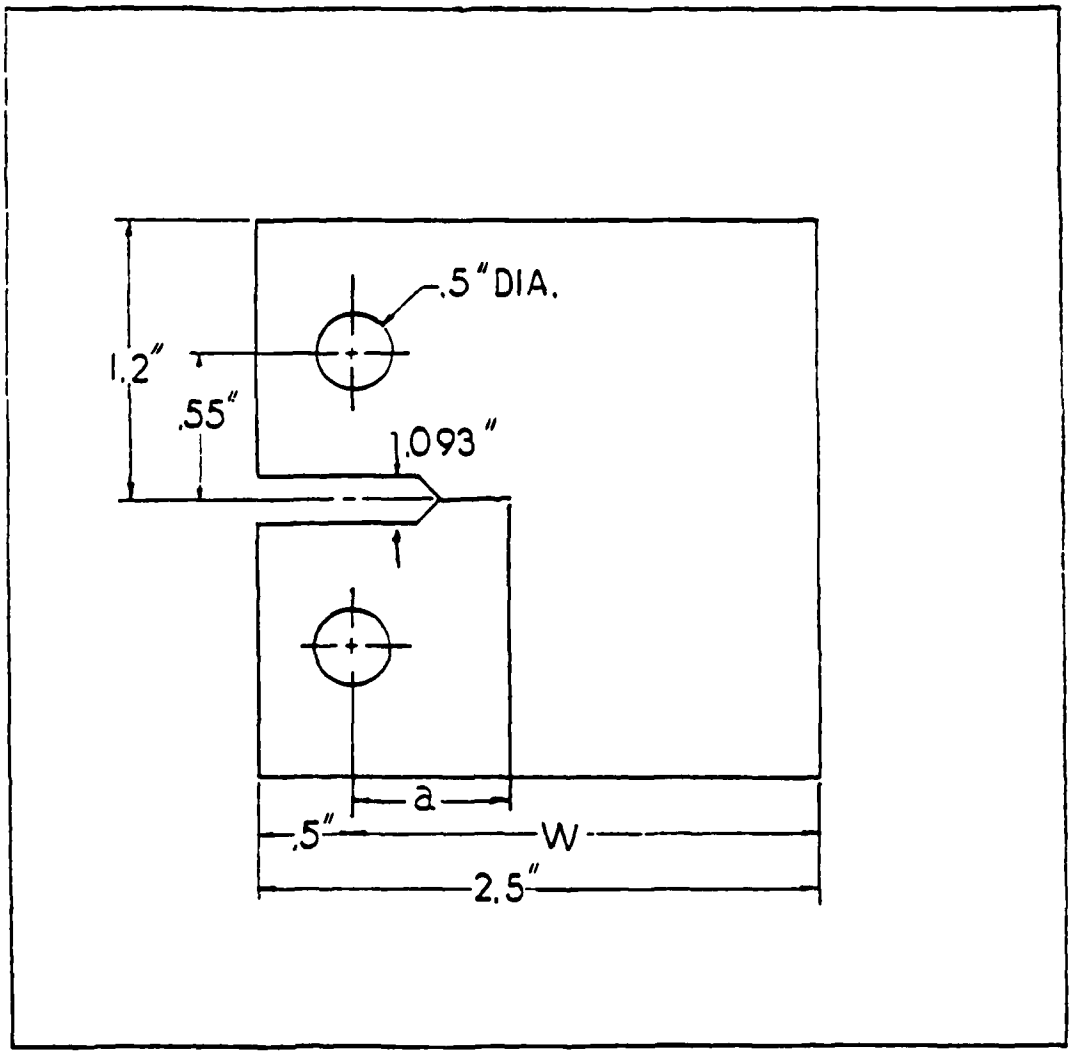

Figure 3.4 Compact Tension Specimen Geometry

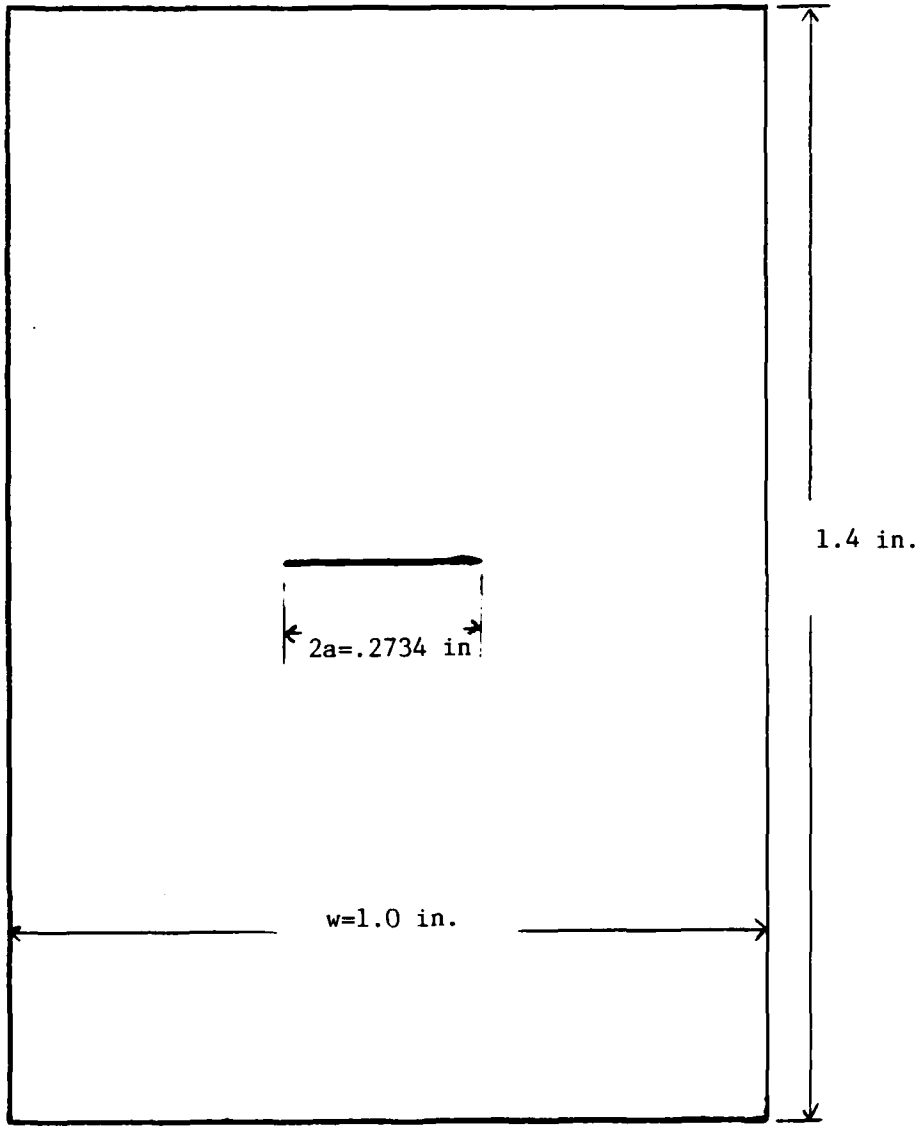

Figure 3.5 Center Cracked Specimen Geometry

$K(ksi\sqrt{In.})$	CTS Load (Lbs.)	Center Cracked Plate Load (lbs.)
35	1710.0	8029.9
45	2198.0	10300.0

Table 3.1 Specimen Loads and Stress Intensity Factors

A stress/strain tolerance investigation was performed to find a balance between accuracy and computer computation time. Several analyses under plane stress conditions were performed using different values of stress and strain tolerances. The results from both meshes repeated Hinnerichs' findings that computer time increases rapidly as the stress/strain tolerances are reduced to .01 [6]. It was also noted that the change in plastic work, from one tolerance analysis to the next, for each of the cases investigated, diminished as .01 was approached, See Figure 3.6. One may observe from Figure 3.6 that the center cracked specimen is least affected by the change in stress/strain tolerances. This can be attributed to smaller area per element near the crack tip. Using stress and strain tolerances of .01 as a datum point, tolerances were increased to provide no more than a 2% error in plastic work over one computer loading cycle, this allowed a minimum of 5 load cycles in 2500 seconds of central processor time on the CDC CYBER 845 computer for all cases studied. This

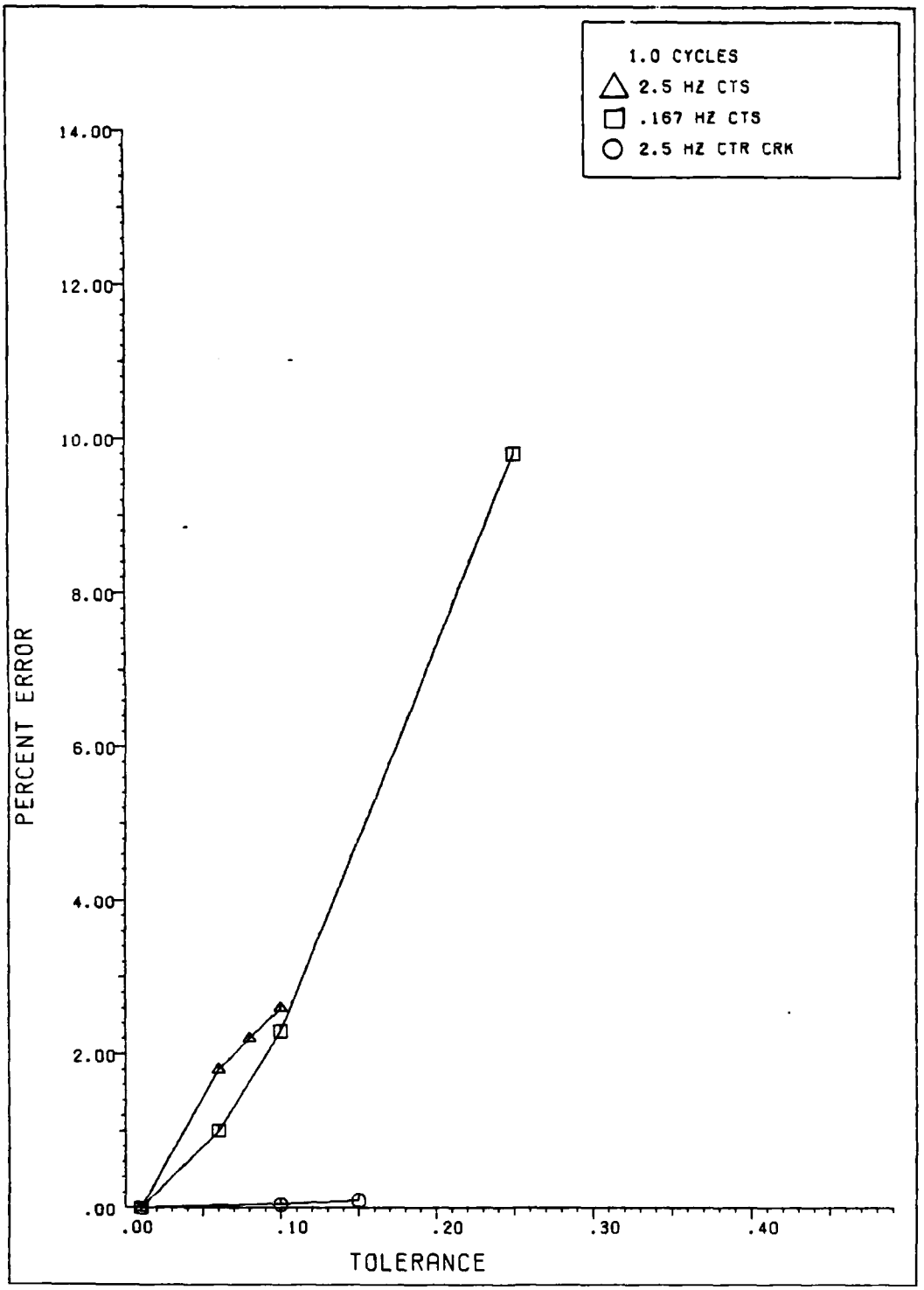

FIG 3.6 ERROR VS. STRESS/STRAIN TOLERANCE SETTING

process established the tolerances for the CTS and the center cracked specimen. Stress/strain tolerances in this study were set at .06 and .10 for the CTS and center cracked specimen respectively.

IV. Results and Discussion

Throughout this chapter, comparisons will be made of three cases under two different stress intensity factors, 35 and 45 ksi $\sqrt{in}$:

(1) CTS with 2.5 Hz. Load Cycling

(2) CTS with .167 Hz. Load Cycling

(3) Center cracked specimen with 2.5 Hz. Load Cycling

All three cases model the material properties of IN-100 at 1350^{o} F subjected to a completely reversed (R-ratio = -1.0) cyclic load. Previous work by Wilson [11], which dealt with only case (1), was verified as part of this study. The desire to investigate interesting findings in Wilson's work with the 2.5 Hz. CTS, along with the continuing need for better understanding of high temperature, low cycle fatigue, led to the inclusion of the other two cases. As discussed in Chapter III, steps were taken to insure the same degree of accuracy and same stress intensity factors exists in each case so valid comparisons can be made. The results are separated into three areas:

(a) Crack opening displacements behind the crack tip at full negative load.

(b) Profiles of y-stress and y-strain fields in front of the crack tip, (the y components along the horizontal line of symmetry were

chosen since they are the most significant), and

(c) Plastic zone size and shape estimations.

Closure Behind Crack Tip at Full Negative Load

One interesting finding in Wilson's CTS work [11] considered the fact that an incomplete closure behind the crack tip (that is, the open side) existed at full negative load. Looking at the way the CTS is loaded (Figure 3.3), it can be seen that no load is applied directly over the near field of the crack tip. In fact, the loading geometry is much like a cantilever beam. Wilson proposed that the plastic deformation near the crack tip from the full positive load, acts like a fulcrum and prevents full closure. Further, it seems reasonable to assume that a center cracked specimen, with uniform loading directly over the near field of the crack tip (Figure 3.4), would close completely upon full negative loading. Figures 4.1 through 4.4 refute this idea. Even though the 2.5 Hz. center cracked specimen is characterized by more full closure than the CTS at 2.5 Hz. and .167 Hz., the highly viscoplastically deformed area surrounding the crack tip still prevents full closure. The .167 Hz. CTS has the least closure and the 2.5 Hz. CTS closure is in between. One should notice the difference that a number of cycles makes. This change can be observed in Figures 4.1 and 4.2

(or 4.3 and 4.4 at 45 ksi$\sqrt{\text{in}}$); the lack of full closure on the first full negative load (.75 cycles) becomes slightly worse as cycles increase to the fourth full negative load (3.75 cycles). Also note the difference caused by the stress intensity factors in Figure 4.1 versus Figure 4.3 and Figure 4.2 versus Figure 4.4. The lack of full closure increases significantly as stress intensity factor is increased from 35 to 45 ksi$\sqrt{\text{in}}$. The reasons for this phenomenon becomes evident by examining the state of stress and strain in front of the crack tip.

y-Stress and Total y-Strain Fields in Front of Crack Tip

The y-stress versus total y-strain curves for all three cases at both 35 and 45 ksi$\sqrt{\text{in}}$ are presented in Figures 4.5 through 4.10. These figures plot the stress/strain values in the near field of the crack tip (.004 inches in front of the crack tip). Comparing Figure 4.5 with Figure 4.6, one can see the effect of varying only cyclic frequency. At 2.5 Hz., the full load has 0.1 seconds to be applied while the .167 Hz. case has 1.5 seconds. The result is higher positive stress and lower total strain in the 2.5 Hz. case. This phenomenon is known as rate sensitivity. The .167 Hz. specimen, consequently, experiences more plastic strain which is the reason why there is less closure behind the crack tip at full negative load. This larger region of plastic strain results in greater compressive stresses (Figure 4.6) as the surrounding

material attempts return to its pre-strained state. Looking at Figure 4.7, the center cracked specimen develops approximately the same maximum tensile stress as the 2.5 Hz. CTS, but the total y-strain and the maximum y-compressive stress is much greater than either CTS cases. The uniform distributed loading in the positive direction acting on the center cracked specimen increases the tensile y-stress field throughout the material and causes much more plastic strain than either CTS case. At this point, one would expect less closure behind the crack tip, at full negative load, than even the .167 Hz. CTS. However, the uniform distributed load in the negative direction increases the compressive y-stress field throughout the material. This compressive y-stress field does more work in overcoming the larger plastic deformation to produce the most closure behind the crack tip. The large compressive stresses in the 2.5 Hz. center cracked specimen, depicted in Figure 4.7, are further evidence of this phenomenum. Of the three cases, the center cracked specimen experiences the widest range of stresses and total strains in the near field of the crack tip.

Increasing the stress intensity factor from 35 to 45 ksi$\sqrt{in}$, as shown in Figures 4.8 - 4.10, has the expected effect of increasing tensile and compressive stresses; which in addition, produces a greater amount of compressive plastic strain. It is this greater amount of

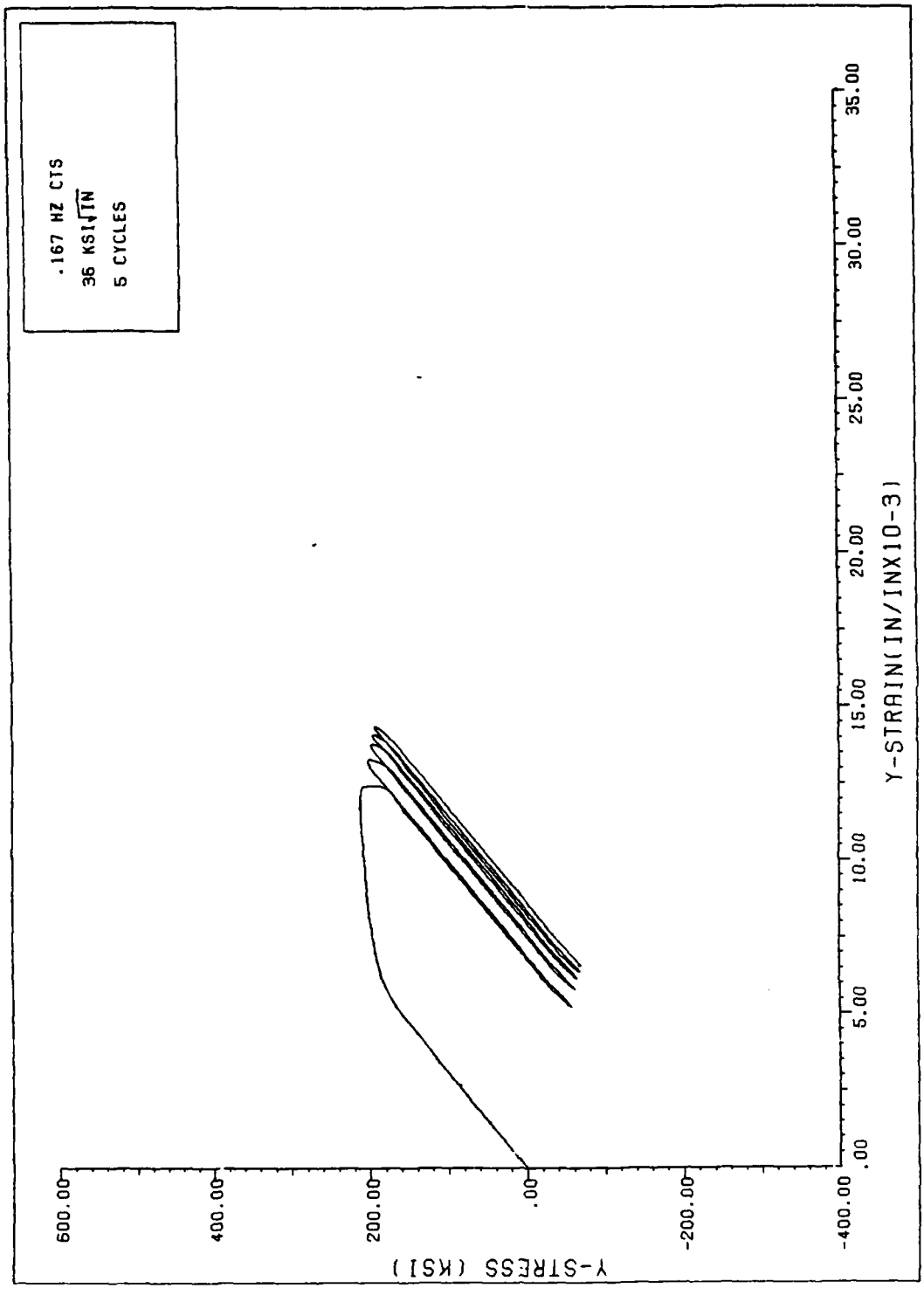

FIG 4.6 Y-STRESS VS. TOTAL Y-STRAIN

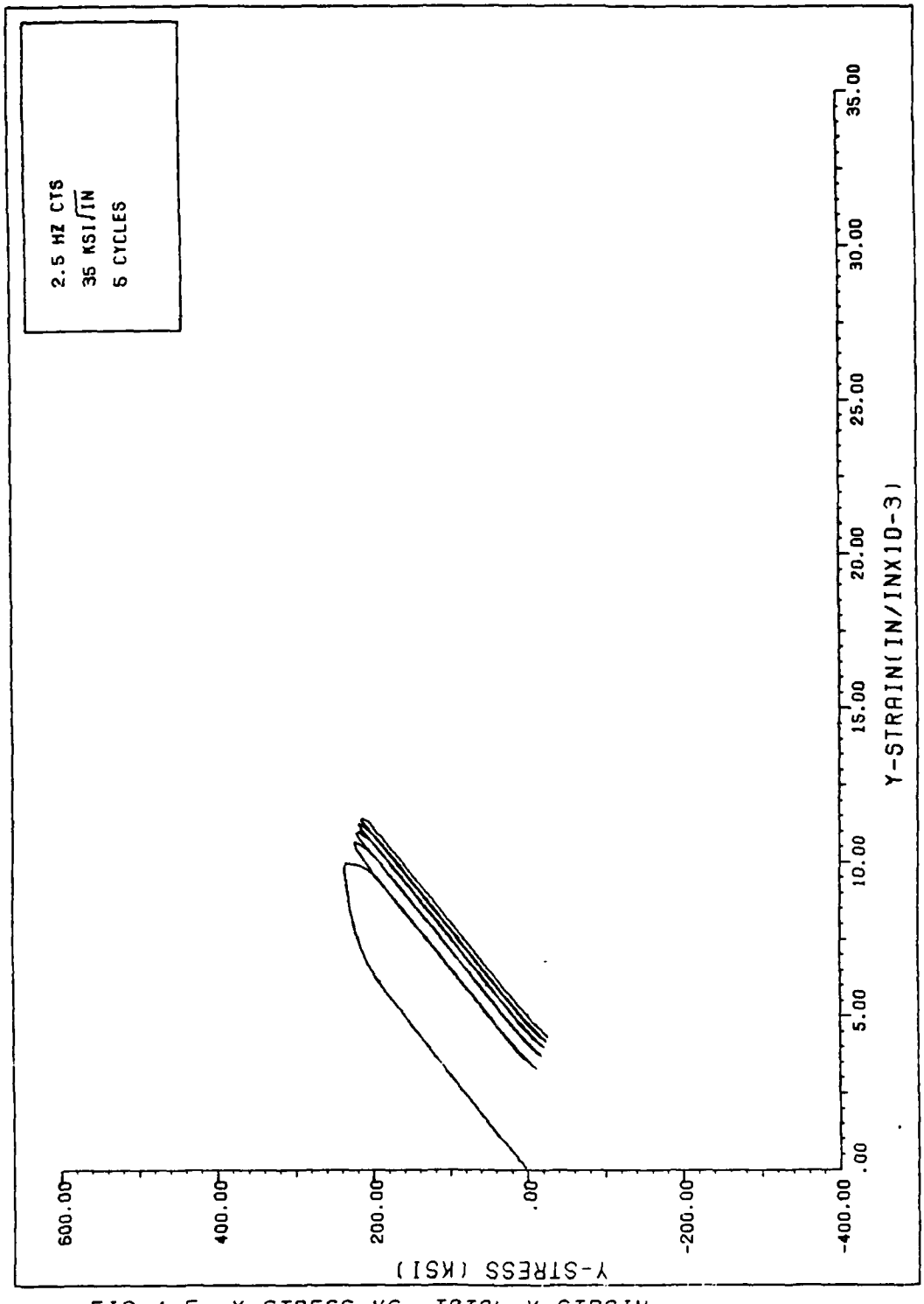

FIG 4.5 Y-STRESS VS. TOTAL Y-STRAIN

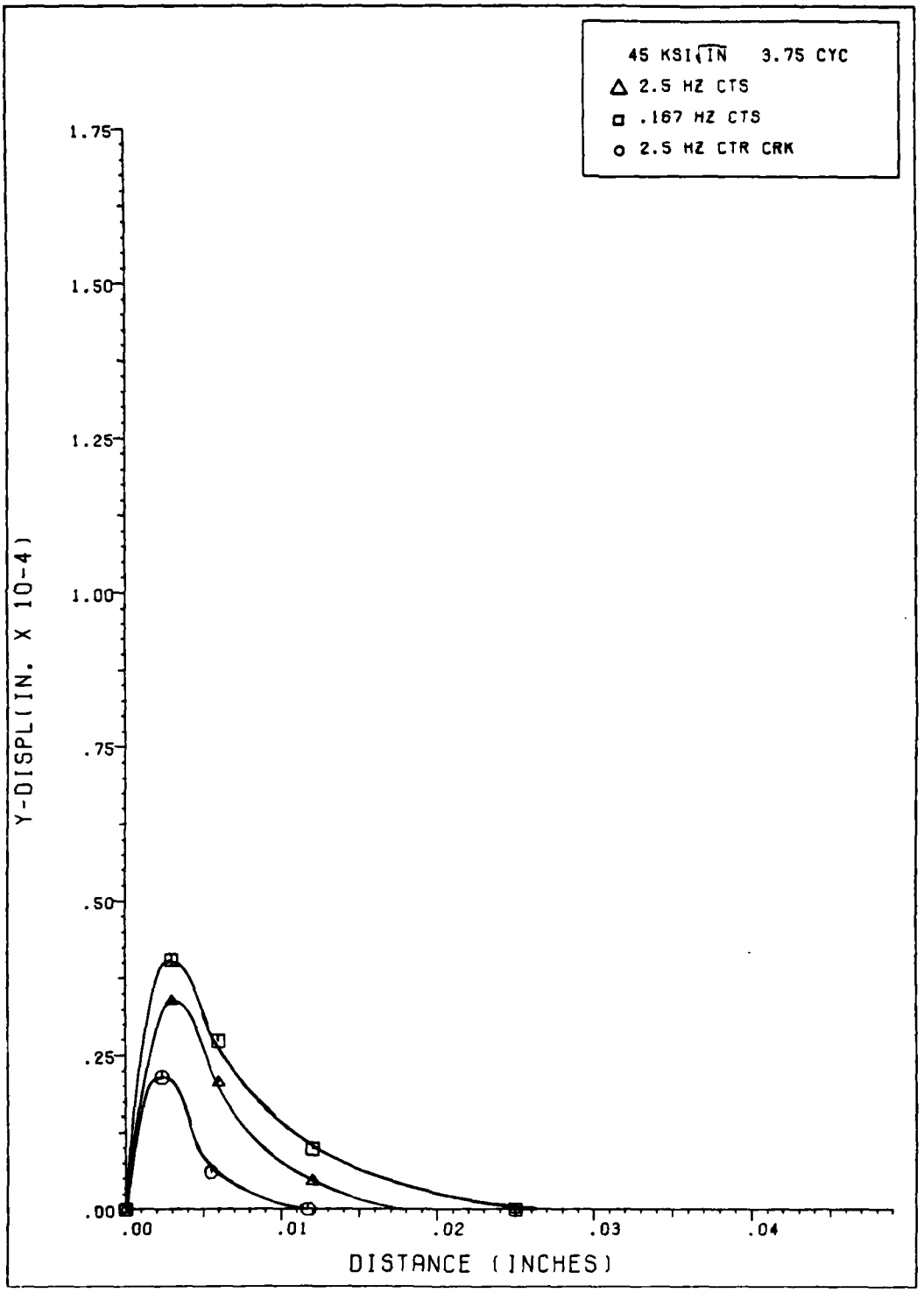

FIG 4.4 Y-DISPL BEHIND CRACK (FULL NEG. LOAD)

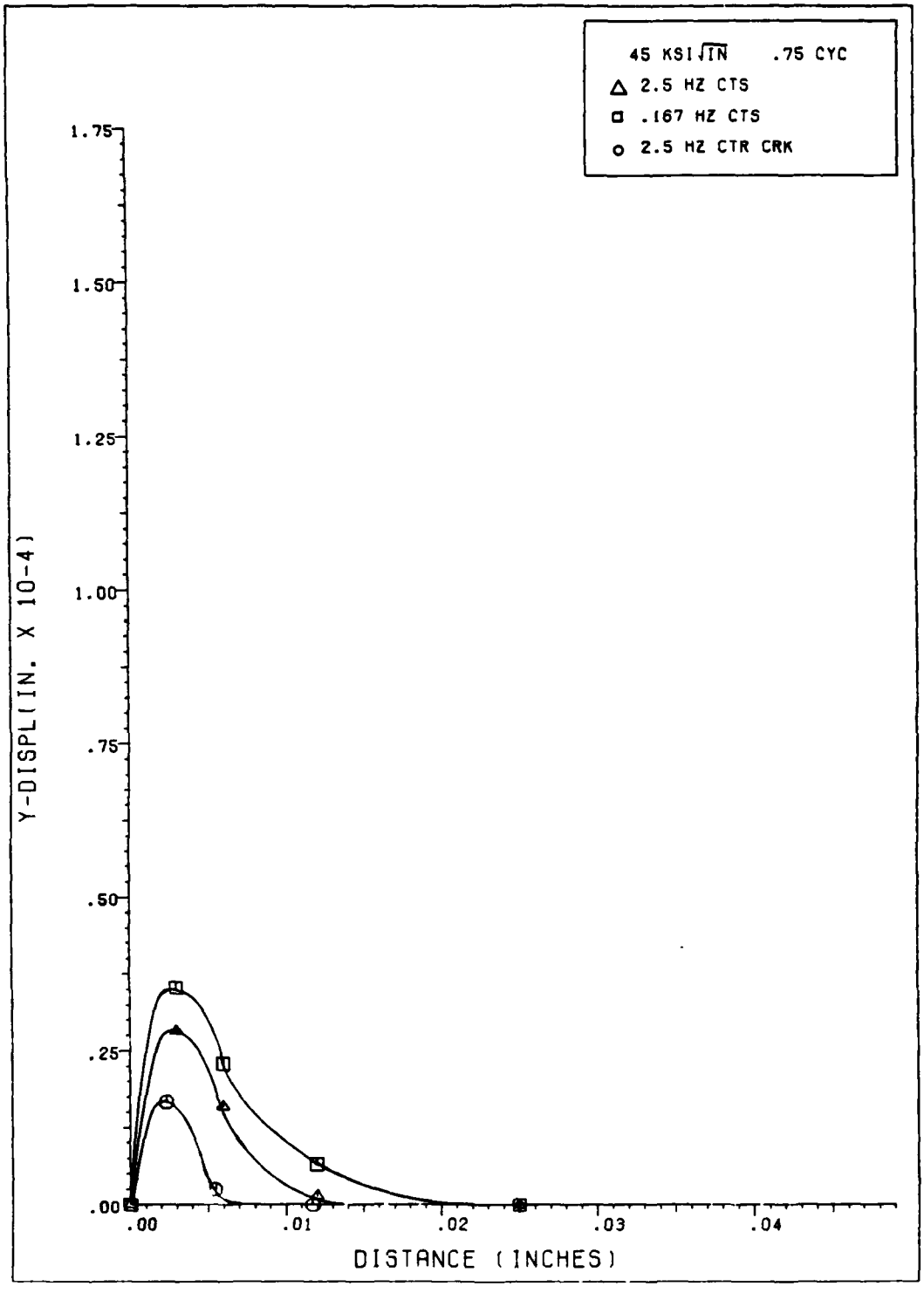

FIG 4.3 Y-DISPL BEHIND CRACK (FULL NEG. LOAD)

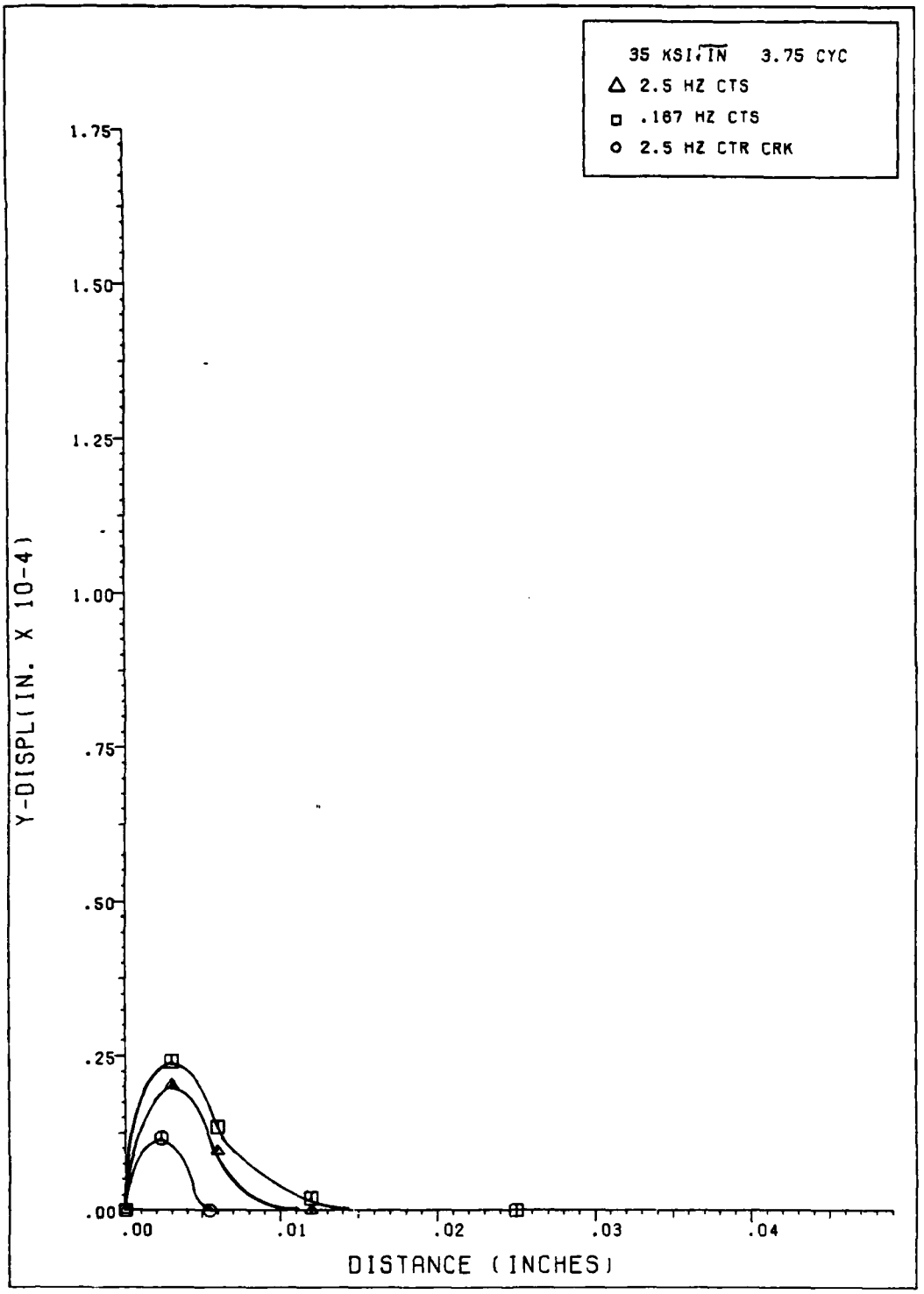

FIG 4.2 Y-DISPL BEHIND CRACK (FULL NEG. LOAD)

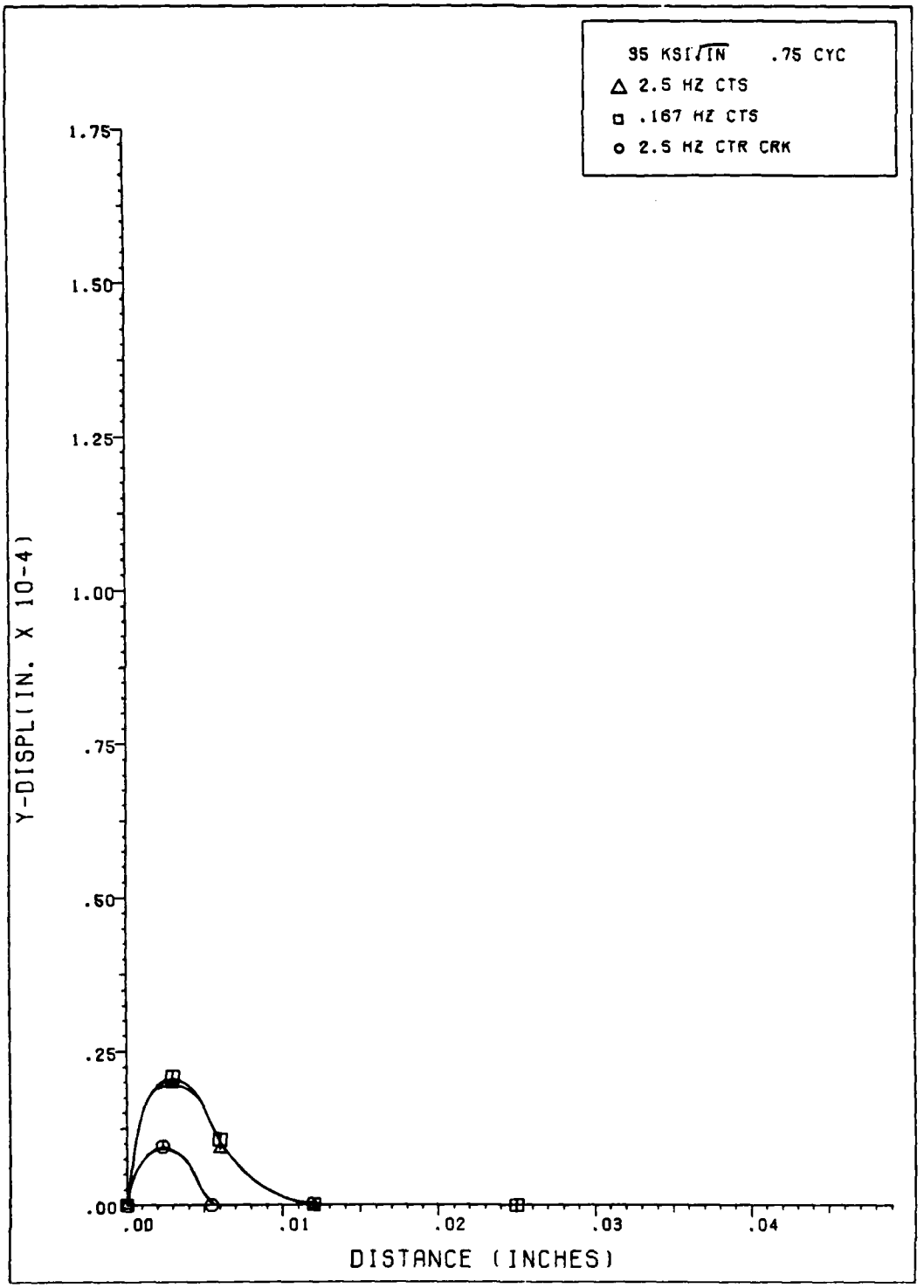

FIG 4.1 Y-DISPL BEHIND CRACK (FULL NEG. LOAD)

compared with the region of negative plastic strain under full negative load, at 35 ksi$\sqrt{in.}$ Figures 4.33 through 4.35 represent the 45 ksi$\sqrt{in}$ cases. The region of negative plastic straining is approximately one fourth the area of the region of positive straining in all cases. These regions can be thought of as residual compressive stress zones, since the residual stress must be overcome before the region can be plastically strained in tension. The result of these residual compressive stress zones, when large enough, is the redistribution of stresses in the form of the discontinuities seen in the y-stress versus distance in front of the crack tip figures. Note that the region of negative plastic straining in the two 2.5 Hz. center cracked specimen cases and the 45 ksi$\sqrt{in}$ CTS at .167 Hz. case (Figures 4.32, 4.35, and 4.34) have the size and position corresponding to the size and position of the y-stress discontinuities in Figures 4.13 and 4.14.

the raw data printout of Bodner-Partom plastic strain. It is noteworthy that the region closest to the crack tip does not return to a state of zero strain even during full negative load.

One way to define compressive plastic straining is to compare total strain at full negative load with total strain at full positive load. When the difference exceeds the appropriate value in Table 4.2, compressive plastic straining has occurred. Unlike Table 4.1, Table 4.2 accounts for the full range of elastic strain, that is, elastic strain in tension plus elastic strain in compression. The results in Table 4.2 can be verified by estimating the linear range of the stress strain curves Figures 4.5 through 4.10.

Case	Plastic Strain in/in	Total Strain in/in 35 ksi $\sqrt{in}$	Total Strain in/in 45 ksi $\sqrt{in}$
(1) 2.5 Hz. CTS	.001	.013	.013
(2) .167 Hz. CTS	.001	.011	.011
(3) 2.5 Hz. Ctr. Crk.	.001	.013	.013

Table 4.2 Total Elastic Strain Range from Full Tension to Full Compression

Plastic Zone

The actual size and shape of the plastic zone will help explain the material behavior. Figures 4.30 through 4.32 show the regions of plastic strain under full positive load

Bodner-Partom results, will be used to define the yield point and the beginning of the plastic zone. Table 4.1 lists the total strain occurring in the three cases when 0.1% plastic strain has been achieved. These results can be verified by reviewing the y-stress/y-strain curves (Figures 4.5 through 4.10).

Case	Plastic Strain in/in	Total Strain 35 ksi$\sqrt{in}$	Total Strain 45 ksi$\sqrt{in}$
(1) 2.5 Hz. CTS	.001	.007	.007
(2) .167 Hz. CTS	.001	.006	.006
(3) 2.5 Hz. Ctr. Crk.	.001	.007	.007

Table 4.1 Total Elastic Strain Range Under Tension

The .167 Hz. Case, with the .001 plastic strain removed, matches the normal elastic range of .5% based on observations in the theory of elasticity [5]. The higher values at 2.5 Hz. are due to the rate sensitivity of the material; that is, high loading rates push up the yield point since less time is available for plastic straining to redistribute the stress.

Using the values in Table 4.1, an approximation can be made to determine where each strain field goes plastic under tension by using the full positive load portion of Figures 4.28 and 4.29. This method is a good approximation for full positive load plastic straining when compared with

discontinuity. Further investigation considering strain in front of the crack is warranted.

The total y-strain field at 4.25 cycles (full positive load) for all three cases is compared with the total y-strain field at 3.75 cycles (full negative load), in Figure 4.28 for 35 ksi$\sqrt{in}$ and Figure 4.29 for 45 ksi$\sqrt{in}$. The total y-strain appears to increase exponentially close to the crack tip. This corresponds to the exponential rise in stresses close to the crack tip predicted by Linear Elastic Fracture Mechanics. The Bodner-Partom Constitutive Law, with its ability to model viscoplastic material behavior, allows the prediction of this phenomenon. The center cracked specimenexhibits the highest y-strain throughout the near field of the crack tip under full positive load, and, except for the region right next to the crack tip in the 35 ksi$\sqrt{in}$ case, the center cracked specimen has the lowest value of strain at full negative load. The load geometry for this case puts the center cracked specimen through a much wider range of strains than the CTS loading geometry.

A criteria is needed to determine when plastic straining occurs. Conventional strength of materials normally defines yield point as .2% permanent deformation represented in a uniaxial stress/strain curve [19]. Consequently, the plastic strain components in the y direction will be used to predict when an element undergoes significant plastic strain. 0.1% plastic strain, based on the

discontinuity. To better illustrate the effect of cycling on the y-stress field near the crack tip, the y-stress at the first positive load is compared with the y-stress for the fifth full positive load for each case at 35 and 45 ksi$\sqrt{in.}$ - see Figures 4.20 through 4.25. These six figures clearly demonstrate the viscoplastic property of stress redistribution due to time dependent plastic straining. The highest stresses near the crack tip are gradually redistributed through time-dependent plastic strain. For example, in Figure 4.10 the stress field at 4.25 cycles starts out with lower stress values, but drops off less rapidly than the .25 cycle results.

The stress field from the fourth full negative load (3.75 cycles) is superimposed on the stress field from the fifth full positive load (4.25 cycles) in Figures 4.26 and 4.27. This way, it will be easier to see the effect of a negative load stress field on the subsequent positive load stress field. As expected, the discontinuities coincide with the maximum compression stresses. The center cracked specimen at 35 ksi $\sqrt{in}$ and 45 ksi $\sqrt{in}$ along with the .167 CTS at 45 ksi $\sqrt{in}$ have higher magnitudes of compressive stress than the other cases without discontinuities. Presumably, these stresses are large enough to cause negative plastic deformation with resulting residual compressive stresses. These residual stresses effectively subtract from the maximum tensile stresses forming the

K_I does not produce the same stress near the crack tip when applied at different cyclic frequencies; now it is evident that the same K_I does not produce the same stress near the crack tip when applied to different load geometries. Now that the stress field in the so-called virgin material has been analyzed, what is the effect of cycling with completely reversed load on the stress field?

After approximately five complete cycles at 35 ksi$\sqrt{in}$, the y-stress field under full positive load has gone through some changes. Looking at Figure 4.13, one immediately notices a discontinuity, or sudden dip, in the center cracked specimen. The discontinuity, .004 inches from the crack tip, was not expected. Figure 4.14, at 45 ksi$\sqrt{in}$, shows the discontinuity has become more pronounced and has moved further away from the crack tip (.008 inches). The.167 Hz. CTS seems to be developing a discontinuity also. Note also, Figures 4.13 and 4.14 verify the conclusion that the same K_I does not produce the same y-stress near the crack tip when applied to different load geometries. Figures 4.15 through 4.19 trace the development of the center cracked specimen discontinuity over 5 cycles at 45 ksi$\sqrt{in}$. Clearly the size of the discontinuity is related to the magnitude of the compressive stress at full negative load. It will be shown that negative [illegible]stic straining, produced by the compressive stress, results in a region of residual compressive stress corresponding to the

considering R-ratio = - 1.0, results close to the fifth cycle will be considered stabilized. The next series of figures allow a closer examination of the stress and strain field in front of the crack tip.

Figure 4.11 shows y-stress as a function of distance in front of the crack tip at full positive load on the first cycle. The center cracked specimen curve verifies that a higher stress field exists throughout the specimen compared to both CTS curves. Note however, the 2.5 Hz. CTS approaches convergence with the center cracked specimen curve close to the crack tip. This seems to verify that the same K_I will produce similar characteristics in different structures. The contrary of this will become apparent in the subsequent analysis of this study's results. The 2.5 Hz. CTS has the expected higher stress level compared to the .167 Hz. CTS close to the crack tip. This results from the rate sensitivity discussed earlier. The 2.5 Hz. CTS curve drops rapidly below the .167 Hz. CTS curve and rejoins away from the crack tip. The explanation for this lies behind the lower load rate which allows more time for the plastic strain process in the .167 Hz. CTS to distribute the stress over more elements, this process produces lower stress close to the crack tip and slightly higher stress in neighboring elements. Figure 4.12, at 45 ksi$\sqrt{in}$, essentially magnifies the 35 ksi$\sqrt{in}$ results. It is already clear that the same

compressive plastic strain that results in even less closure behind the crack tip than in the 35 ksi$\sqrt{in}$ cases. Notice now, especially in Figures 4.9 and 4.10, that negative plastic straining is occurring in the compressive region of the stress/strain curves. This is causing an overlapping of the curves as each cycle enters the region of full negative load. The ability to account for plastic straining in compression as well as plastic strain in tension is a characteristic of the Bodner material idealization [10].

Reviewing, in order, Figures 4.5 through 4.10, the maximum compressive stresses progressively approach the maximum tensile stresses in magnitude, this is a direct result of the increasing size of the plastic zone, resists closure and the return to the undeformed state. Finally, compressive stresses have grown large enough, especially in Figures 4.9 and 4.10, to cause plastic strain in the negative direction.

In all six stress/strain curves there is a noticeable ratcheting (stepped movement) to the right. The rate of change in the ratcheting diminishes as cycles increase to a point where further plastic straining may cease. Work by Wilson [11] showed that, for an R-ratio of 0.1, this stable zone occurred after 23 cycles. Due to the prohibitive central processor time, associated with completing the possible high number of cycles for a stable plastic zone

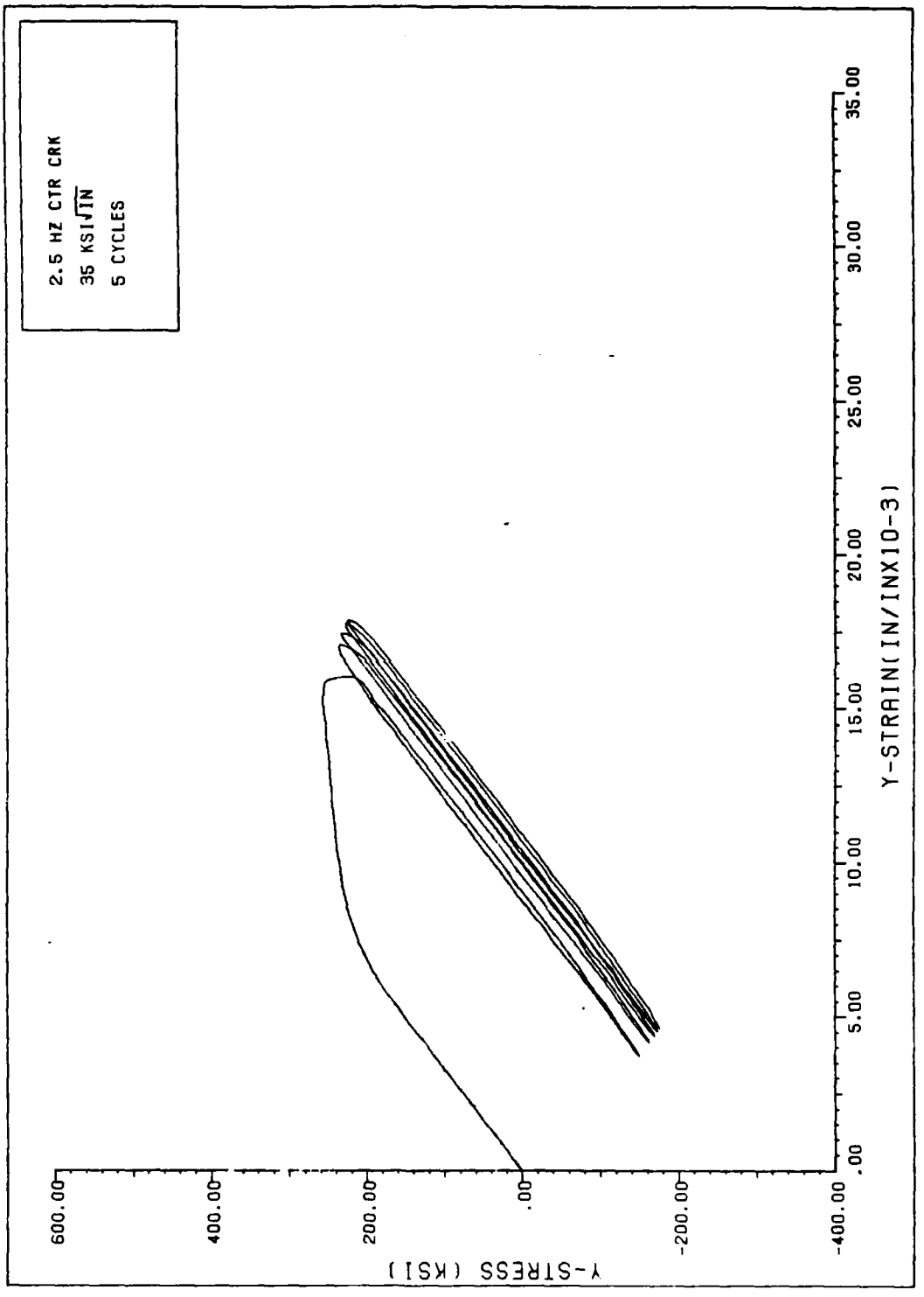

FIG 4.7 Y-STRESS VS. TOTAL Y-STRAIN

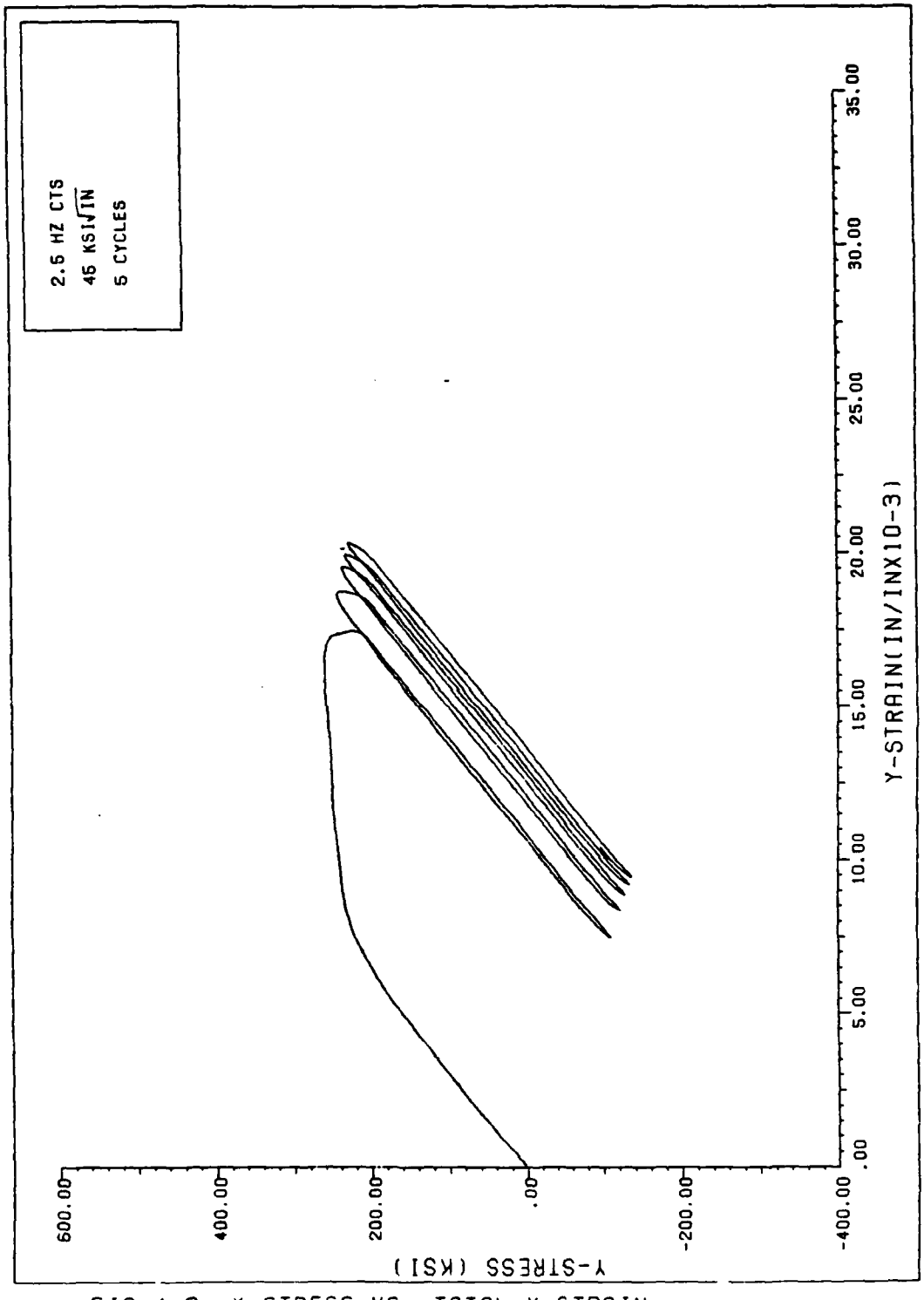

FIG 4.8 Y-STRESS VS. TOTAL Y-STRAIN

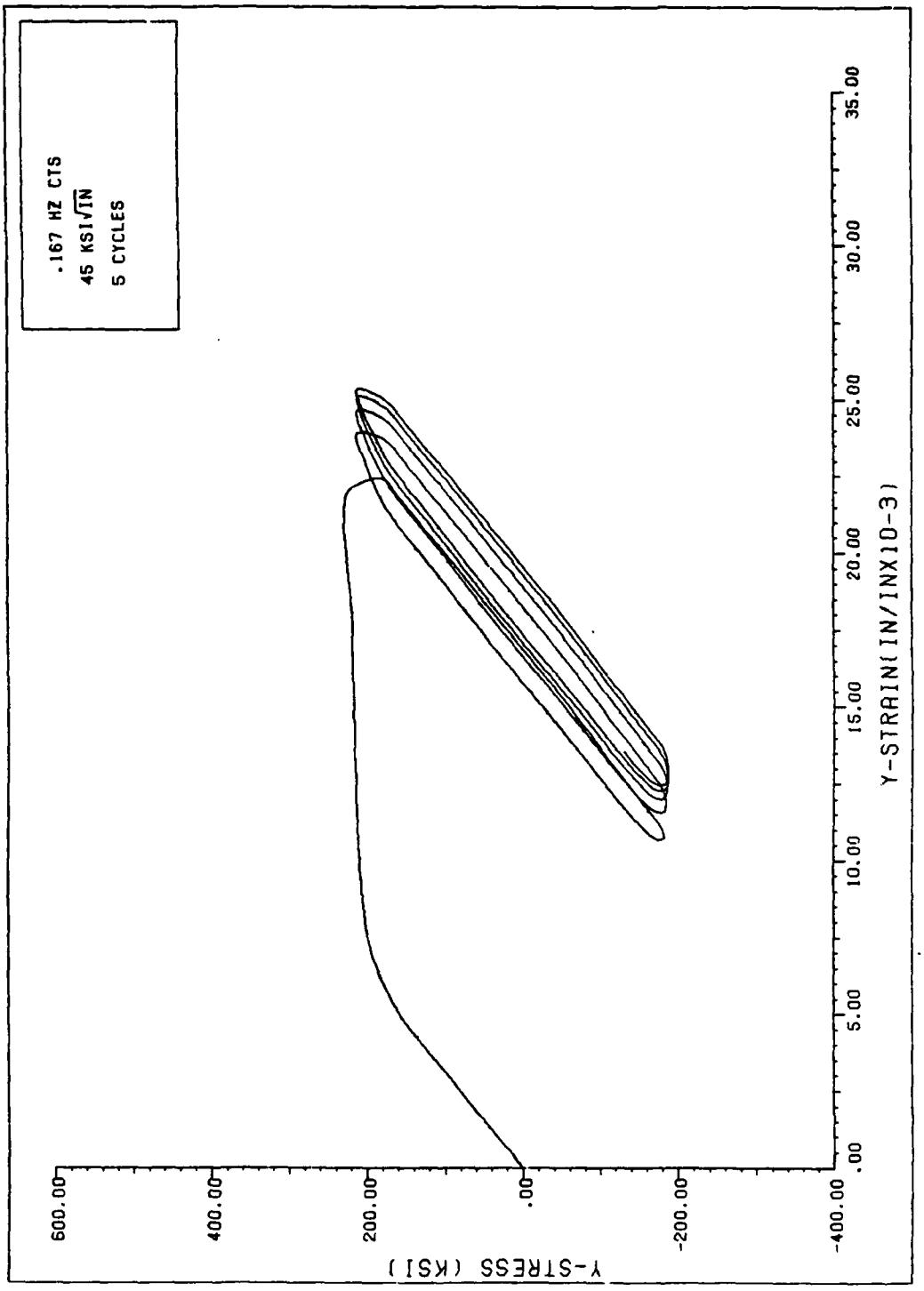

FIG 4.9 Y-STRESS VS. TOTAL Y-STRAIN

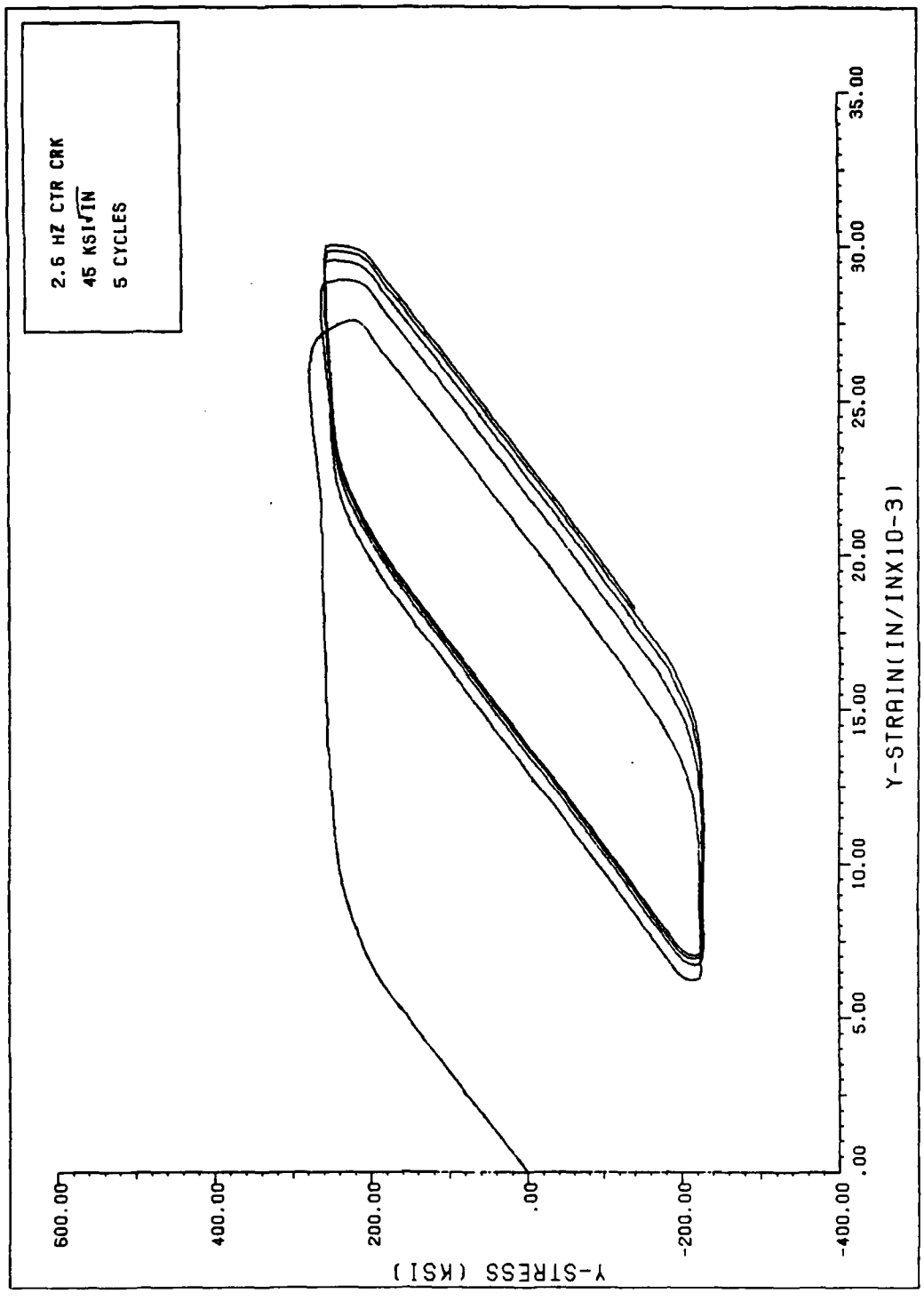

FIG 4.10 Y-STRESS VS. TOTAL Y-STRAIN

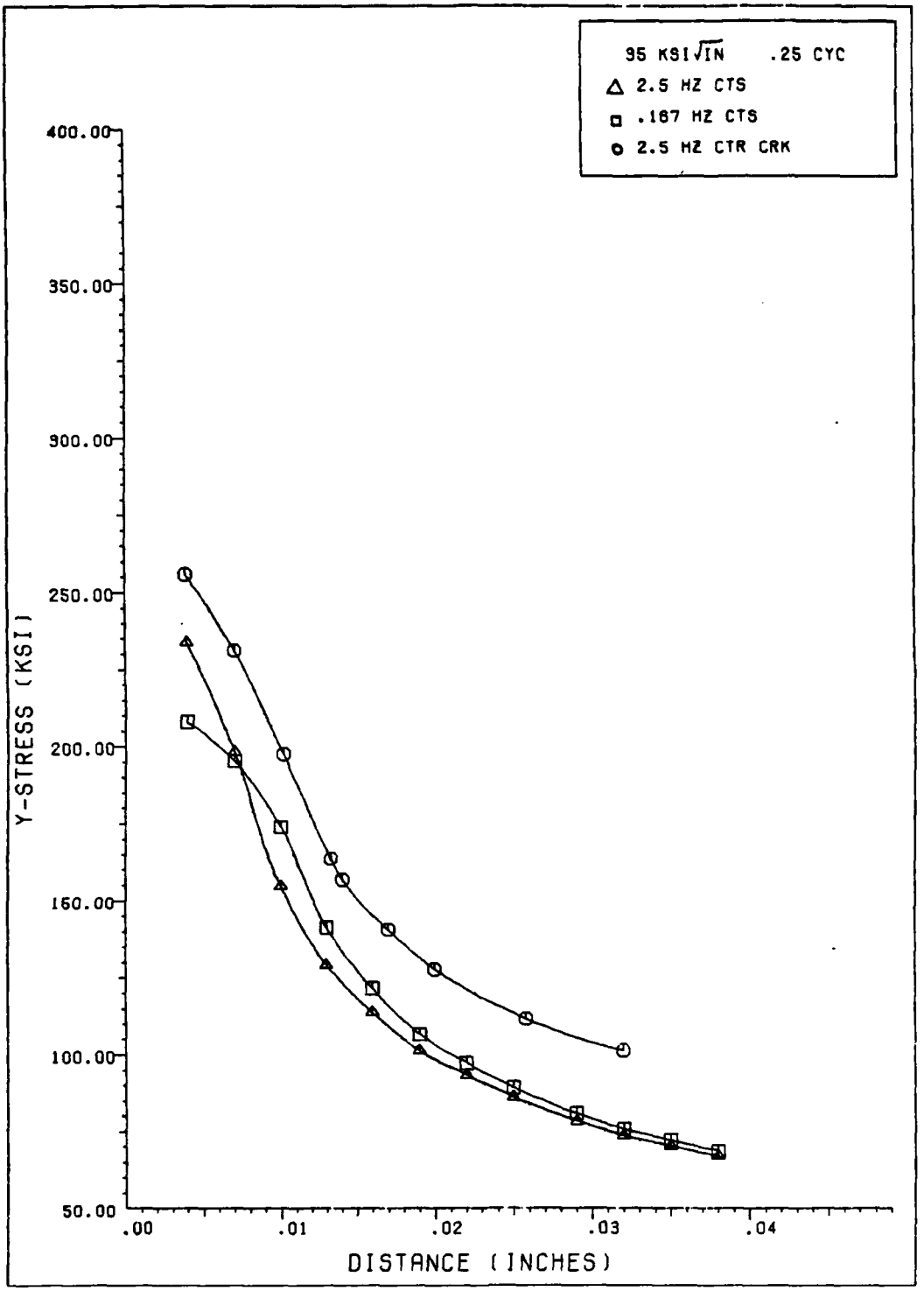

FIG 4.11 Y-STRESS IN FRONT OF CRACK (FULL POS LD)

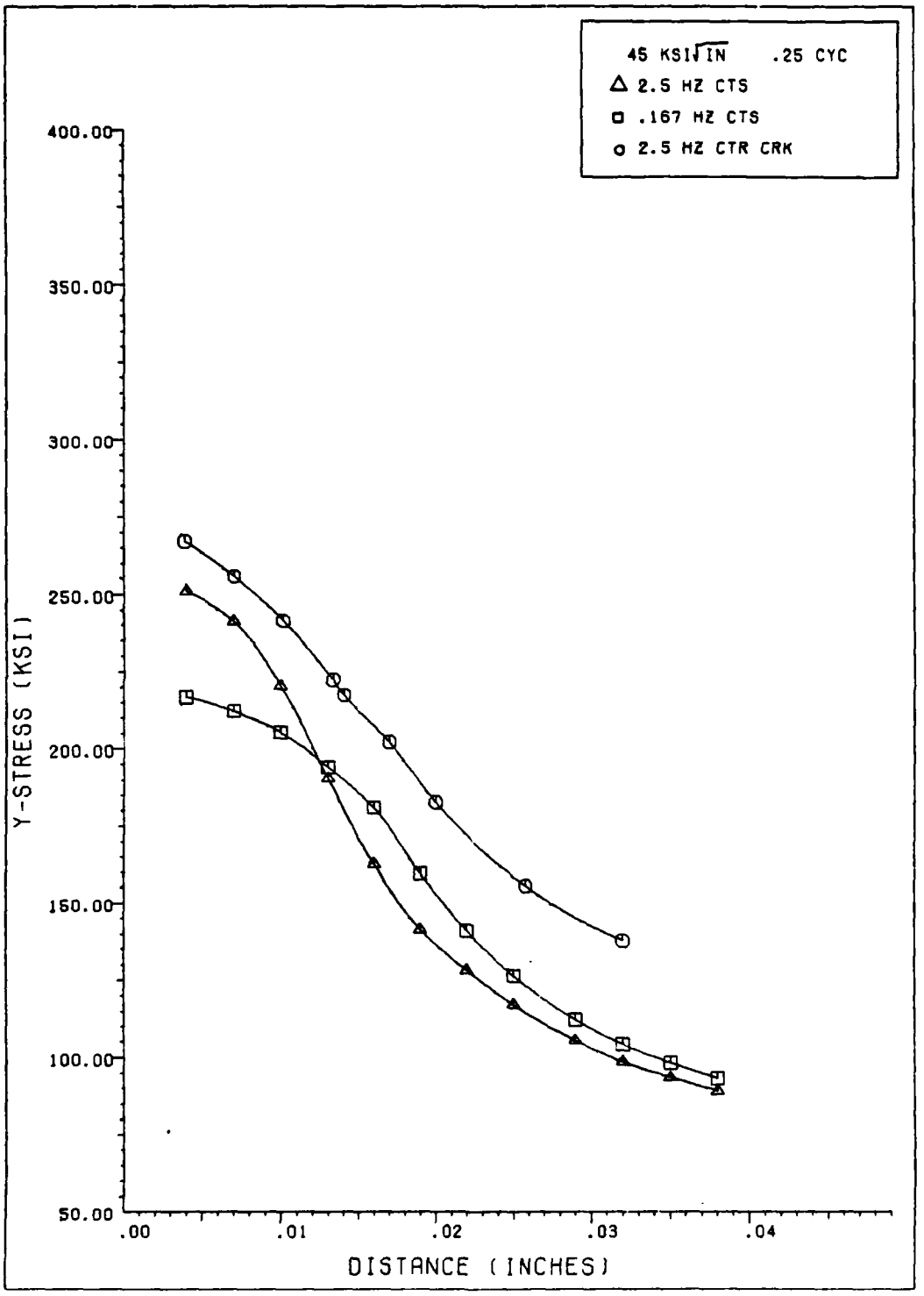

FIG 4.12 Y-STRESS IN FRONT OF CRACK (FULL POS LD)

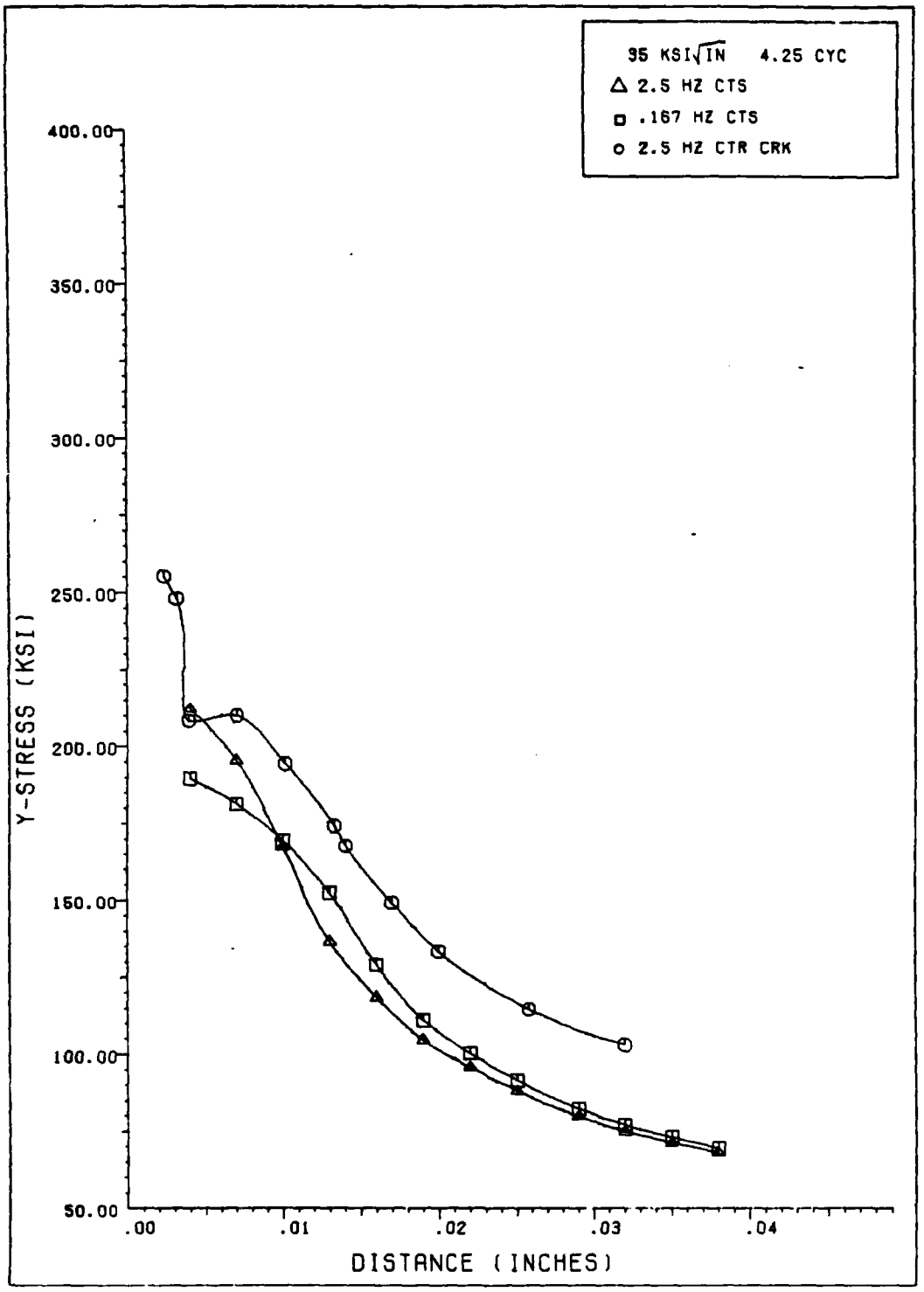

FIG 4.13 Y-STRESS IN FRONT OF CRACK (FULL POS LD)

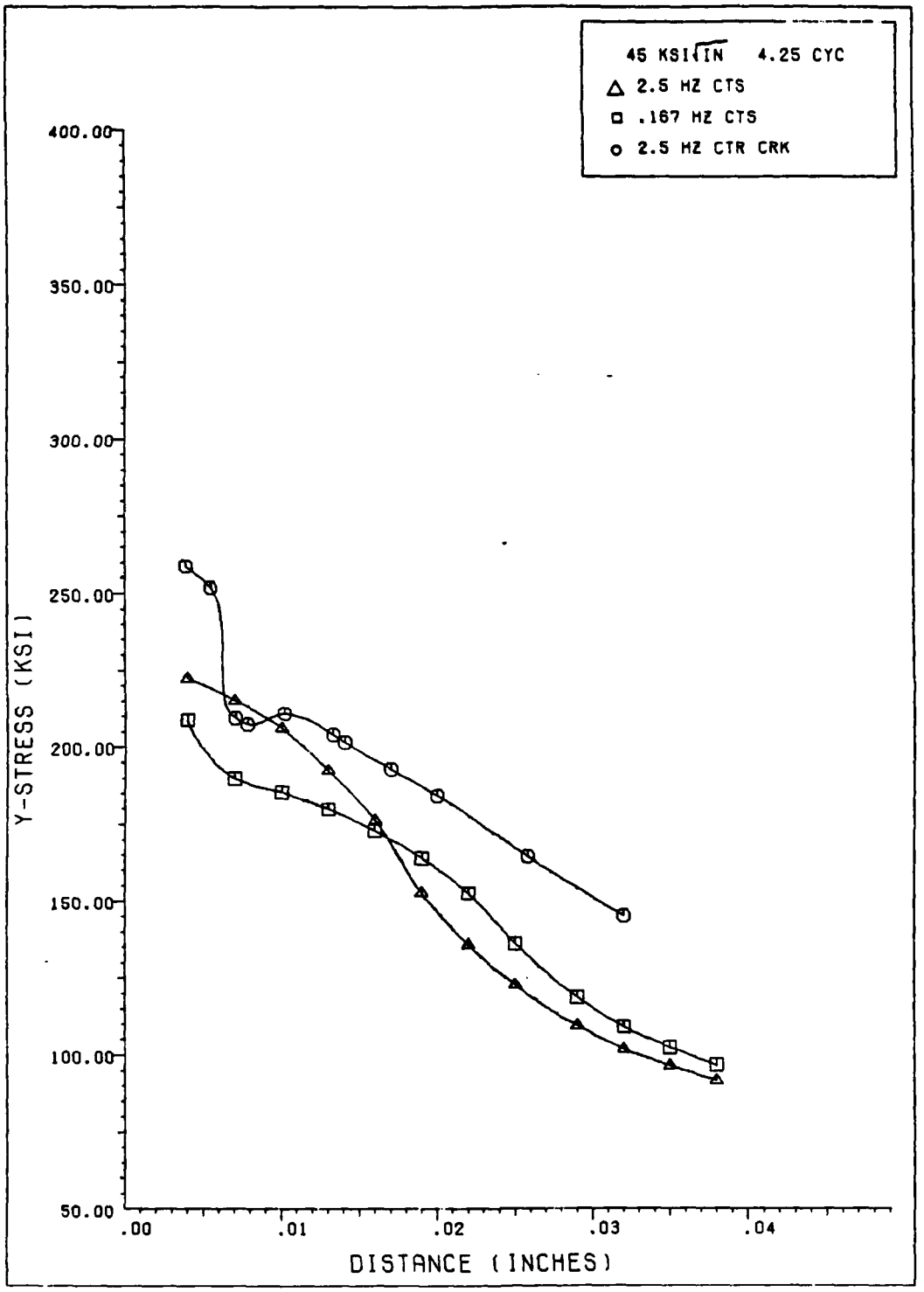

FIG 4.14 Y-STRESS IN FRONT OF CRACK (FULL POS LD)

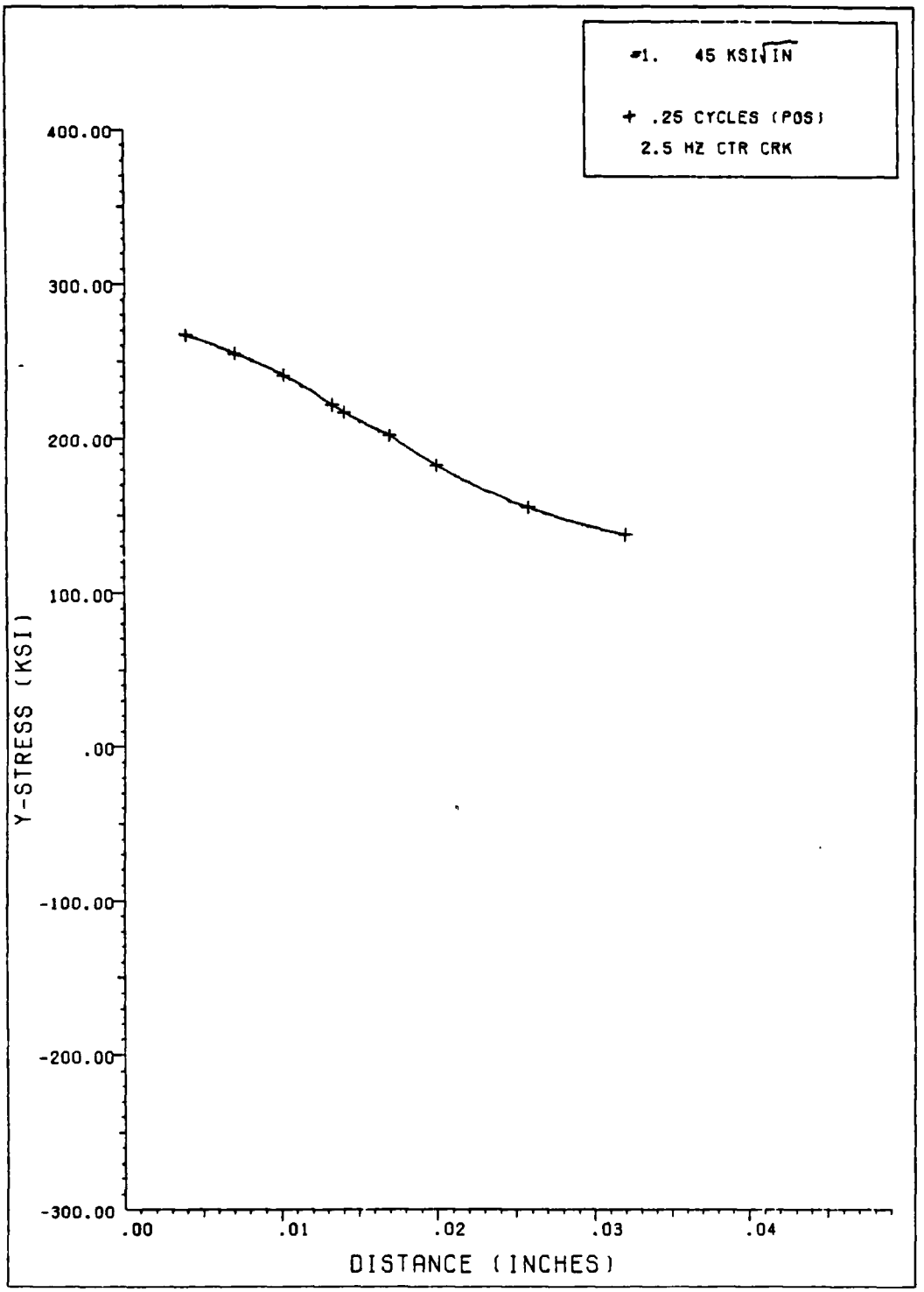

FIG 4.15 Y-STRESS IN FRONT OF CRACK

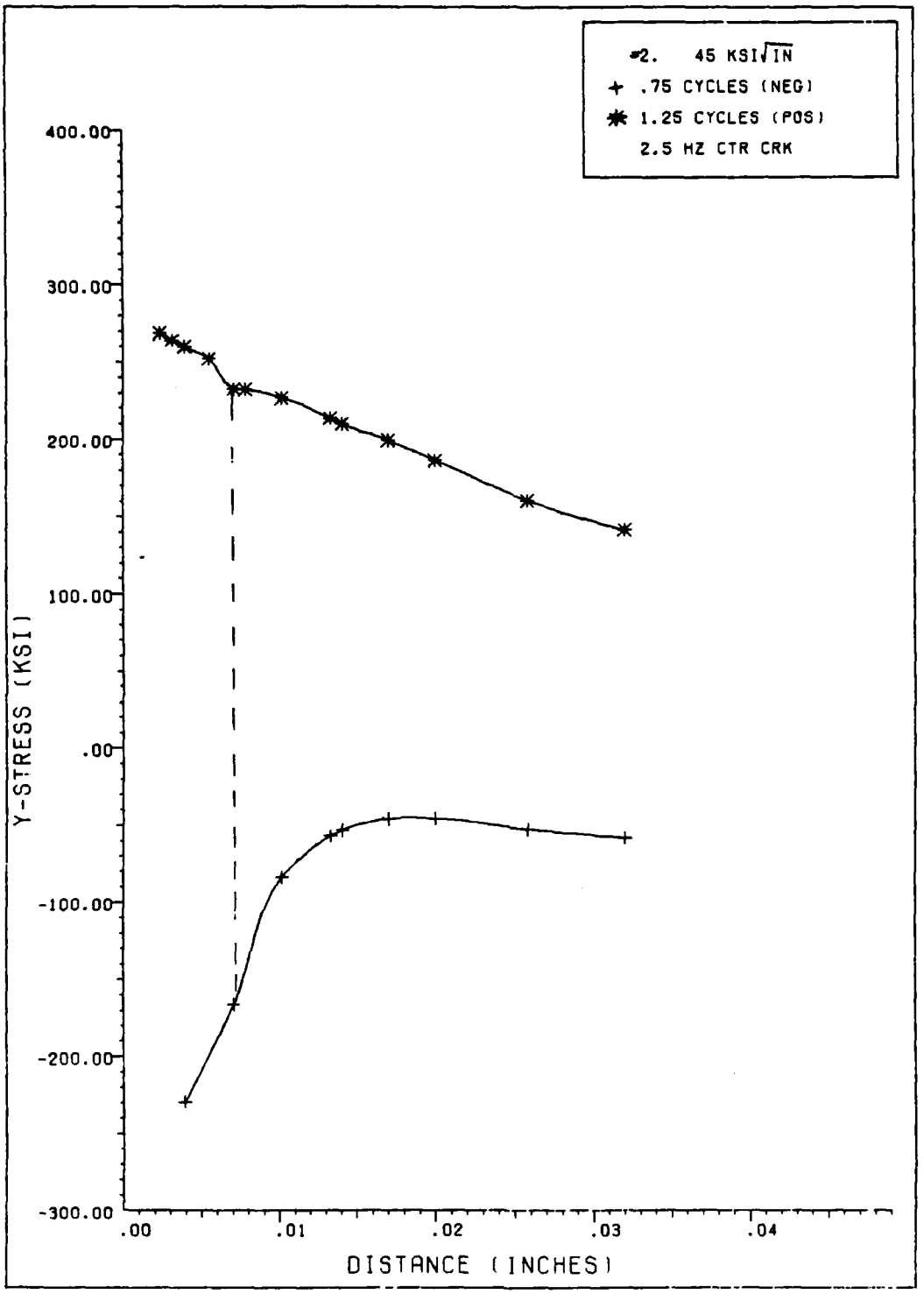

FIG 4.16 Y-STRESS IN FRONT OF CRACK

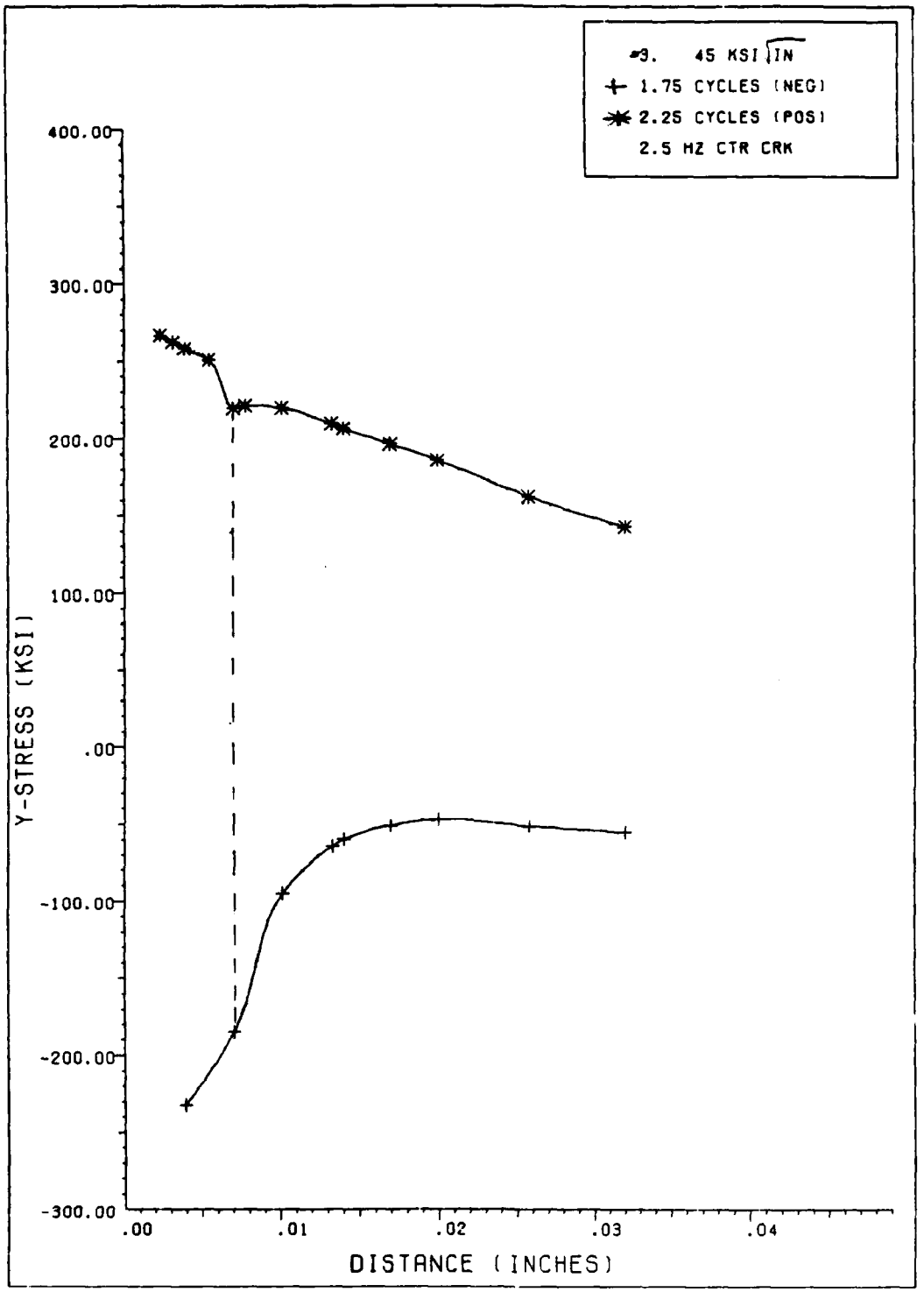

FIG 4.17 Y-STRESS IN FRONT OF CRACK

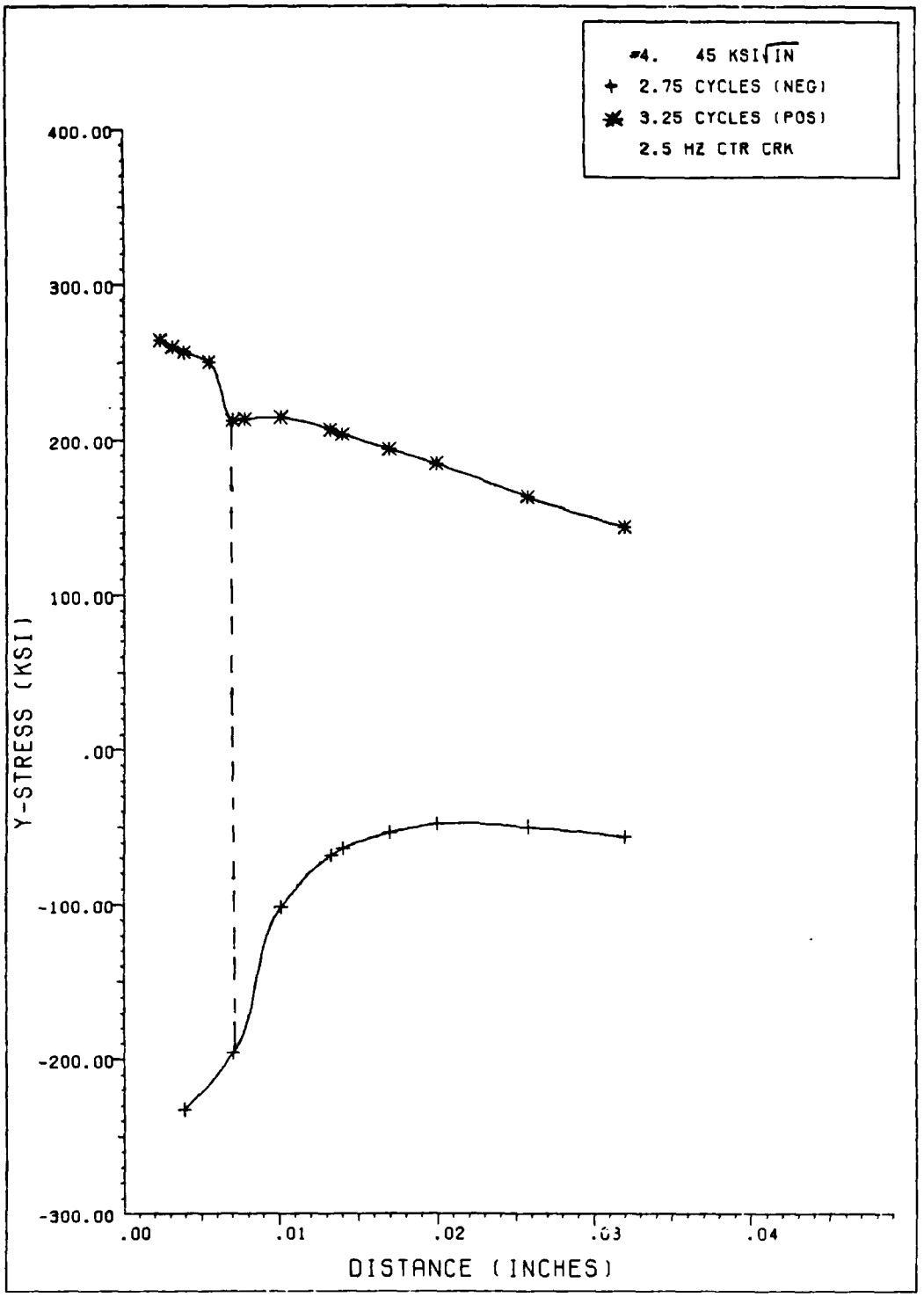

FIG 4.18 Y-STRESS IN FRONT OF CRACK

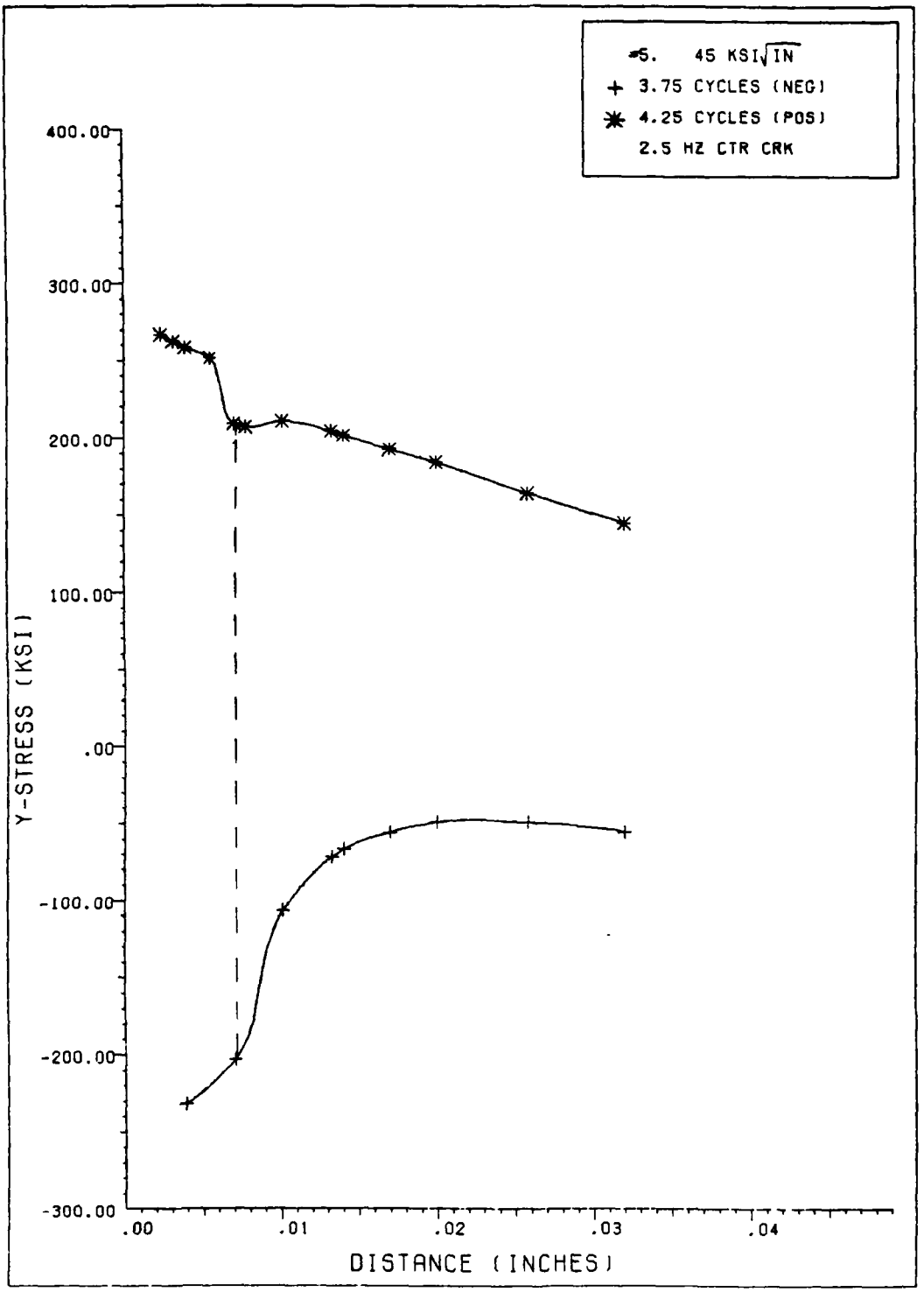

FIG 4.19 Y-STRESS IN FRONT OF CRACK

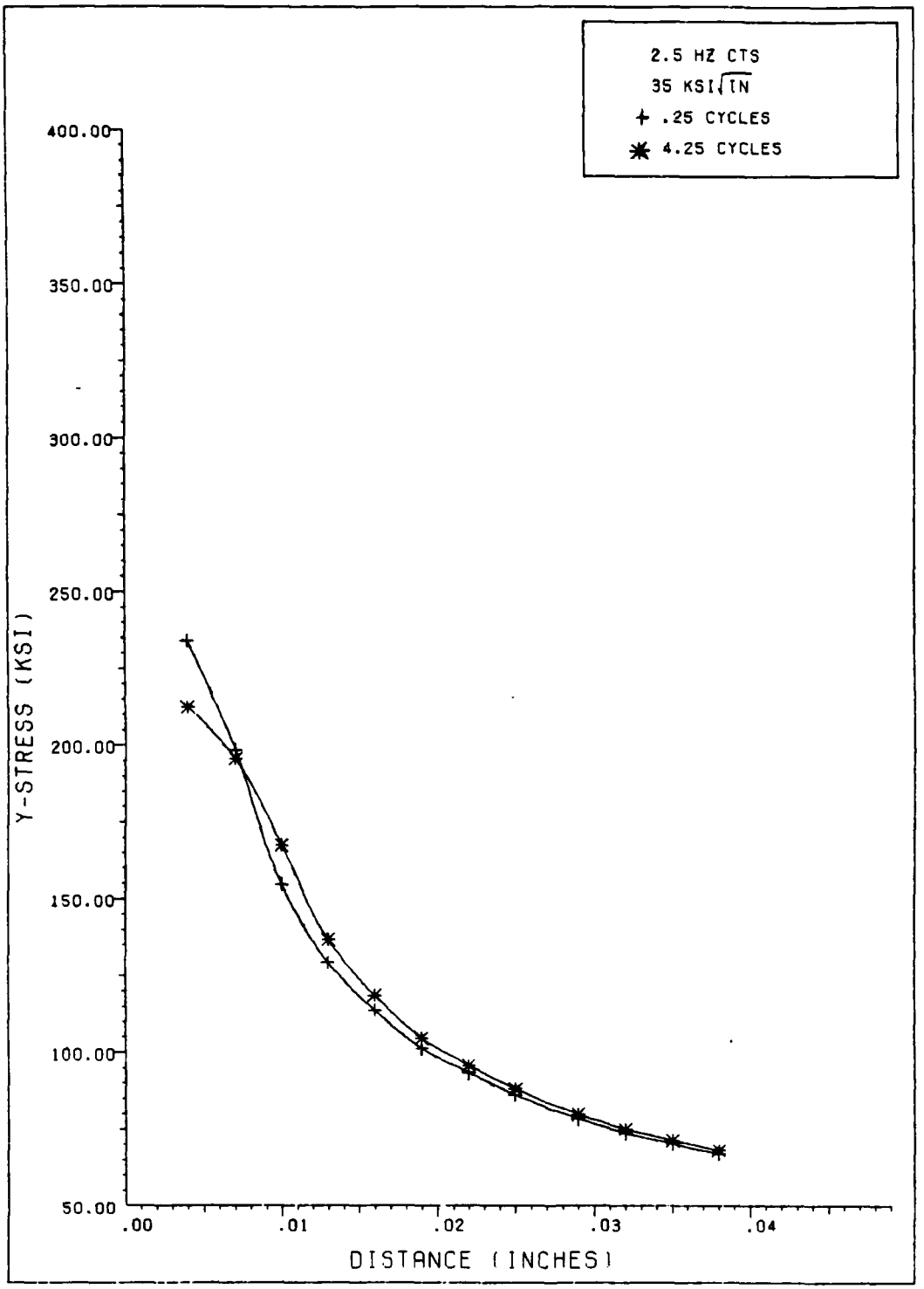

FIG 4.20 Y-STRESS IN FRONT OF CRACK (FULL POS LD)

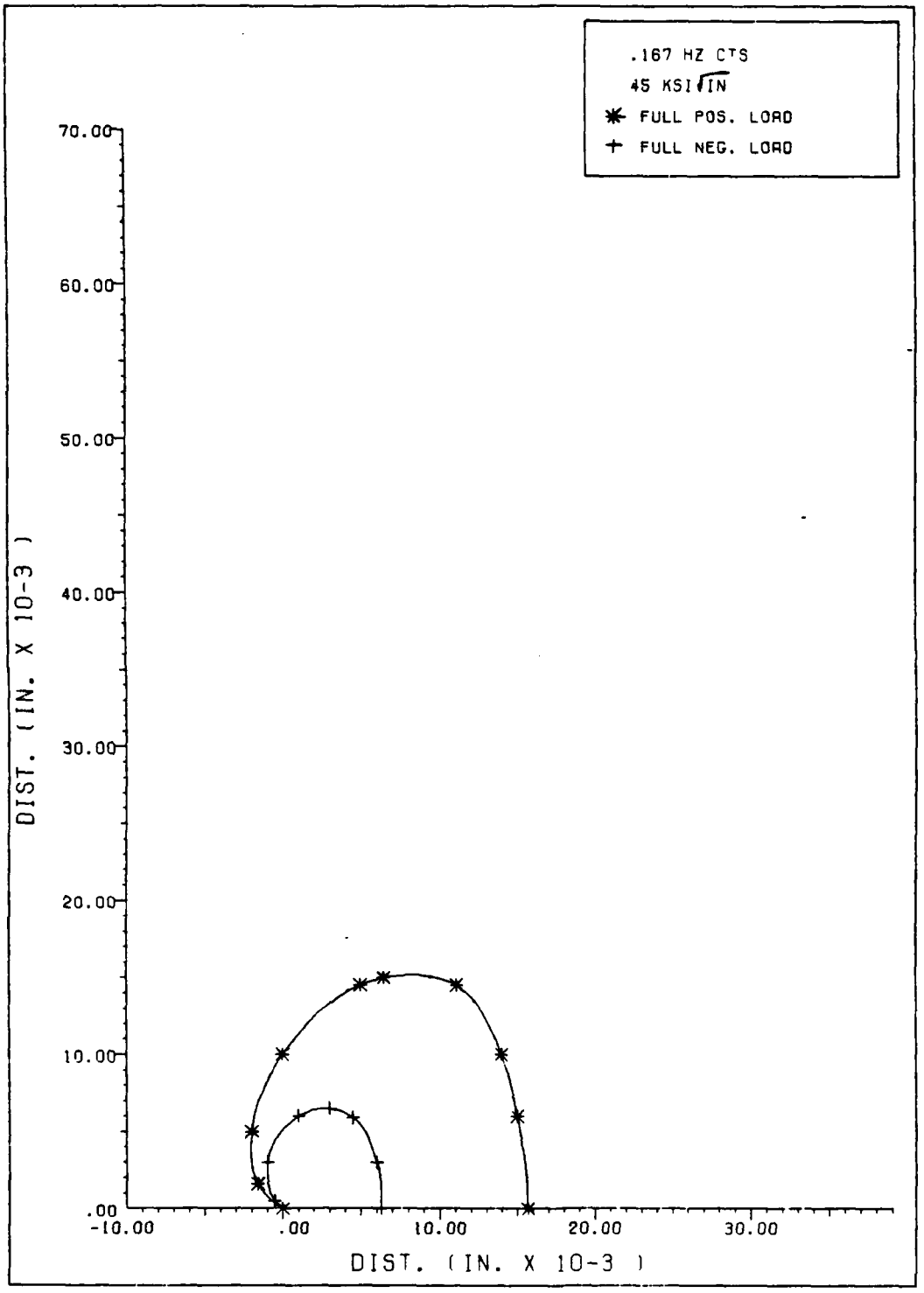

FIG 4.34 REGION OF PLASTIC STRAINING

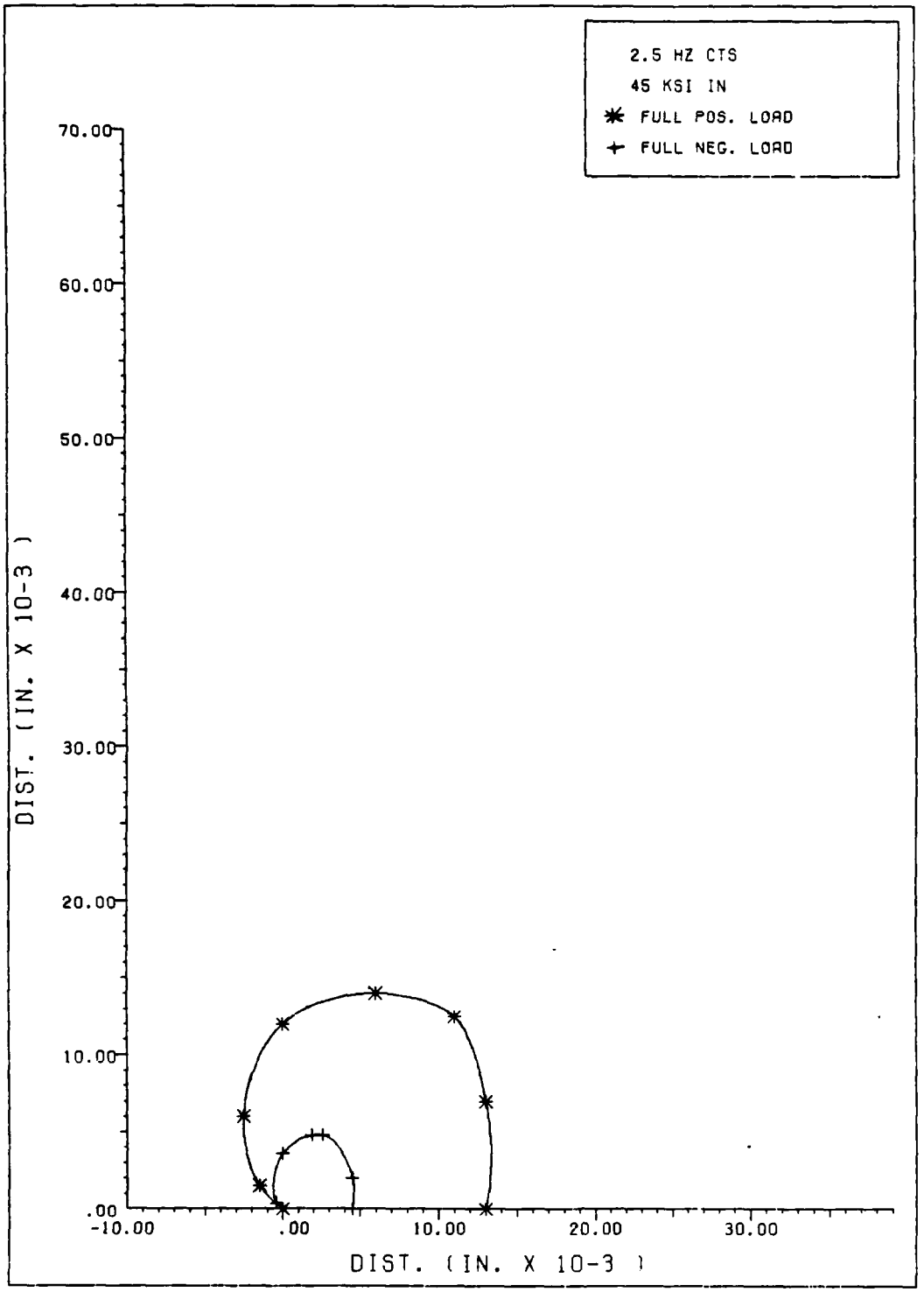

FIG 4.33 REGION OF PLASTIC STRAINING

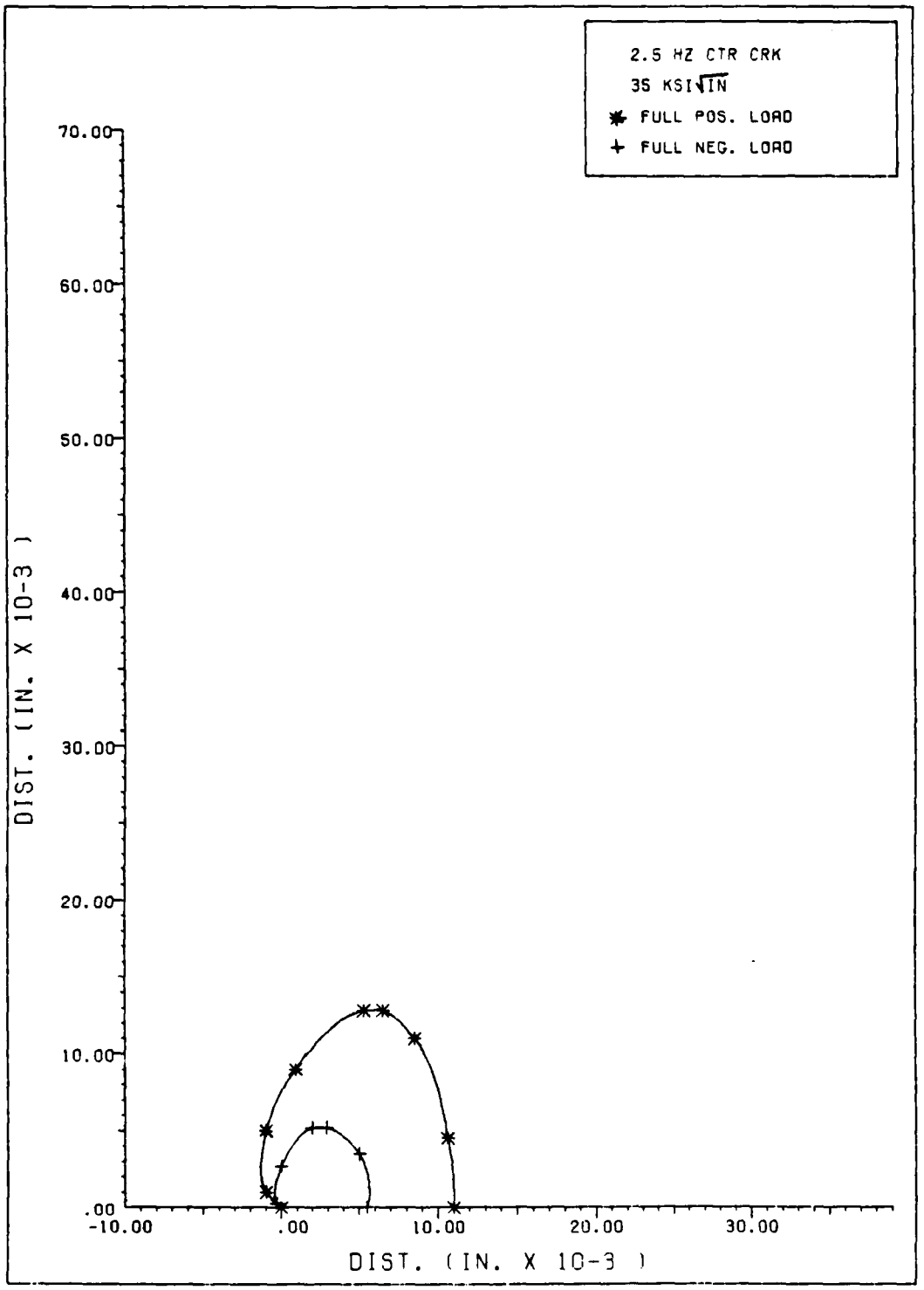

FIG 4.32 REGION OF PLASTIC STRAINING

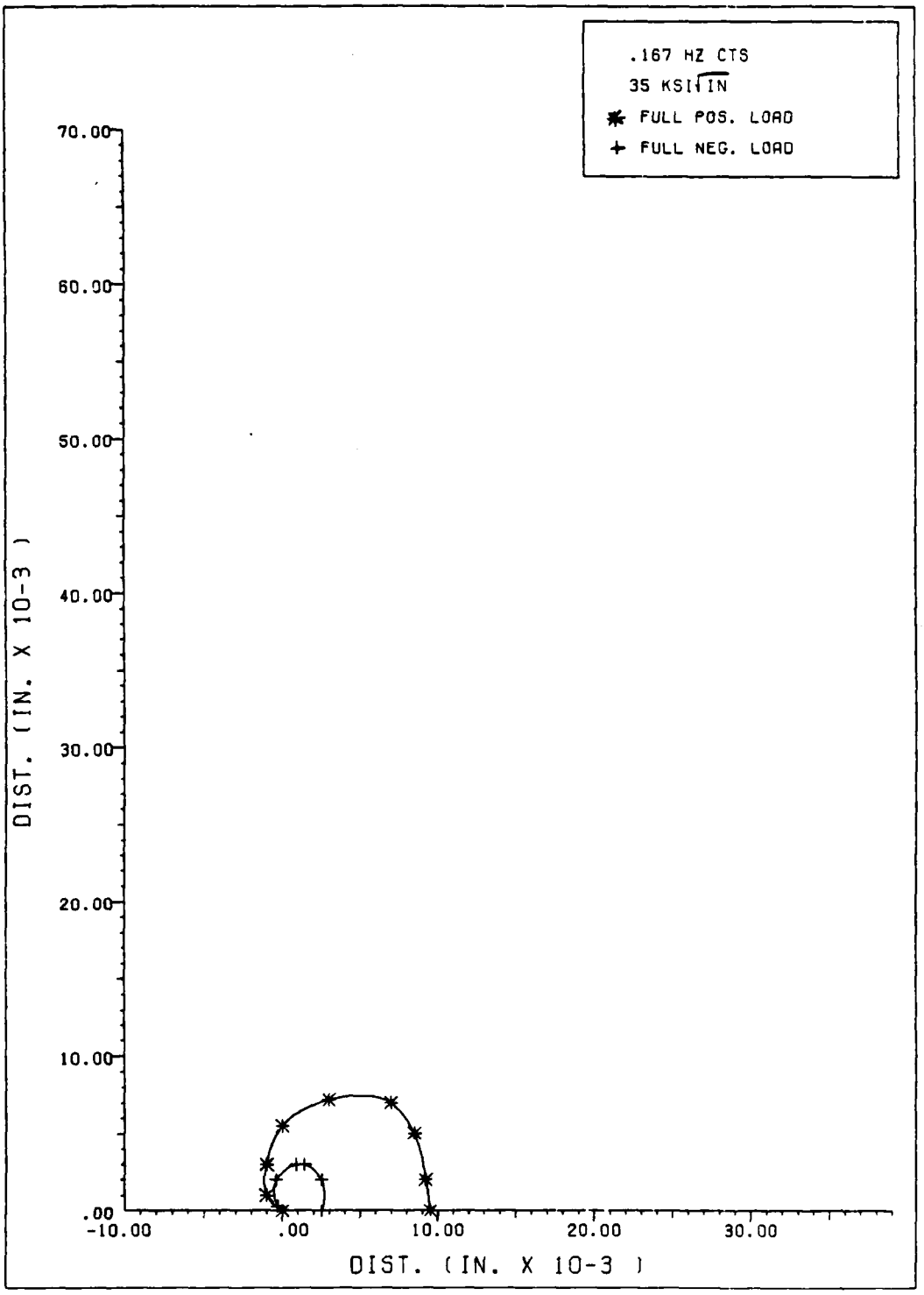

FIG 4.31 REGION OF PLASTIC STRAINING

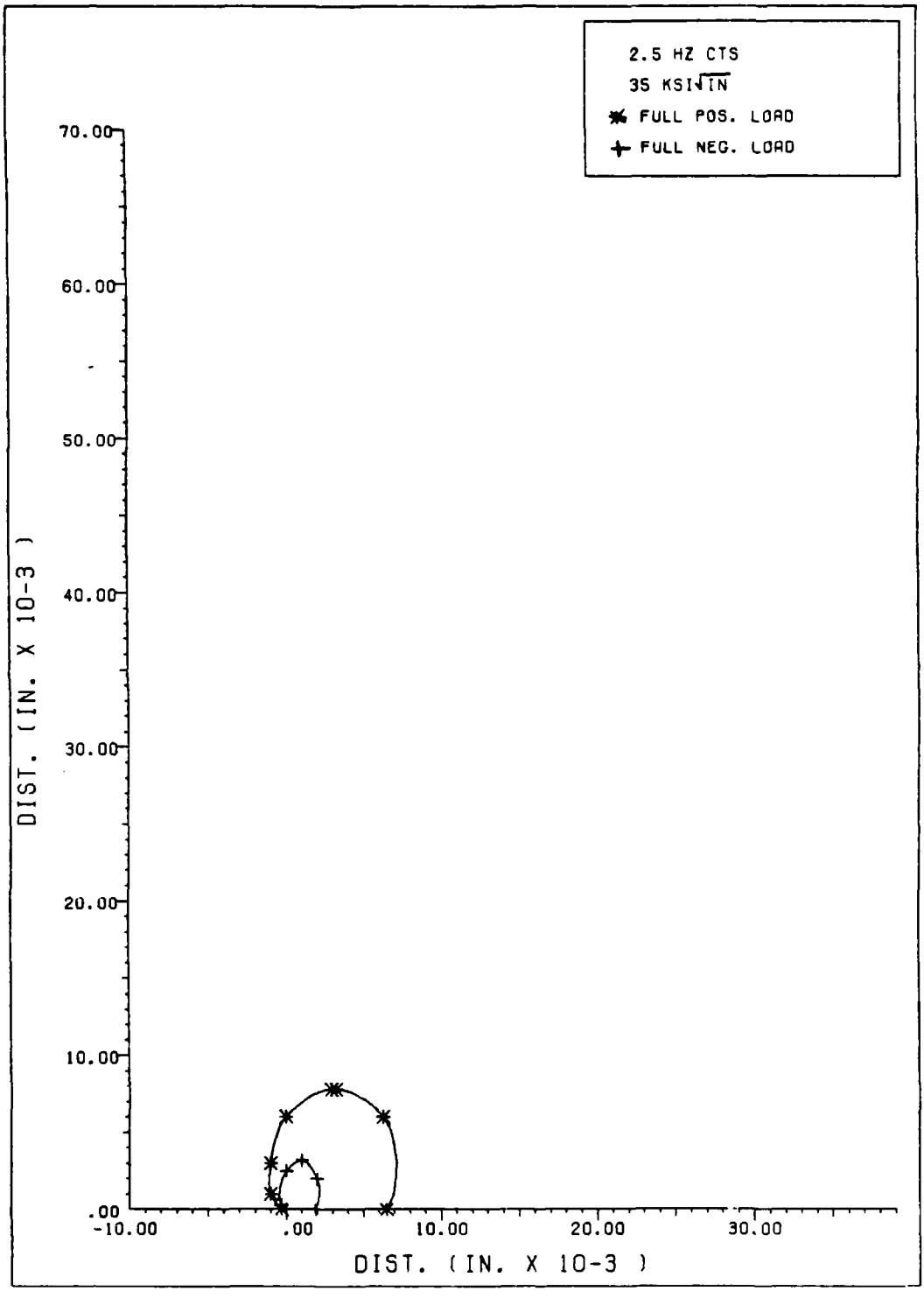

FIG 4.30 REGION OF PLASTIC STRAINING

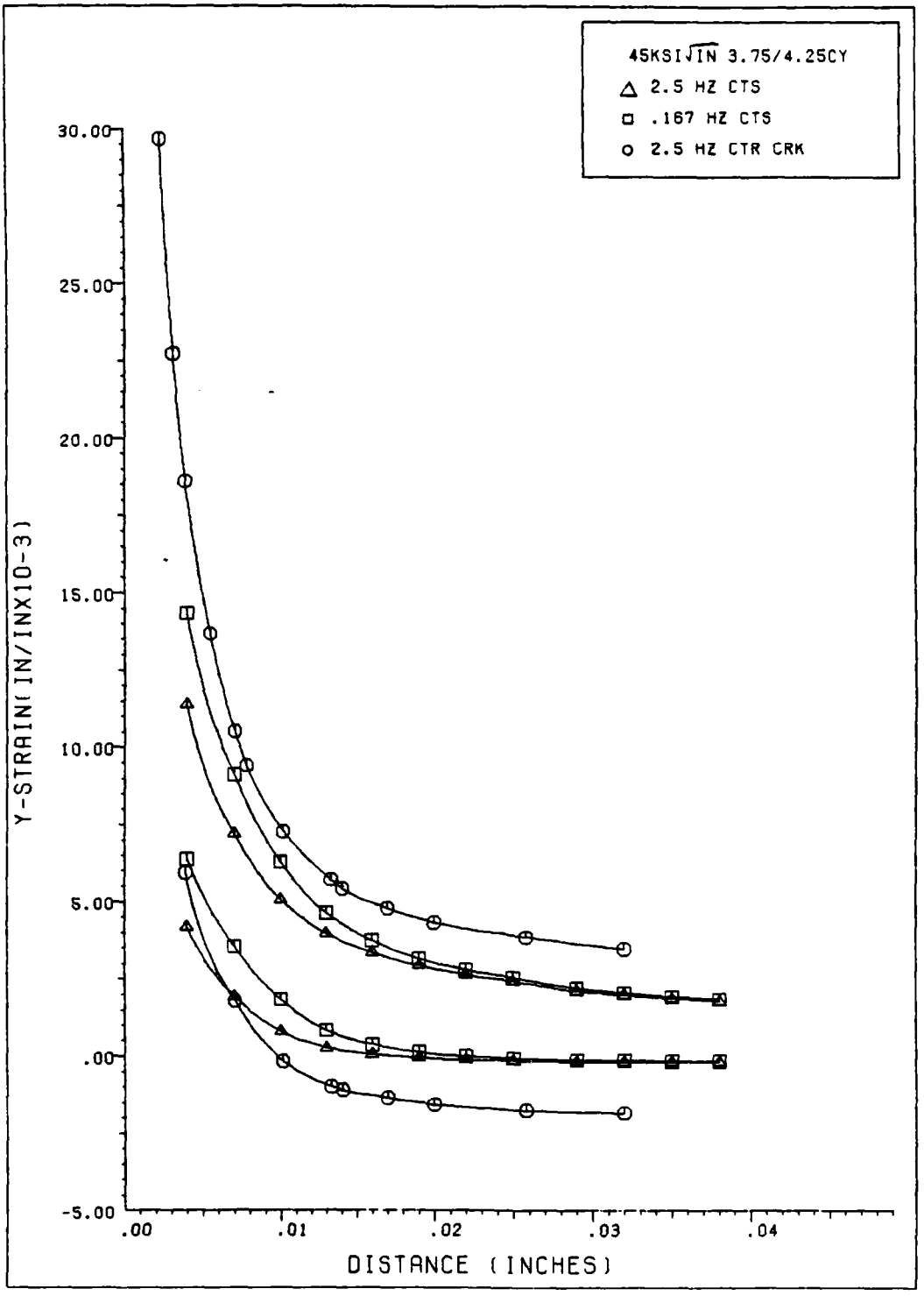

FIG. 4.29 Y-STRAIN IN FRONT OF CRACK TIP

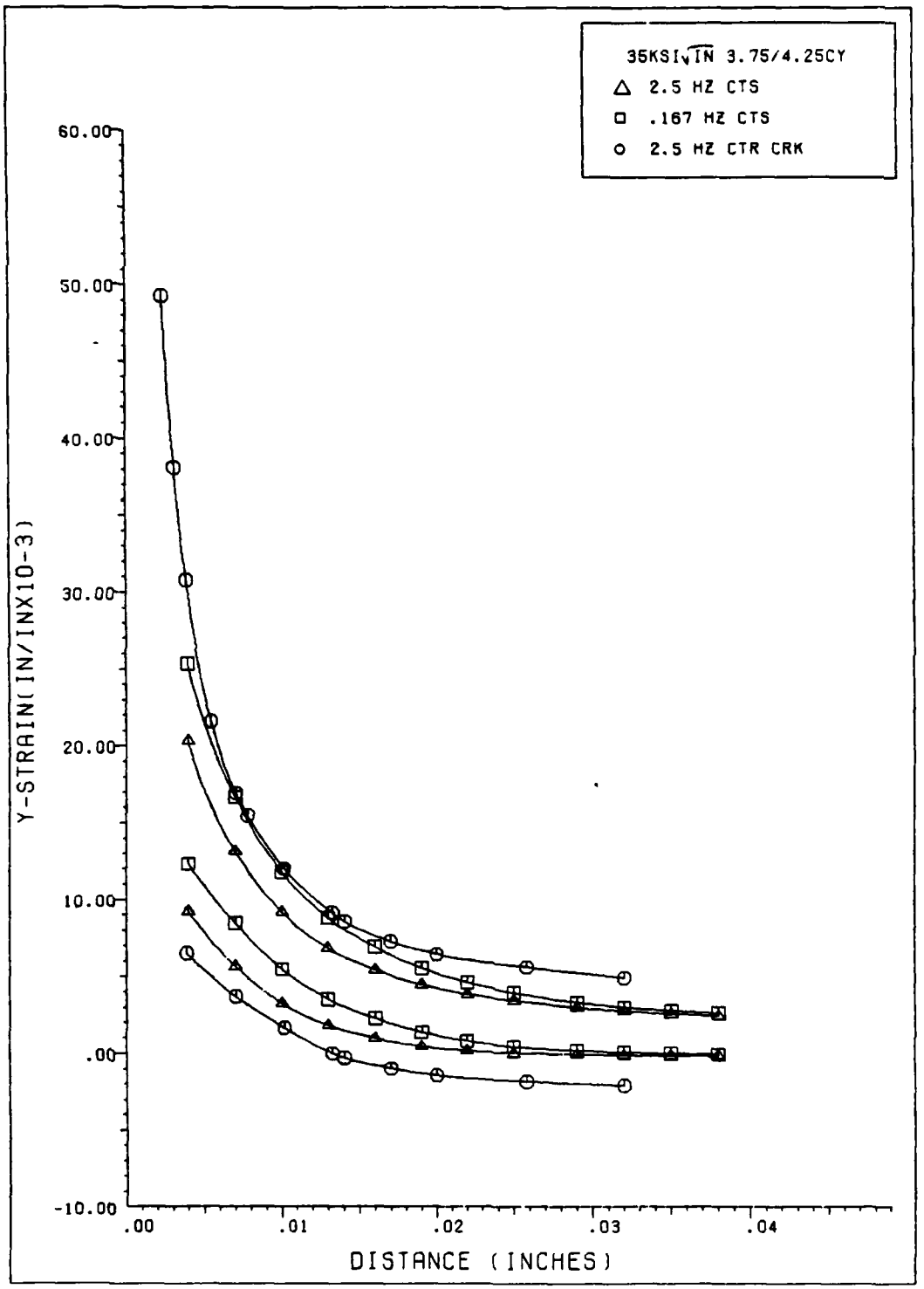

FIG. 4.28 Y-STRAIN IN FRONT OF CRACK TIP

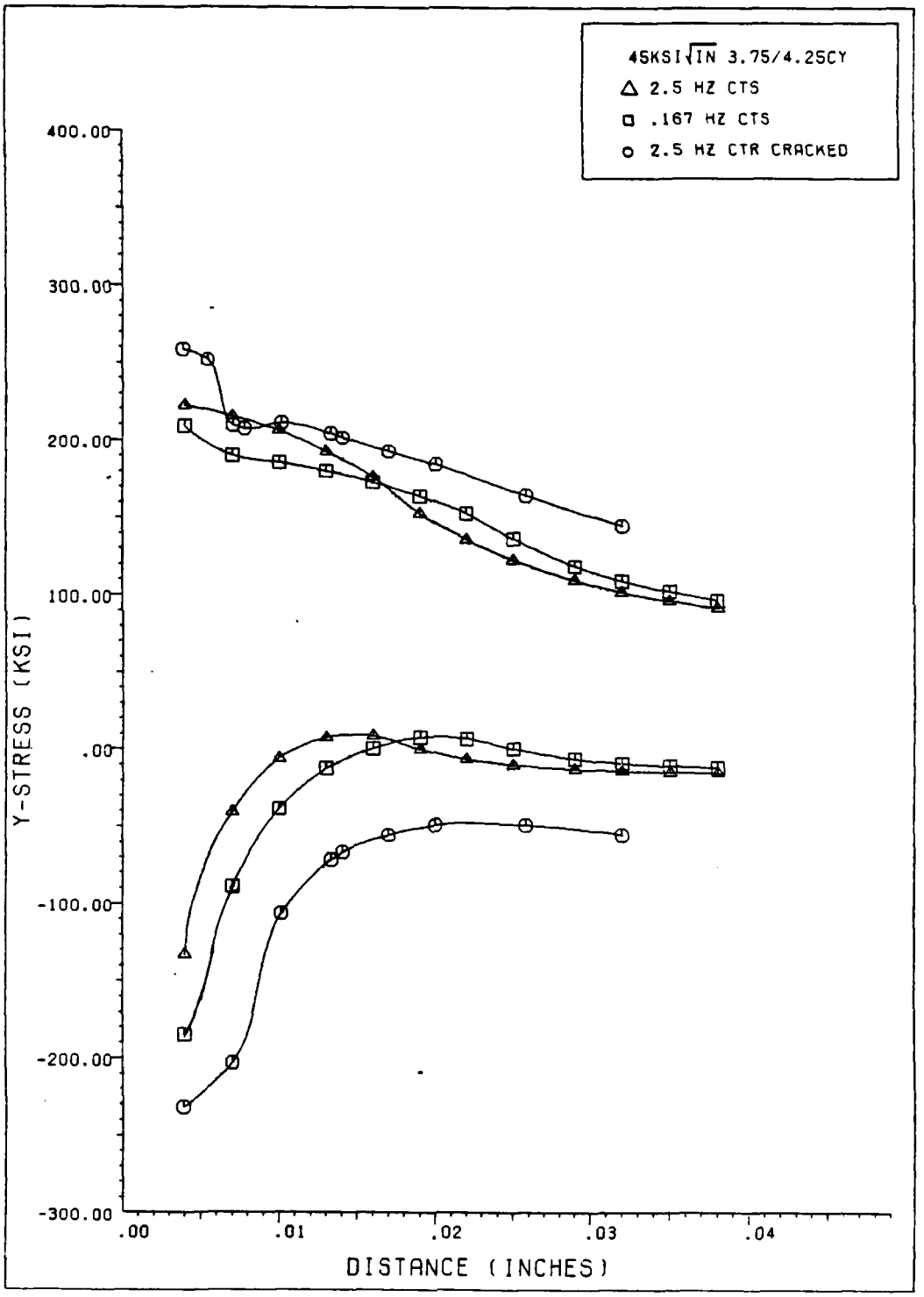

FIG. 4.27 Y-STRESS IN FRONT OF CRACK TIP

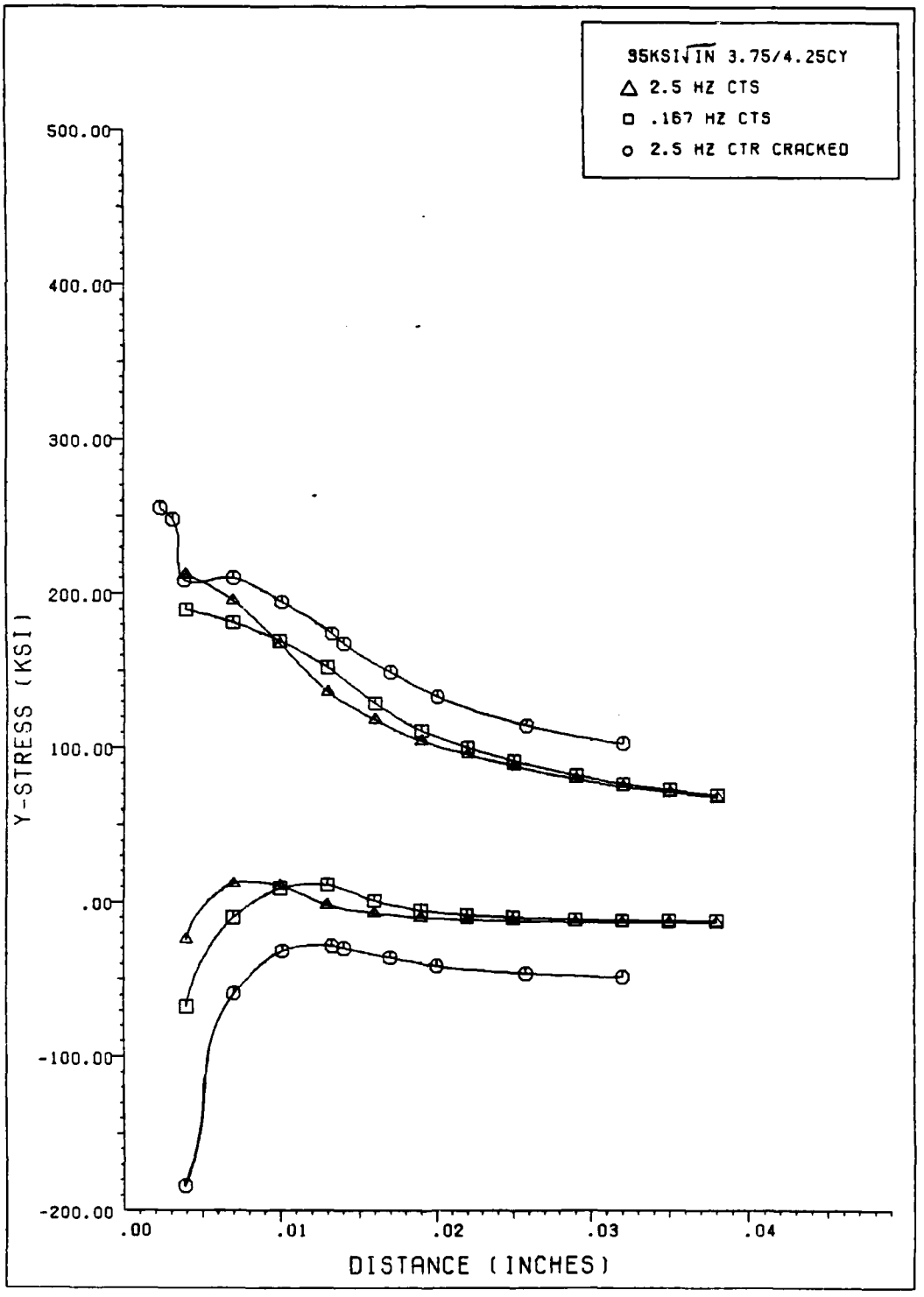

FIG. 4.26 Y-STRESS IN FRONT OF CRACK TIP

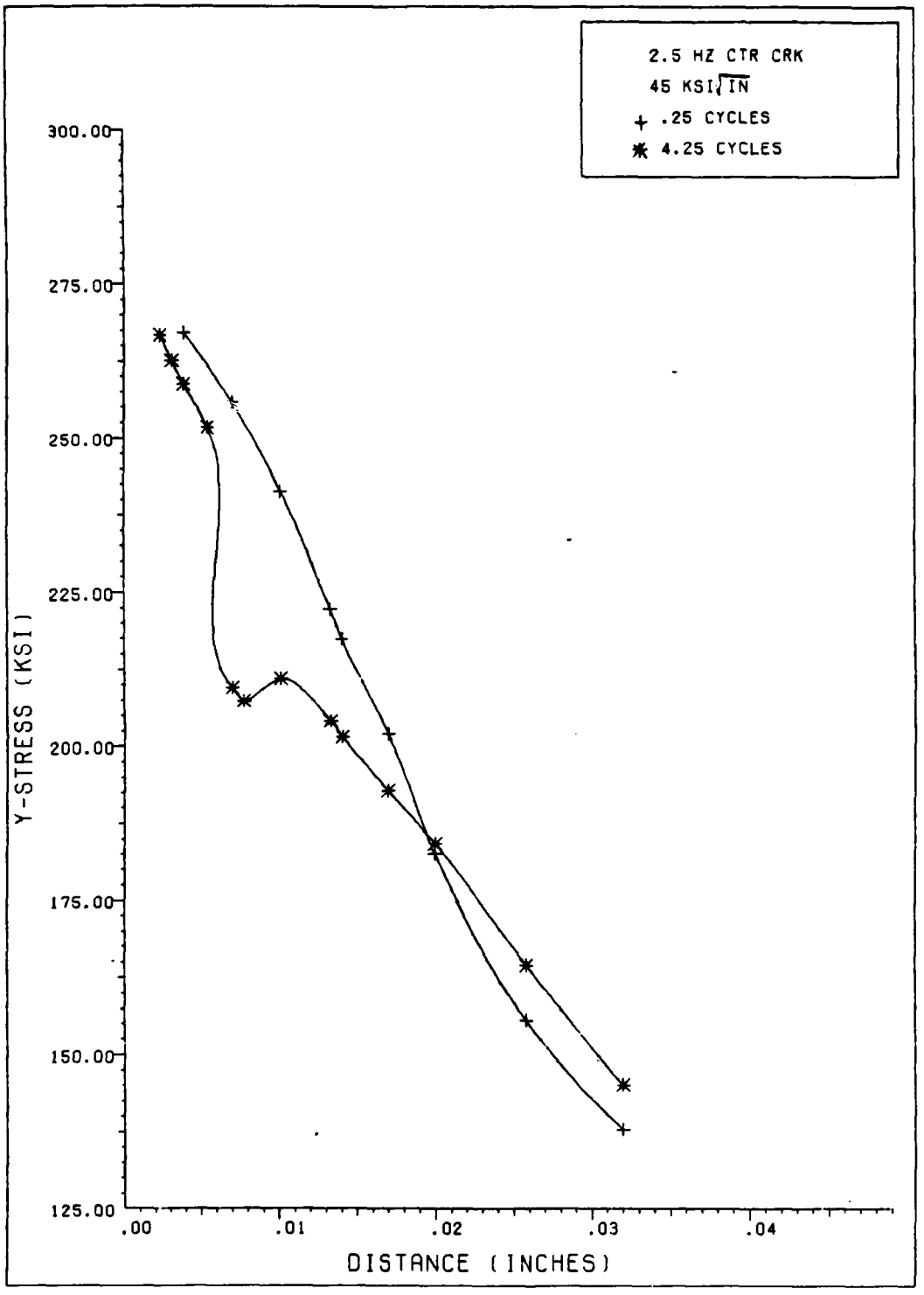

FIG 4.25 Y-STRESS IN FRONT OF CRACK (FULL POS LD)

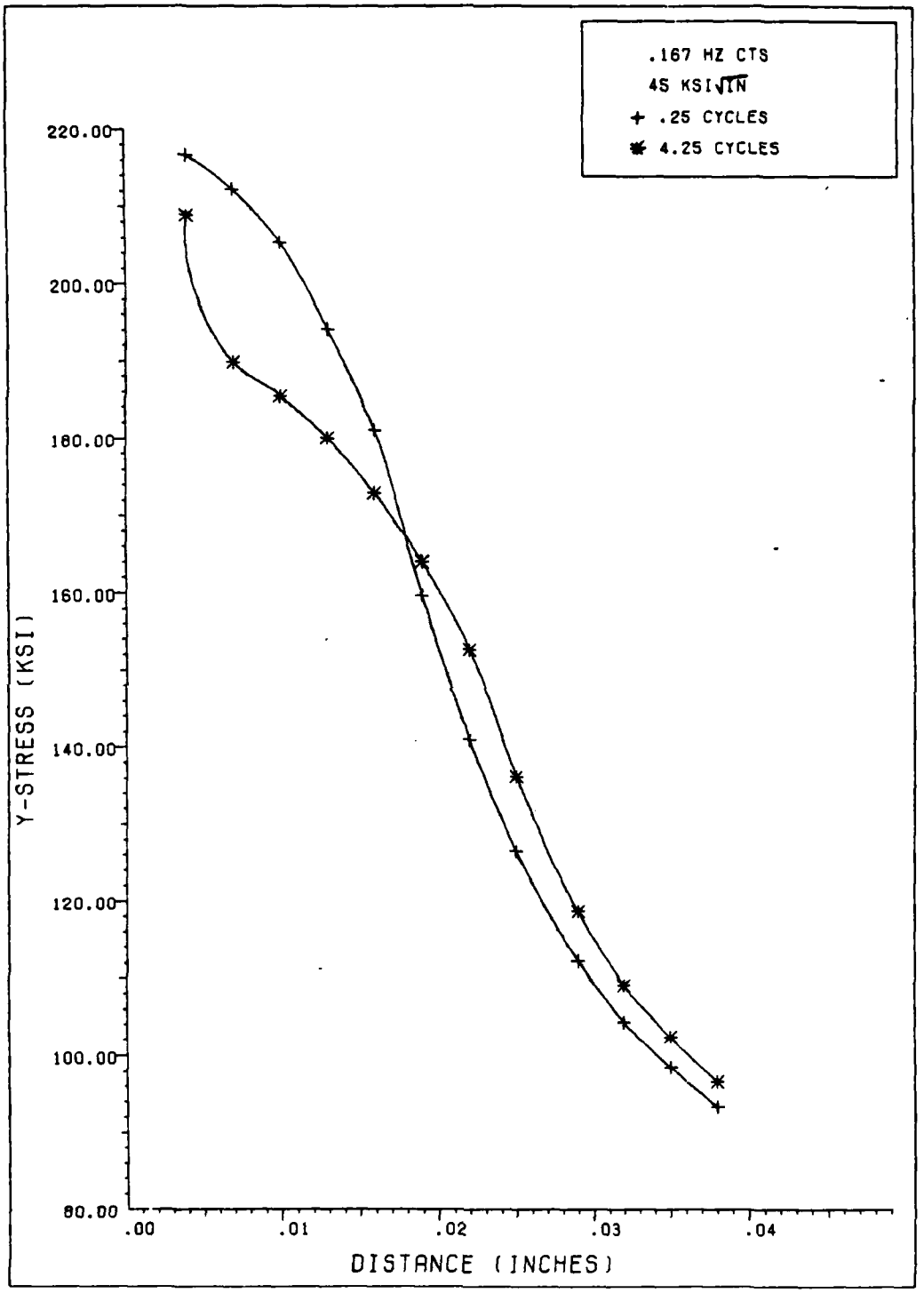

FIG 4.24 Y-STRESS IN FRONT OF CRACK (FULL POS LD)

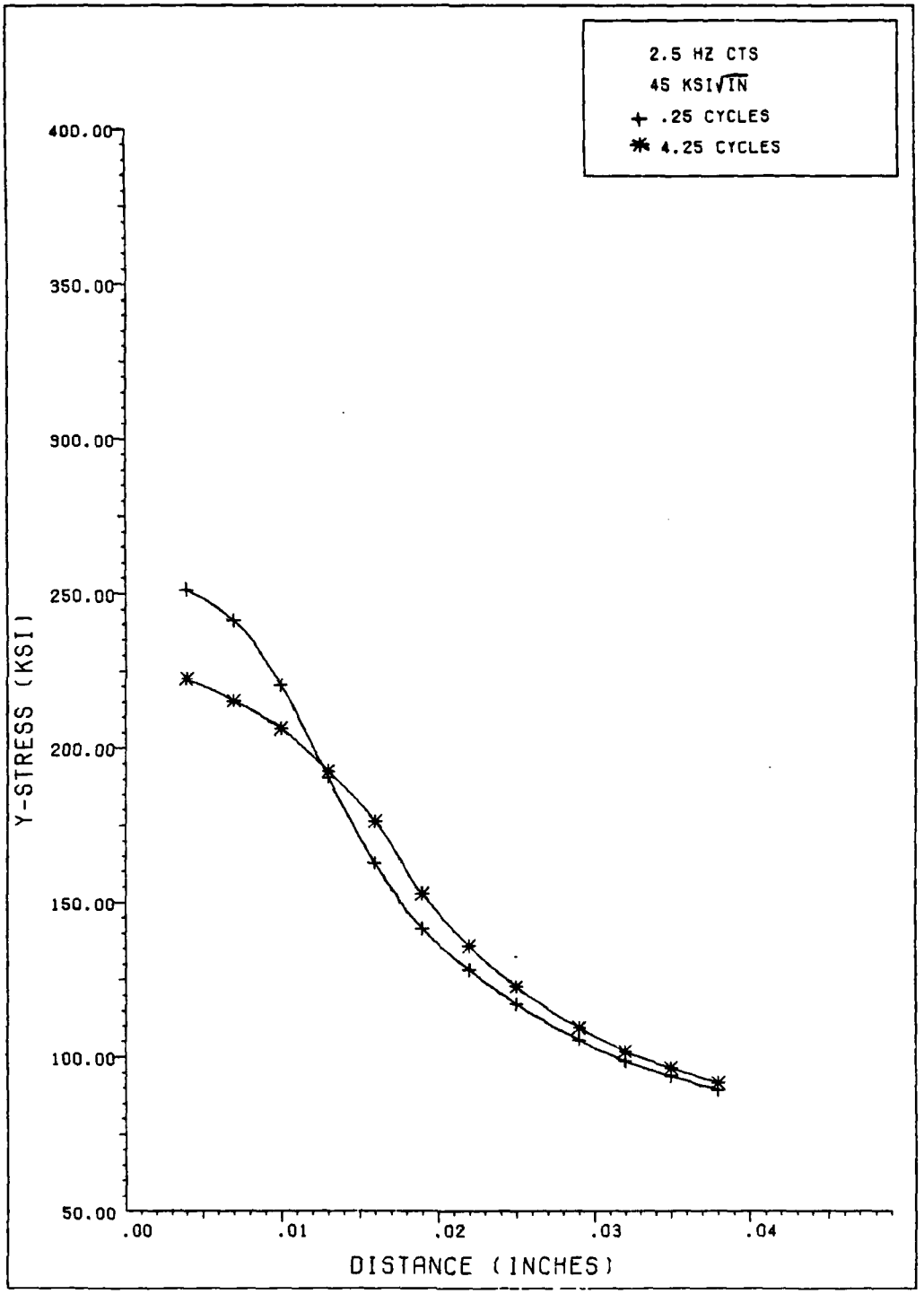

FIG 4.23 Y-STRESS IN FRONT OF CRACK (FULL POS LD)

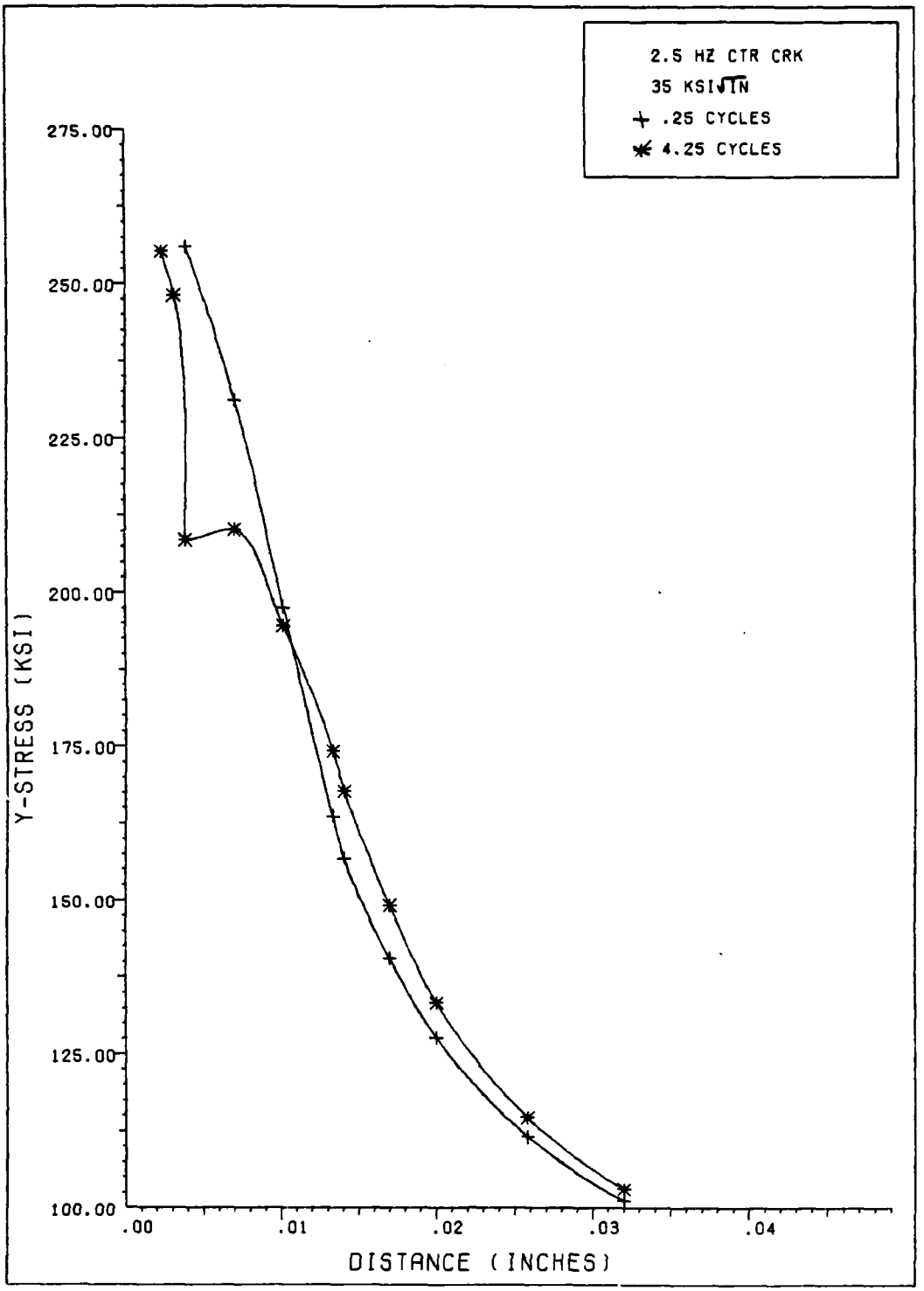

FIG 4.22 Y-STRESS IN FRONT OF CRACK (FULL POS LD)

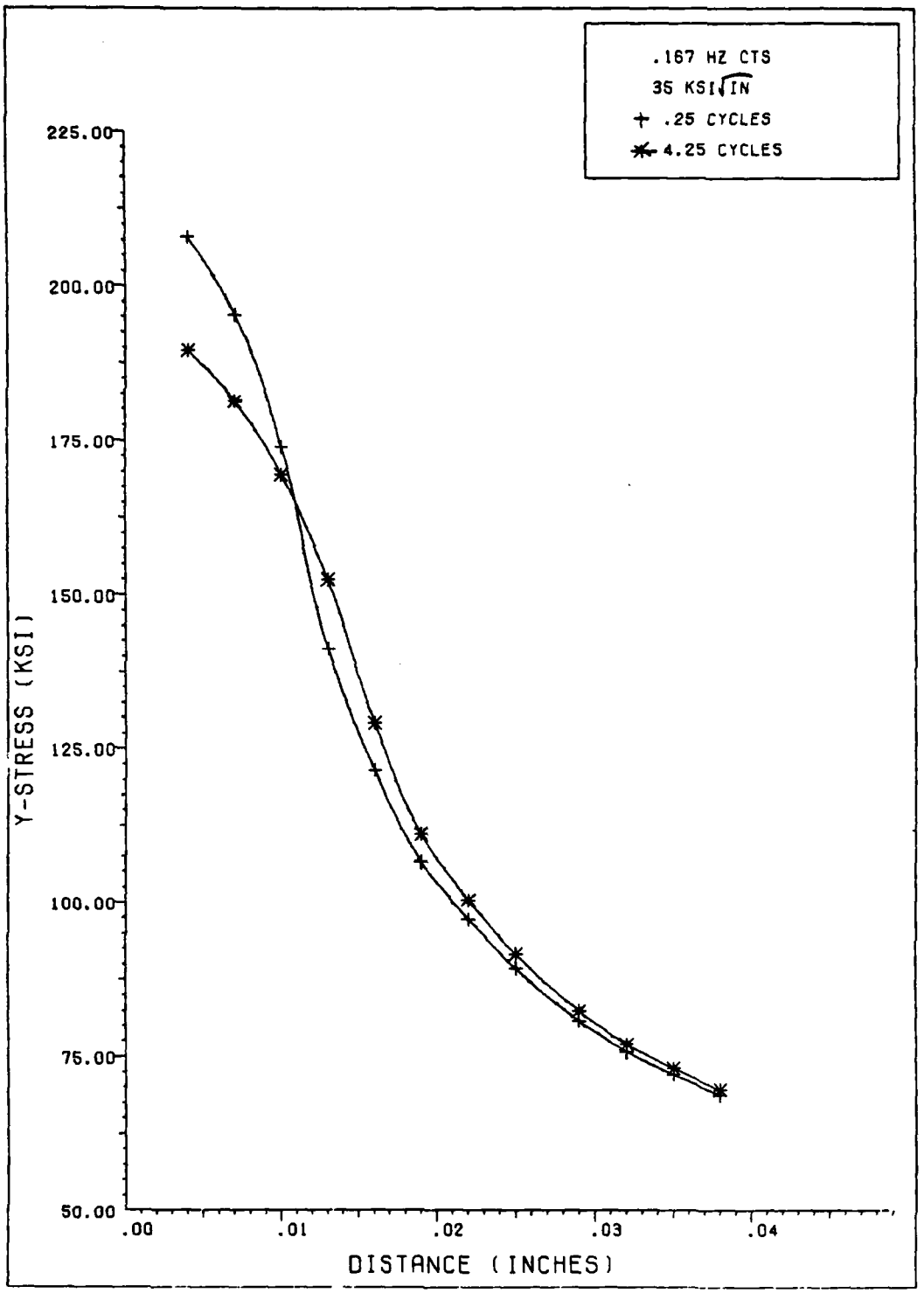

FIG 4.21 Y-STRESS IN FRONT OF CRACK (FULL POS LD)

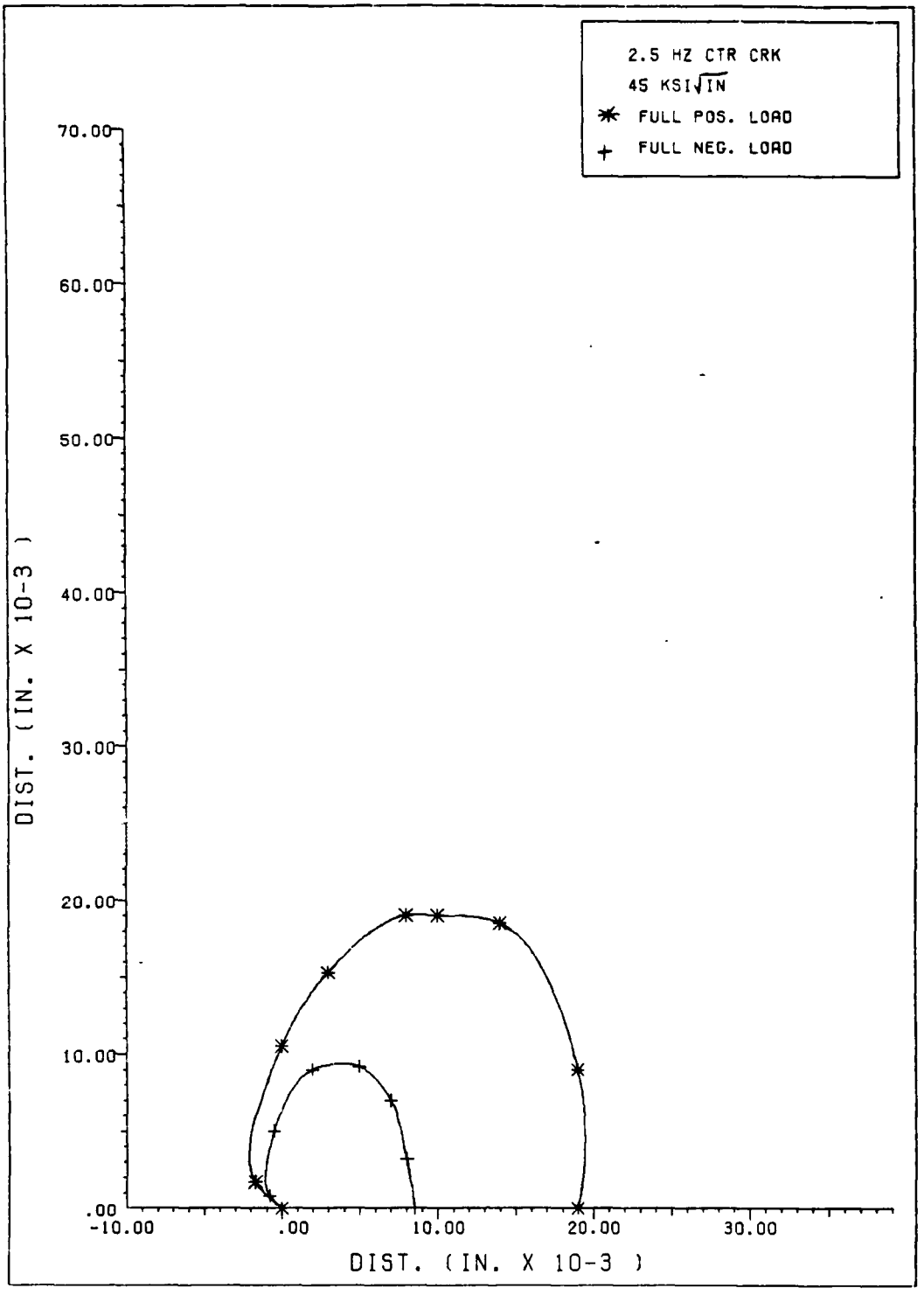

FIG 4.35 REGION OF PLASTIC STRAINING

V. Conclusions

The following conclusions for IN-100 at 1350° F can be made relative to the work carried on within the study:

1. None of the three cases, at either 35 or 45 ksi$\sqrt{in}$, close completely in the region immediately behind the crack tip, even at full negative load. This phenomenon is a result of the large region of plastic strain formed during full positive load.

2. As the number of cycles increase and the region of plastic strain fully develops, slightly less closure occurs behind the crack tip.

3. As K_I is increased, the region of plastic strain grows, and significantly less closure occurs behind the crack tip.

4. The amount of closure for the center cracked specimen is greater than both CTS cases, but significantly, it does not close all the way.

5. The size of the plastically strained region at the crack tip is a major factor determining the amount of closure behind the crack tip. Load and specimen geometry, in the particular case of the center cracked specimen as compared with both CTS cases, has an overriding influence on closure. Furthermore, due to the uniform loading in the center cracked specimen, it experienced a wider range of stresses and strains in both compression and tension throughout the material.

6. Maximum stresses in front of the crack tip decrease and approximately stabilize at a lower value after 5 cycles. This is a result of the time dependent plastic strain and the redistribution of stresses.

7. The same stress intensity factor, K_I, does not produce the same stresses near the crack tip when applied to different geometries of frequencies. The differences increase as K_I increases and/or as the number of cycles increases.

8. Lower maximum stresses and increased total strain in front of the crack tip are achieved when a lower cyclic load frequency is used. This is the characteristic of load rate sensitivity, which is due to the redistribution of stresses through time-dependent plastic strain.

9. After cycling at a -1.0 R-ratio, a discontinuity, or small region of significantly lower stress in the stress field in front of the crack tip, develops. This is a result of residual compressive stresses at the discontinuity location caused by negative plastic straining during full negative load. This phenomenon occurred only in the center cracked specimen at 35 and 45 ksi$\sqrt{in}$ and the 45 ksi$\sqrt{in}$ CTS at .167 Hz. Also, these cases exhibited the most amount of negative plastic straining during full negative load.

10. An analysis of the region undergoing plastic straining near the crack tip, at full positive and full

negative loads, verifies that the discontinuity is a result of residual compressive stress.

11. The region of compressive plastic straining during full negative load is approximately one fourth the area of the region tensile plastic straining during full positive load.

Bibliography

1. Hill, R. J., Reimann, W. H., Ogg, J. S., "A Retirement-For-Cause Study of an Engine Turbine Disk," AFWAL-TR-81-2984, Wright Patterson AFB, Ohio, 1981.

2. Harris, J. A., Jr., Sims, D. L., Annis, C. G., Jr., "Concept Definition: Retirement for Cause of F-100 Rotor Components," AFWAL-TR-80-4118, Wright Patterson AFB, Ohio, 1980.

3. Hopkins, S. W., Besuner, P. M., Rau, C. A. Jr., Allison, D. W., Eischen, J. W., Robinson, J. N., and Wachob, H. F., "Cost/Risk Analysis for Disk Retirement," AFWAL TR-83-4089, Wright Patterson AFB, Ohio, 1983.

4. Larsen, J. M. and Nicholas, T., "Load Sequence Crack Growth Transients in a Superalloy at Elevated Temperature," Fracture Mechanics: Fourteenth Symposium, Vol. II, Testing and Applications, ASTM STP 791, J. C. Lewis and G. Sines, Eds., American Society for Testing and Materials, 1983, pp. 536-552.

5. Collins, J. A., Failure of Materials in Mechanical Design, New York: John Wiley & Sons, 1981.

6. Hinnerichs, T. D., "Viscoplastic and Creep Crack Growth Analysis by the Finite Element Method," AFWAL-TR-80-4140, Wright Patterson AFB, Ohio, 1981.

7. Hinnerichs, T., Nicholas, T., and Palazotto, A., "A Hybrid Experimental-Numerical Procedure for Determining Creep Crack Growth Rates," Journal of Engineering Fracture Mechanics, Vol. 16, No. 2, pp. 265-277, 1982.

8. Hinnerichs, T. D., Palazotta, A. N., Nicholas, T., "Evaluation of Creep Crack Growth Criteria for IN-100 at Eleveted Temperature," AIAA Journal, Vol. 21, No. 3, pp. 438-445, March 1983.

9. Smail, J. W., "The Viscoplastic Crack Growth Behavior of a Compact Tension Specimen Using the Bodner-Partom Flow Law," Journal of Engineering Fracture Mechanics, Vol. 19: 1, pp. 137-158 (1984).

10. Keck, J. E., "The High Temperature Viscoplastic Fatigue Behavior of a Compact Tension Specimen Using the Bodner-Partom Flow Law," M. S. Thesis, Department of Aeronautics and Astronautics, Air Force Institute of Technology, Wright-Patterson AFB, Ohio, 1982.

11. Wilson, R. E. and Palazotto, A. N., "Viscoplastic Fatigue in a Superalloy at Elevated Temperature Considering a Zero Mean Stress," presented at the 25th AIAA structures, Structural Dynamics and Material Conference, Published in the Conference Proceedings as Paper, AIAA-84-0931: pp. 264-274 (1984).

12. Stouffer, D. C., "A Constitutive Representation for IN-100," AFWAL-TR-81-4039, Wright Patterson AFB, Ohio, 1981.

13. Bodner, S. R., Partom, I., and Partom, Y., "Uniaxial Cyclic Loading of Elastic-Viscoplastic Materials," Journal of Applied Mechanics, Vol. 46: pp. 805-810 (December, 1979).

14. Zienkiewicz, O. C., The Finite Element (Third Edition), New York: McGraw-Hill Book Company, 1977.

15. Cook, R. D., Concepts and Applications of Finite Element Analysis (Second Edition), New York: John Wiley & Sons, 1981.

16 Owen, D. R. J., and Hinton, E., Finite Elements in Plasticity Theory and Practice, Swansea, U.K.: Pineridge Press Limited, 1980.

17. Clauss, F. J., Engineer's Guide to High-Temperature Materials, Reading, Massachusetts: Addison-Wesley Publishing Company, 1969.

18. Broek, D., Elementary Engineering Fracture Mechanics, Boston: Martinus Nijhoff Publishers, 1983.

19. Smith, C. O., The Science of Engineering Materials, Englewood Cliffs, New Jersey: Prentice-Hall, Inc., 1969.

Appendix A

The computer program, VISCO, modified by Wilson [11] for negative R-ratio cyclic loading was changed in several areas. The changes, while significant to the results of this study, did not interfere with the proven Bodner-Partom viscoplastic computation procedure. This fact was verified by duplicating Wilson's results using this version of VISCO.

The modifications to VISCO in this study can be divided into three major categories: cosmetics, specimen adaptation and output enhancement. Cosmetics included commenting out unused code (00276-00287, 00299, 00300, 00908-00913) and removal of unused subroutines (geom, func and disp). The category of specimen adaptation deals with the integral boundary conditions originally inserted by Wilson [11] to prevent negative displacements along the crack edge during negative cycling (00697-00700). This modification was necessary to represent the center cracked specimen boundary conditions. Further, the center cracked specimen mesh had different elements of interest in front of the crack tip (00864-00865, 00976-00994, 01071-01072). Output enhancement included format changes (01003, 01006, 01008) and output limitation (00936-00939, 00973-00974) which combined to make data more accessible for

analysis. One modification added Z, the Bodner-Partom hardness parameter to the output (00866). The final modification output enhancement turned out to be the most significant.

Due to the nature of this study, result comparison of unique cases, it was critical that output of results could be directed consistently at the precise moment of interest. The original timestep algorithm used to direct output had a built-in inaccuracy which accrued each time results were printed. For example, when the moment of interest was full positive load after two cycles, data at +83.7% load was printed. Further, the subsequent full negative load data was actually based on only -71.5% load. Since this error accrued as cycles increased, output close to desired cyclic load was hard to come by. After two simple modifications: adding line 00253 and changing line 00291 from "TP=0", to the present form, loads, even in the worst case (.167 Hz. CTS), were never off more than 4% of desired load.

```
00001       PROGRAM WILSON(INPUT=0,OUTPUT=0,TAPE5=INPUT,TAPE6=OUTPUT,TAPE7=0,
00002      1TAPE9,TAPE1,TAPE2,TAPE3,TAPE4,TAPE8,TAPE25)
00003 C
00004 C         FINITE ELEMENT ANALYSIS PROGRAM OF TWO DIMENSIONS
00005 C         PLANE STRESS & PLANE STRAIN OPTIONS
00006 C         GAUSS-SEIDEL ITERATION SOLUTION ROUTINE
00007 C         ELEMENT NODES I,J,K, MUST BE NUMBERED COUNTER CLOCKWISE
00008 C       DIMENSION AND COMMON STATEMENTS
00009 C
00010         COMMON /A/AREA(382)
00011         COMMON /NPINV/SXX(235,9),SXY(235,9),SYX(235,9),SYY(235,9)
00012         COMMON /BC/NPB(235),NFIX(235),SLOPE(235)
00013         COMMON /NPNAP/NP(382,9),NAP(235)
00014         COMMON /DISPL/DSX(235),DSY(235)
00015         COMMON /LOAD/XLOAD(235),YLOAD(235),FX(10),FY(10),NF,FRATE,NFA(10),
00016        1NFN(10)
00017         COMMON /BMAT/XORD(235),YORD(235),NPI(382),NPJ(382),NPK(382)
00018         COMMON /STRESS/SIGXX(382),SIGXY(382),SIGYY(382),SIGZZ(382)
00019         COMMON/STOL/DSIGXX(382),DSIGXY(382),DSIGYY(382),DSIGZZ(382)
00020         COMMON /VISCO/EVPX(382),EVPXY(382),EVPY(382),EVPZ(382),EPEFF(382),
00021        1DPEFF(382)
00022         COMMON /D/DX(382),DY(382),DXY(382),DZ(382)
00023         COMMON /WORK/WPP(382),WPC(382),WPE(382)
00024         COMMON /PROP/ET(382),XU(382),TH(382),PS,MAT
00025         COMMON /JINT/JEL(10),JN(10,382),XN(10,382),YN(10,382),CJINT,JPATH
00026         COMMON /BODNER/DZ2,EN,Z1,ZO,ZI,EMO,RN,AC
00027         COMMON/CRACK/ICR,ICRR,NCR(29,4),SXXC(29),SXYC(29),SYXC(29),
00028        1SYYC(29),TCRACK(29),YLOD(29)
00029         COMMON /CSTAR/DXDT(235),DYDT(235),DDT
00030         COMMON/HARD/WKPLAS(382)
00031         DIMENSION LM(3),B(6,6),D(6,6),S(6,6)
00032 C
00033 C       READ AND PRINT OF DATA
00034 C
00035         WRITE(6,99)
00036         READ (5,*)NDATA,MESHE,MESHN,MESHOLD,SCAL,MPRINT
00037         PRINT (6,*)"NUMBER OF MESH DATA SETS=",NDATA
00038         PRINT (6,*)"ADDED ELEMENTS=",MESHE,"ADDED NODES=",MESHN
00039         PRINT (6,*)"OLD ELEMENTS REUSED=",MESHOLD
00040         PRINT (6,*)" PLOT SCALE FACTOR IS ",SCAL
00041         READ (5,*)PS,MAT
00042         IF (PS .EQ. 0.)PRINT (6,*)" PLANE STRESS SOLUTION"
00043         IF (PS .GT. 0.)PRINT (6,*)" PLANE STRAIN SOLUTION"
00044         IF (MAT .EQ. 0)PRINT (6,*)"VISCOUS SUBROUTINE BEING USED"
00045         IF (MAT .GT. 0.)PRINT (6,*)"BODNER'S SUBROUTINE BEING USED"
00046         IF (MAT .GT. 0)READ(5,*)DZ2,EN,Z1,ZO,ZI,EMO,RN,AC
00047         IF (MAT .GT. 0)PRINT (6,*)"DZ2=",DZ2,"EN=",EN,"Z1=",Z1,"ZO=",ZO,
00048        1"ZI=",ZI,"EMO=",EMO,"RN=",RN,"AC=",AC
00049         READ (5,*)NUMBC,NCPIN,NOPIN,NCYCM,TOLER,XFAC
00050         WRITE(6,103)NUMBC
00051         WRITE(6,104)NCPIN
00052         WRITE(6,105)NOPIN
00053         WRITE(6,106)NCYCM
00054         WRITE(6,107)TOLER
00055         WRITE(6,108)XFAC
00056         READ(5,*)VP,YIELD,HP,VC,ALPHA,RAM,BERG,DTINIT,DTMAX,TMAX
00057         DT=DTINIT
00058         READ (5,*)TPRINT,STOPCY,XMOVE1,XMOVE2,TMOVE3
00059         READ (5,*)NC,PMAX,PO,PERIOD
00060         PRINT(6,*)"CYCLIC LOAD CODE: 1=IN;0=OUT,IN USE  ",NC
00061         PRINT(6,*)"CYCLIC MAX AMPLITUDE OF LOAD REQUIRED   ",PMAX
00062         PRINT(6,*)"STATIC AMPLITUDE    ",PO
00063         PRINT(6,*)"CYCLIC PERIOD VALUE IN SECONDS     ",PERIOD
00064         PRINT(6,*)"FLUIDITY CONSTANT=  ",VP
00065         IF(MAT .EQ. 0)PRINT(6,*)"YIELD= ",YIELD," PLASTIC SLOPE= ",HP
```

```
      PRINT(6,*) " CREEP EXPONENT=",ALPHA," CREEP COEFF=",VC
      PRINT (6,*)"RAMBRG-OSGD COEFF=",RAM,"RAMBRG-OSGD EXPON=",BERG
      PRINT (6,*)"TIME STEP=  ",DT
      PRINT (6,*)"MAXIMUM TIMESTEP=",DTMAX
      PRINT (6,*)"PRINT TIME=  ",TPRINT
      PRINT (6,*)"MAX TIME =  ",TMAX
      READ (5,*)TSTRESS,TEPS,VM,PE,SLOPEA
      PRINT (6,*)"STRAIN TOLERANCE IS ",TEPS
      PRINT(6,*)"STRESS TOLERANCE IS",TSTRESS
      NN=1
      CALL MESH(NUMNP,NUMEL,NDATA,SCAL,MESHE,MESHN,MPRINT,MESHOLD)
      WRITE(6,112)
      READ(5,4)(NPB(L),NFIX(L),SLOPE(L),L=1,NUMBC)
      WRITE(6,4)(NPB(L),NFIX(L),SLOPE(L),L=1,NUMBC)
      READ(5,*)NF,FRATE,NODE,OPE,CEPT,RT,CONV
      PRINT (6,*)" LOADED NODES=",NF," FORCE RATE=",FRATE
      PRINT(6,*) "NODE PT OF INTEREST=",NODE,"SLOPE=",OPE
      PRINT(6,*) "TIME CONVERSION FOR SHARP=",CONV
      PRINT(6,*) "INTERCEPT=",CEPT,"RELEASE TIME=",RT
      PRINT(6,*)"MALVERN VERSION CODE LIN=-1.,EXP=0.,POW=+1. IN USE ",VM
      PRINT(6,*)"POWER VERSION EXPONENT VALVE IS",PE
      PRINT(6,*)"THE A VALUE USED IN EXPMALVERN IS",SLOPEA
      READ(5,*)(NFA(I),I=1,NF)
      IF(PO.LT.0)READ(5,*)(NFN(I),I=1,NF)
      PRINT(6,*)"POSITIVE LOADED NODES=",(NFA(I),I=1,NF)
      PRINT(6,*)"NEGATIVE LOADED NODES=",(NFN(I),I=1,NF)
      DO 40 I=1,NF
      J=NFA(I)
      READ(5,*)FX(I),FY(I)
 40   PRINT (6,*)"NODE ",J," XLOAD=",FX(I)," YLOAD=",FY(I)
      READ (5,*)ICR,TCRACK(1)
      PRINT (6,*)"THE NUMBER OF NODES TO BE CRACKED=",ICR
      IF (ICR .EQ. 0)GO TO 940
      DO 2000 I=1,ICR
      READ (5,*)(NCR(I,K),K=1,4)
2000  PRINT (6,*)(NCR(I,K),K=1,4)
      READ(5,*)(TCRACK(I),I=1,ICR)
      DO 930 I=1,ICR
      PRINT(6,*)"NODE  ",NCR(I,1),"PDPS AT TIME   ",TCRACK(I)
930   CONTINUE
940   CONTINUE
      READ (5,*)JPATH
      PRINT(6,*)"NUMBER OF J INTEGRAL PATHS=",JPATH
      IF (JPATH .EQ. 0)GO TO  910
      DO 900 I=1,JPATH
      READ (5,*)JEL(I)
      PRINT (6,*)"NUMBER OF ELEMENTS IN PATH",I,"EQUALS",JEL(I)
      M=JEL(I)
      READ (5,120)(JN(I,K),XN(I,K),YN(I,K),K=1,M)
120   FORMAT (I5,2E10.2)
      DO 905 K=1,M
905   PRINT (6,*)"JN=",JN(I,K)," XN= ",XN(I,K)," YN= ",YN(I,K)
900   CONTINUE
910   CONTINUE
C
C     INITIALIZATION
C
      ICRR=1
      NNN=0
      DO 175 L=1,NUMNP
      DO 170 M=1,9
      SXX(L,M)=0.0
      SXY(L,M)=0.0
      SYX(L,M)=0.0
   SYY(L,M)=0.0
```

```
00131         DSX(L)=0.0
00132         DSY(L)=0.0
00133   175   CONTINUE
00134         PRINT(6,*)"NUMNP=",NUMNP
00135         DO 140 L=1,NUMNP
00136         DO 142 M=1,9
00137   142   NP(L,M)=0
00138         NP(L,10)=0
00139         NP(L,1)=L
00140   140    CONTINUE
00141 C
00142 C  CHECK ELEMENTS FOR POSITIVE AREAS   & INITIALIZATION
00143 C
00144         DO 180 N=1,NUMEL
00145         DX(N)=0.
00146         DY(N)=0.
00147         DZ(N)=0.
00148         DXY(N)=0.0
00149         DPEFF(N)=0.
00150         EVPX(N)=0.
00151         EVPY(N)=0.
00152         EVPZ(N)=0.
00153         EVPXY(N)=0.
00154         EPEFF(N)=0.
00155         SIGXX(N)=0.
00156         SIGYY(N)=0.
00157         SIGZZ(N)=0.
00158         SIGXY(N)=0.
00159         WPP(N)=0.
00160         WPE(N)=0.
00161         WPC(N)=0.
00162         I=NPI(N)
00163         J=NPJ(N)
00164         K=NPK(N)
00165         AJ    =XORD(J)-XORD(I)
00166         AK    =XORD(K)-XORD(I)
00167         BJ    =YORD(J)-YORD(I)
00168         BK    =YORD(K)-YORD(I)
00169   176   AREA(N)=(AJ*BK-BJ*AK)/2.
00170         ACHECK=ACHECK+AREA(N)
00171   180   CONTINUE
00172         PRINT *,"TOTAL ELEMENT AREA=",ACHECK
00173 C
00174 C       FORMATION OF STIFFNESS ARRAY
00175 C
00176         DO 200 N=1,NUMEL
00177         CALL BMATRIX (N,B)
00178         CALL DMATRIX(N,D)
00179 C
00180 C ASSEMBLE B D B MATRIX PRODUCT FOR ELEMENT N
00181 C
00182         DO 182 J=1,6
00183         DO 182 I=1,3
00184         S(I,J)=0.
00185         DO 182 K=1,3
00186   182   S(I,J)=S(I,J)+D(I,K)*B(K,J)
00187         DO 183 J=1,6
00188         DO 183 I=1,3
00189   183   D(J,I)=S(I,J)
00190         DO 184 J=1,6
00191         DO 184 I=1,6
00192         S(I,J)=0.
00193         DO 184 K=1,3
00194   184   S(I,J)=S(I,J)+D(I,K)*B(K,J)
00195 C   ASSEMBLE TOTAL STIFFNESS MATRIX IN COMPACTED FORM
```

```
C
C  NP(N,M) ARRAY  INDICATES NONZERO COLUMNS M IN ROW N
C
      LM(1)=NPI(N)
      LM(2)=NPJ(N)
      LM(3)=NPK(N)
      DO 200 L=1,3
      DO 200 M=1,3
      LX=LM(L)
      MX=0
  185 MX=MX+1
      IF(NP(LX,MX)-LM(M))190,195,190
  190 IF(NP(LX,MX))185,195,185
  195 NP(LX,MX)=LM(M)
      IF(MX-10)196,702,702
  196 SXX(LX,MX)=SXX(LX,MX)+S(2*L-1,2*M-1)
      SXY(LX,MX)=SXY(LX,MX)+S(2*L-1,2*M)
      SYX(LX,MX)=SYX(LX,MX)+S(2*L,2*M-1)
  200 SYY(LX,MX)=SYY(LX,MX)+S(2*L,2*M)
C
C     COUNT OF ADJACENT NODAL POINTS
C
      DO 206 M=1,NUMNP
      MX=1
  205 MX=MX+1
      IF(NP(M,MX))206,206,205
  206 NAP(M)=MX-1
C
C     INVERSION OF NODAL POINT STIFFNESS
      CALL NPINV(NUMNP)
C     MODIFICATION OF BOUNDARY FLEXIBILITY
C
      CALL BCOND(NUMBC)
C
C     ITERATION ON NODAL POINT DISPLACEMENTS
C
      T=0.
      TP=0
      PI=1.
      CALL LOAD(DT,T,NUMEL,NUMNP,PI,RT,PMAX,PO,PERIOD,NC,CYCNO,
     1STOPCY)
      CALL SOLVE(NUMNP,NUMEL,NCPIN,NOPIN,NCYCM,TOLER,XFAC,T,DT,PI)
      CALL OUTPUT(NUMEL,NUMNP,T,DT,NNN)
      DO 410 N=1,NUMEL
      SIGEFF=(SIGXX(N)**2+SIGYY(N)**2+SIGZZ(N)**2-SIGXX(N)*SIGYY(N)
     1 -SIGYY(N)*SIGZZ(N)-SIGZZ(N)*SIGXX(N)+3.*SIGXY(N)**2)**.5
      PII=YIELD/SIGEFF
      IF (PII .LT. PI)I=N
  410 IF (PII .LT. PI)PI=PII
      PRINT (6,*)"ELEMENT ",I," YIELDS AT ",PI," * TOTAL LOAD"
      DO 400 I=1,NUMNP
      DSX(I)=DSX(I)*PI
  400 DSY(I)=DSY(I)*PI
      DDT=PI/FRATE
      CALL WORK(NUMEL,T,PI)
      CALL OUTPUT(NUMEL,NUMNP,T,DT,NN)
      T=0.001
      TP=.001
  310 T=T+DT
      TP=TP+DT
      DO 600 I=1,NUMNP
      DXDT(I)=DSX(I)
  600 DYDT(I)=DSY(I)
  500 IF(MAT.EQ.0)CALL VISCOUS(NUMEL,VP,YIELD,HP,DT,RAM,BERG,VC,ALPHA,
     1SLOPEA,PE,VM)
```

```
00262        CALL LOAD(DT,T,NUMEL,NUMNP,PI,RT,PMAX,PO,PERIOD,NC,CYCNO,
00263       1STOPCY)
00264        CALL SOLVE(NUMNP,NUMEL,NCPIN,NOPIN,NCYCM,TOLER,XFAC,T,DT,PI)
00265        CALL STRESS(NUMEL,NN,T,DT,P,TEPS,TP,TSTRESS,YIELD)
00266        IF (P .GT. 1.0)GO TO 500
00267        IF (P .GE. 0.8 .AND. P .LE. 1.)GO TO 510
00268        IF (P .GE. 0.65 .AND. P .LT. 0.8)DT=1.25*DT
00269        IF(T.GE.STOPCY)DTMAX=50.
00270        IF (P .LT. 0.65)DT=1.5*DT
00271        IF (DT .GT. DTMAX)DT=DTMAX
00272  510   CALL STRESS(NUMEL,NNN,T,DT,P,TEPS,TP,TSTRESS,YIELD)
00273        CALL WORK(NUMEL,T,PI)
00274        IF(ICR .GT. 0)CALL NODEPOP(T,DT,DTINIT,TP,TPRINT,NUMNP,NODE,OPE,
00275       1CEPT,RT,CONV)
00276 C      IF((CYCNO.GE.(XMOVE1-.05)).AND.(CYCNO.LE.(XMOVE1+.05)))
00277 C     1CALL GEOM(MESHE,MESHN,NUMEL)
00278 C      IF((CYCNO.GE.(XMOVE1-.05)).AND.(CYCNO.LE.(XMOVE1+.05)))
00279 C     1CALL DISP(MESHN)
00280 C      IF((CYCNO.GE.(XMOVE1-.05)).AND.(CYCNO.LE.(XMOVE1+.05)))
00281 C     1CALL FUNC(NUMEL)
00282 C      IF((CYCNO.GE.(XMOVE2-.05)).AND.(CYCNO.LE.(XMOVE2+.05)))
00283 C     1CALL DISP(MESHN)
00284 C      IF((CYCNO.GE.(XMOVE2-.05)).AND.(CYCNO.LE.(XMOVE2+.05)))
00285 C     1CALL FUNC(NUMEL)
00286 C      IF((T.GE.TMOVE3).AND.(T.LE.(TMAX-.05)))CALL DISP(MESHN)
00287 C      IF((T.GE.TMOVE3).AND.(T.LE.(TMAX-.05)))CALL FUNC(NUMEL)
00288        IF(T.GE.STOPCY)TPRINT=50.
00289        IF (TP .LT. TPRINT)GO TO 300
00290        CALL OUTPUT(NUMEL,NUMNP,T,DT,NN)
00291        TP=TP-TPRINT
00292  300   IF (T .LT. TMAX)GO TO 310
00293        CALL OUTPUT(NUMEL,NUMNP,T,DT,NN)
00294        CALL DPLOT(NUMEL,NUMNP,T,SCAL,YIELD)
00295        GO TO 150
00296 C
00297 C      PRINT OF ERRORS IN INPUT DATA
00298 C
00299 C701   WRITE(6,711)N
00300 C      GO TO 150
00301   702  WRITE(6,712)LX
00302     4  FORMAT(2I10,F10.5)
00303    99  FORMAT(1H1)
00304   103  FORMAT(29H NUMBER OF BOUNDARY POINTS  =I4/)
00305   104  FORMAT(29H CYCLE PRINT INTERVAL       =I4/)
00306   105  FORMAT(29H OUTPUT INTERVAL OF RESULTS =I4/)
00307   106  FORMAT(29H CYCLE LIMIT                =I4/)
00308   107  FORMAT(29H TOLERANCE LIMIT            =G12.4/)
00309   108  FORMAT(29H OVER RELAXATION FACTOR     =F6.3)
00310   112  FORMAT (20H BOUNDARY CONDITIONS)
00311   711  FORMAT(32HOZERO OR NEGATIVE AREA, EL. NO.=I4)
00312   712  FORMAT(33HOOVER 8 N.P. ADJACENT TO N.P. NO.I4)
00313 C
00314   150  CONTINUE
00315        END
00316        SUBROUTINE MESH(NNUMNP,NNUMEL,NDATA,SCAL,MESHE,MESHN,MPRINT,MESHOL
00317       1D)
00318 C   THIS PROGRAM GENERATES ANY SPECIFIED NUMBER OF ELEMENTS GIVEN THE
00319 C   COORDINATES OF EIGHT POINTS ON THE BOUNDARY
00320 C
00321        COMMON /BMAT/XORD(235),YORD(235),NPI(382),NPJ(382),NPK(382)
00322        COMMON /NPNAP/NP(382,9),NAP(235)
00323        COMMON /LOAD/XLOAD(235),YLOAD(235),FX(10),FY(10),NF,FRATE,NFA(10),
00324       1NFN(10)
00325        COMMON /PROP/ET(382),XU(382),TH(382),PS,MAT
```

```
C      READ AND INITIALIZATION OF DATA
C
       NUMEL=0
       NUMNP=0
       NNUMNP=0
       NNUMEL=0
       NNDATA=0
       NDIR=0
       CALL PLOTS(0.,0.,9)
       CALL PLOT (0.,1.,-3)
    FORMAT(4I5,5E12.5)
    FORMAT(4I5,3E12.5)
 70   FORMAT (1I10,2E20.8)
      READ(5,10) INITNP,INITEL,E,XNU,THE
    FORMAT(2I5,5E12.5)
       PRINT 20,INITNP,INITEL
    FORMAT(/,* INITNP=*,I3,3X,*INITEL=*,I3)
       READ 10,NDIVX,NDIVY
       PRINT (6,*)" NDIVX=",NDIVX," NDIVY=",NDIVY
       IF (NDIVX .EQ. 0)GO TO 600
       READ 40,(XCOR(I),YCOR(I),I=1,8)
 40    FORMAT (2E20.8)
       PRINT 50,(N,XCOR(N),N,YCOR(N),N=1,8)
 50    FORMAT (* XCOR(*,I1,*)=*,F10.5,5X,*YORD(*,I1,*)=*,F10.5)
C
       NUMEL=2*(NDIVX)*(NDIVY)
       NUMNP=(NDIVX+1)*(NDIVY+1)
C
C  CALCULATE NODAL POINT COORDINATES
       DX=NDIVX
       DX=1.0/DX
       DY=NDIVY
       DY=1.0/DY
       IEND=NDIVY+1
       JEND=NDIVX+1
       J1=0
       DO 250 I=1,IEND
       R=(I-1)
       RY=R*DY
       DO 240 J=1,JEND
       R=(J-1)
       RX=R*DX
       J1=J1+1
C  SHAPE FUNCTIONS
       RN(1)=1.0*(1.0-RX)*(1.0-RY)*(1.0-2.0*RX-2.0*RY)
       RN(2)=+4.0*(RX)*(1.0-RX)*(1.0-RY)
       RN(3)=-1.0*(RX)*(1.0-RY)*(1.0-2.*RX+2.0*RY)
       RN(4)=+4.0*(RX)*(RY)*(1.0-RY)
       RN(5)=-1.0*(RX)*(RY)*(3.0-2.0*RX-2.0*RY)
       RN(6)=+4.0*(RX)*(1.0-RX)*RY
       RN(7)=-1.0*(1.0-RX)*(RY)*(1.0+2.0*RX-2.0*RY)
       RN(8)=+4.0*(1.0-RX)*(RY)*(1.0-RY)
C
       XXORD(J1)=0.0
       YYORD(J1)=0.0
       DO 230 K=1,8
       XXORD(J1)=XXORD(J1)+RN(K)*XCOR(K)
       YYORD(J1)=YYORD(J1)+RN(K)*YCOR(K)
 230   CONTINUE
 240   CONTINUE
 250   CONTINUE
C
C  CALCULATE NP ARRAY
```

AD-A151 702 CRACK CLOSURE CHARACTERISTICS CONSIDERING CENTER CRACKED AND COMPACT TENS..(U) AIR FORCE INST OF TECH WRIGHT-PATTERSON AFB OH SCHOOL OF ENGI.. C L HENKEL 2/2

UNCLASSIFIED DEC 84 AFIT/GAE/AA/84D-9 F/G 20/11 NL

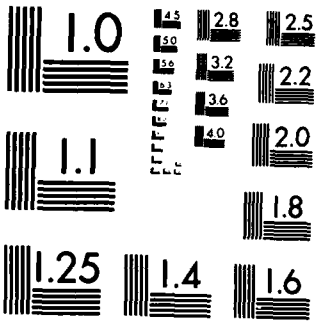

MICROCOPY RESOLUTION TEST CHART
NATIONAL BUREAU OF STANDARDS-1963-A

```
00391 C
00392       I2=0
00393       DO 340 I=1,NDIVY
00394       J1=(I-1)*(NDIVX+1)+1
00395       IF (NDIR .EQ. 0)GO TO 500
00396       IF (NDIR .EQ. 1)NDIR=0
00397       GO TO 510
00398  500  NDIR=1
00399  510  CONTINUE
00400       DO 330 J=1,NDIVX
00401       I2=I2+2
00402       I1=I2-1
00403       J2=J1+1
00404       J4=J1+(NDIVX+1)
00405       J3=J4+1
00406       D1=(XXORD(J3)-XXORD(J1))**2+(YYORD(J3)-YYORD(J1))**2
00407       D2=(XXORD(J4)-XXORD(J2))**2+(YYORD(J4)-YYORD(J2))**2
00408       IF (D1 .GT. 1.01*D2)GO TO 320
00409       IF (D1 .GT. .99*D2 .AND. NDIR .EQ. 0)GO TO 320
00410       NDIR=0
00411       NP(I1,1)=J1
00412       NP(I1,2)=J3
00413       NP(I1,3)=J4
00414       NP(I2,1)=J1
00415       NP(I2,2)=J2
00416       NP(I2,3)=J3
00417       GO TO 329
00418  320  NDIR=1
00419       NP(I1,1)=J1
00420       NP(I1,2)=J2
00421       NP(I1,3)=J4
00422       NP(I2,1)=J2
00423       NP(I2,2)=J3
00424       NP(I2,3)=J4
00425  329  CONTINUE
00426       J1=J2
00427  330  CONTINUE
00428  340  CONTINUE
00429 C
00430 C  OUTPUT STATEMENTS
00431 C
00432       PRINT (8,*)
00433       PRINT (6,*)"THE NODAL POINT COORDINATES ARE THE FOLLOWING"
00434       IFAC=INITNP-1
00435       DO 420 I=1,NUMNP
00436       I1=I+IFAC
00437       XORD(I1)=XXORD(I)
00438       YORD(I1)=YYORD(I)
00439  110  FORMAT (* NODAL PT *,I4,5X,*XCORD=*,E15.8,5X,*YCORD=*,E15.8)
00440  420  CONTINUE
00441 C
00442       IFAC=INITEL-1
00443 C  CALCULATE NPI  NPJ  NPK  ARRAYS
00444       DO 440 I=1,NUMEL
00445       I1=I+IFAC
00446       ET(I1)=E
00447       XU(I1)=XNU
00448       TH(I1)=THE
00449       NPI(I1)=NP(I,1)+INITNP-1
00450       NPJ(I1)=NP(I,2)+INITNP-1
00451       NPK(I1)=NP(I,3)+INITNP-1
00452    FORMAT(* ELEMENT *,I4,5X,*NPI=*,I3,3X,*NPJ=*,I3,3X,*NPK=*,I3,3X,
00453      1*E0=*,E12.5,3X,*NU=*,E12.5,3X,*T=*,E12.5)
00454  440  CONTINUE
00455  600  CONTINUE
```

```
      NNDATA=NNDATA+1
      NNUMEL=NUMEL+INITEL-1+MESHE-MESHOLD
      NNUMNP=NUMNP+INITNP-1+MESHN
      IF (NNDATA .LT. NDATA)GO TO 5
      IF(MESHE.GT.0)READ(7,61)(N,NPI(N),NPJ(N),NPK(N),ET(N),XU(N),
     1TH(N),L=1,MESHE)
      IF(MESHN.GT.0)READ(7,70)(N,XORD(N),YORD(N),L=1,MESHN)
      IF (MPRINT .GT. 0)PRINT 110,(I,XORD(I),YORD(I),I=1,NNUMNP)
      IF(MPRINT.GT.0)PRINT 120,(L,NPI(L),NPJ(L),NPK(L),ET(L),XU(L),TH(L)
     1,L=1,NNUMEL)
      PRINT (6,*)" TOTAL NUMBER NODE POINTS=",NNUMNP
      PRINT (6,*)" TOTAL NUMBER OF ELEMENTS=",NNUMEL
C
C  PLOT ROUTINE      XXXXXXXXXXXXXXXXXXX
      CALL FACTOR (SCAL)
      HGHT=.1/SCAL
      PRINT(6,*)"HGHT=",HGHT
      DO 480 I=1,NNUMEL
      I1=NPI(I)
      I2=NPJ(I)
      I3=NPK(I)
      CALL PLOT (XORD(I1),YORD(I1),+3)
      CALL PLOT ( XORD(I2), YORD(I2),+2)
      CALL PLOT ( XORD(I3), YORD(I3),+2)
      CALL PLOT ( XORD(I1), YORD(I1),+2)
      CALL PLOT(XORD(I1),YORD(I1),+3)
      XD1=ABS(XORD(I1)-XORD(I2))*SCAL
      XD2=ABS(XORD(I1)-XORD(I3))*SCAL
      XD3=ABS(XORD(I2)-XORD(I3))*SCAL
      IF(XD1.LT..15.AND.XD2.LT..15.AND.XD3.LT..15)GO TO  480
      XCENT=(XORD(I1)+XORD(I2)+XORD(I3))/3.-.1/SCAL
      YCENT=(YORD(I1)+YORD(I2)+YORD(I3))/3.
      RATIO=I
      IF (RATIO .LT. 10.)XCENT=XCENT+.1/SCAL
      CALL NUMBER(XCENT,YCENT,HGHT,RATIO,0.,-1)
480   CONTINUE
      CALL FACTOR(1.)
      CALL PLOTE(N)
      RETURN
      END
      SUBROUTINE BMATRIX(N,B)
      COMMON /A/AREA(382)
      COMMON /BMAT/XORD(235),YORD(235),NPI(382),NPJ(382),NPK(382)
      DIMENSION B(6,8)
      I=NPI(N)
      J=NPJ(N)
      K=NPK(N)
      AJ    =XORD(J)-XORD(I)
      AK    =XORD(K)-XORD(I)
      BJ    =YORD(J)-YORD(I)
      BK    =YORD(K)-YORD(I)
      TAREA=2.*AREA(N)
      B(1,1)=(BJ-BK)/TAREA
      B(1,2)=0.
      B(1,3)=(BK    )/TAREA
      B(1,4)=0.
      B(1,5)=-(BJ    )/TAREA
      B(1,6)=0.
      B(2,1)=0.
      B(2,2)=(AK-AJ)/TAREA
      B(2,3)=0.
      B(2,4)=-(AK    )/TAREA
      B(2,5)=0.
      B(2,6)=(AJ    )/TAREA
      B(3,1)=(AK-AJ)/TAREA
```

```
      B(3,2)=(BJ-BK)/TAREA
      B(3,3)=-(AK    )/TAREA
      B(3,4)=(BK     )/TAREA
      B(3,5)=(AJ    )/TAREA
      B(3,6)=-(BJ    ) /TAREA
      RETURN
      END
      SUBROUTINE DMATRIX (N,D)
      COMMON /A/AREA(382)
      COMMON /PROP/ET(382),XU(382),TH(382),PS,MAT
      COMMON /BMAT/XORD(235),YORD(235),NPI(382),NPJ(382),NPK(382)
      DIMENSION D(6,6)
      IF (PS .GT. 0.)GO TO 10
      COMM=ET(N)*AREA(N)*TH(N)/(1.-XU(N)**2)
      D(1,1)=COMM
      D(1,2)=COMM*XU(N)
      D(2,1)=COMM*XU(N)
      D(2,2)=COMM
      D(3,3)=COMM*(1.-XU(N))*.5
      GO TO 20
   10 COMM=ET(N)*AREA(N)*(1.-XU(N))*TH(N)/((1.+XU(N))*(1.-2.*XU(N)))
      D(1,1)=COMM
      D(1,2)=COMM*XU(N)/(1.-XU(N))
       D(2,1)=D(1,2)
      D(2,2)=COMM
      D(3,3)=COMM*(1.-2.*XU(N))/(2.*(1.-XU(N)))
   20 CONTINUE
      D(3,2)=0.
      D(3,1)=0.
      D(2,3)=0.
      D(1,3)=0.
      RETURN
      END
      SUBROUTINE NPINV(NUMNP)
      COMMON /NPINV/SXX(235,9),SXY(235,9),SYX(235,9),SYY(235,9)
      DO 210 M=1,NUMNP
      COMM=SXX(M,1)*SYY(M,1)-SXY(M,1)*SYX(M,1)
      TEMP=SYY(M,1)/COMM
      SYY(M,1)=SXX(M,1)/COMM
      SXX(M,1)=TEMP
      SXY(M,1)=-SXY(M,1)/COMM
  210 SYX(M,1)=-SYX(M,1)/COMM
      RETURN
      END
      SUBROUTINE BCOND(NUMBC)
      COMMON /BC/NPB(235),NFIX(235),SLOPE(235)
      COMMON /NPINV/SXX(235,9),SXY(235,9),SYX(235,9),SYY(235,9)
      COMMON /NPNAP/NP(382,9),NAP(235)
      COMMON/CRACK/ICR,ICRR,NCR(29,4),SXXC(29),SXYC(29),SYXC(29),
     1SYYC(29),TCRACK(29),VLOD(29)
      PRINT (6,*)"IN BOUNDARY CONDITION SUBROUTINE NOW"
      DO 240 L=1,NUMBC
      M=NPB(L)
      IF (ICR .EQ. 0)GO TO 310
      DO 300 I=1,ICR
      IF (M .NE. NCR(I,1))GO TO 300
      SXXC(I)=SXX(M,1)
      SXYC(I)=SXY(M,1)
      SYXC(I)=SYX(M,1)
      SYYC(I)=SYY(M,1)
      PRINT (6,*)"SXXC(",I,")=",SXXC(I)
      PRINT (6,*)"SXYC(",I,")=",SXYC(I)
      PRINT (6,*)"SYXC(",I,")=",SYXC(I)
      PRINT (6,*)"SYYC(",I,")=",SYYC(I)
  300 CONTINUE
```

```
00586   310  CONTINUE
00587        IF(NFIX(L)-1)225,220,215
00588   215  C=(SXX(M,1)*SLOPE(L)-SXY(M,1))/(SYX(M,1)*SLOPE(L)-SYY(M,1))
00589        R=1.-C*SLOPE(L)
00590        SXX(M,1)=(SXX(M,1)-C*SYX(M,1))/R
00591        SXY(M,1)=(SXY(M,1)-C*SYY(M,1))/R
00592        SYX(M,1)=SXX(M,1)*SLOPE(L)
00593        SYY(M,1)=SXY(M,1)*SLOPE(L)
00594        GO TO 240
00595   220  SYY(M,1)=SYY(M,1)-SYX(M,1)*SXY(M,1)/SXX(M,1)
00596        GO TO 230
00597   225  SYY(M,1)=0.
00598   230  SXX(M,1)=0.
00599   235  SXY(M,1)=0.
00600        SYX(M,1)=0.
00601   240  CONTINUE
00602        RETURN
00603        END
00604        SUBROUTINE LOAD(DT,T,NUMEL,NUMNP,PI,RT,PMAX,PO,PERIOD,NC,
00605       1CYCNO,STOPCY)
00606        COMMON /LOAD/XLOAD(235),YLOAD(235),FX(10),FY(10),NF,FRATE,NFA(10),
00607       1NFN(10)
00608        COMMON /BMAT/XORD(235),YORD(235),NPI(382),NPJ(382),NPK(382)
00609        COMMON /VISCO/EVPX(382),EVPXY(382),EVPY(382),EVPZ(382),EPEFF(382),
00610       1DPEFF(382)
00611        COMMON /PROP/ET(382),XU(382),TH(382),PS,MAT
00612        COMMON/CRACK/ICR,ICRR,NCR(29,4),SXXC(29),SXYC(29),SYXC(29),
00613       1SYYC(29),TCRACK(29),YLOD(29)
00614        DIMENSION D(6,6),B(6,6)
00615        DO 100 L=1,NUMNP
00616        XLOAD(L)=0.
00617   100  YLOAD(L)=0.
00618        IF (ICR .EQ. 0)GO TO 300
00619        IM=ICRR-1
00620        IF (IM .LE. 0)GO TO 300
00621        M=NCR(IM,1)
00622        DO 200 L=1,NUMNP
00623        TT=TCRACK(IM)+RT-T
00624        IF(L .EQ. M) YLOAD(L)=YLOD(IM)*TT/(RT)
00625        IF(L .EQ. M .AND. TT .LT. 0.)YLOAD(L)=0.
00626        IF(L.EQ.M)PRINT(6,*)"YLOAD ",L," EQUALS ",YLOAD(L)
00627   200  CONTINUE
00628   300  CONTINUE
00629        IF (T.EQ.0.0) T=0.001
00630        P=FRATE*T
00631        PP=P+PI
00632        IF (PP .GT. 1.)PP=1.
00633        NC=1
00634        IF(T.GE.STOPCY)GO TO 25
00635        IF(NC.EQ.1)CALL CYCLIC (T,PMAX,PO,PERIOD,PP,CYCNO)
00636        PRINT(6,*)"PP=     ",PP
00637    25  IF(T.GE.STOPCY) PP=1.
00638        IF(PP.LT.0)GO TO 120
00639        DO 110 I=1,NF
00640        J=NFA(I)
00641        XLOAD(J)=FX(I)*PP
00642   110  YLOAD(J)=FY(I)*PP
00643        GO TO 130
00644   120  DO 125 I=1,NF
00645        J=NFN(I)
00646        XLOAD(J)=FX(I)*PP
00647   125  YLOAD(J)=FY(I)*PP
00648   130  DO 10 N=1,NUMEL
00649        IF (EPEFF(N) .EQ. 0.)GO TO 10
00650        I=NPI(N)
```

```
00651         J=NPJ(N)
00652         K=NPK(N)
00653         CALL DMATRIX(N,D)
00654         SX=D(1,1)*EVPX(N)+D(1,2)*EVPY(N)
00655         SY=D(2,1)*EVPX(N)+D(2,2)*EVPY(N)
00656         SXY=D(3,3)*EVPXY(N)
00657         CALL BMATRIX(N,B)
00658         XLOAD(I)=XLOAD(I)+B(1,1)*SX+B(2,1)*SY+B(3,1)*SXY
00659         YLOAD(I)=YLOAD(I)+B(1,2)*SX+B(2,2)*SY+B(3,2)*SXY
00660         XLOAD(J)=XLOAD(J)+B(1,3)*SX+B(2,3)*SY+B(3,3)*SXY
00661         YLOAD(J)=YLOAD(J)+B(1,4)*SX+B(2,4)*SY+B(3,4)*SXY
00662         XLOAD(K)=XLOAD(K)+B(1,5)*SX+B(2,5)*SY+B(3,5)*SXY
00663         YLOAD(K)=YLOAD(K)+B(1,6)*SX+B(2,6)*SY+B(3,6)*SXY
00664   10    CONTINUE
00665         RETURN
00666         END
00667         SUBROUTINE SOLVE(NUMNP,NUMEL,NCPIN,NOPIN,NCYCM,TOLER,XFAC,T,DT,PI)
00668         COMMON /NPINV/SXX(235,9),SXY(235,9),SYX(235,9),SYY(235,9)
00669         COMMON /LOAD/XLOAD(235),YLOAD(235),FX(10),FY(10),NF,FRATE,NFA(10),
00670        1NFN(10)
00671         COMMON /DISPL/DSX(235),DSY(235)
00672         COMMON /NPNAP/NP(382,9),NAP(235)
00673         COMMON /CSTAR/DXDT(235),DYDT(235),DDT
00674         DDT=DT
00675         NPRINT=0
00676         NUMPT=NCPIN
00677         NUMOPT=NOPIN
00678         NCYCLE=0
00679         RTF=PI+T*FRATE
00680         IF(RTF .LT. 1.)FTOLER=RTF*TOLER
00681         IF(RTF .GE. 1.)FTOLER=TOLER
00682   327   SUM=0.
00683         DO 290 M=1,NUMNP
00684         NUM=NAP(M)
00685         IF (NUM .EQ. 1)PRINT (6,*)"NODE POINT  ",M," IS UNCONNECTED "
00686         IF(SXX(M,1)+SYY(M,1))275,290,275
00687   275   FRX=XLOAD(M)
00688         FRY=YLOAD(M)
00689         DO 280 L=2,NUM
00690         N=NP(M,L)
00691         FRX=FRX-SXX(M,L)*DSX(N)-SXY(M,L)*DSY(N)
00692   280   FRY=FRY-SYX(M,L)*DSX(N)-SYY(M,L)*DSY(N)
00693         DX=SXX(M,1)*FRX+SXY(M,1)*FRY-DSX(M)
00694         DY=SYX(M,1)*FRX+SYY(M,1)*FRY-DSY(M)
00695         DSX(M)=DSX(M)+XFAC*DX
00696         DSY(M)=DSY(M)+XFAC*DY
00697         DO 65 INTT=115,121
00698   65    IF(DSY(INTT).LT.0.)DSY(INTT)=0.
00699         DO 66 INTT=176,177
00700   66    IF(DSY(INTT).LT.0.)DSY(INTT)=0.
00701   10    IF (SXX(M,1))20,40,20
00702   20    IF (SYY(M,1))285,30,285
00703   30    SUM=SUM+ABS(DX/SXX(M,1))
00704         GO TO 290
00705   40    SUM=SUM+ABS(DY/SYY(M,1))
00706         GO TO 290
00707   285   SUM=SUM+ABS(DX/SXX(M,1))+ABS(DY/SYY(M,1))
00708   290   CONTINUE
00709 C
00710 C       CYCLE COUNT AND PRINT CHECK
00711 C
00712         NCYCLE=NCYCLE+1
00713         IF(NCYCLE-NUMPT)305,300,300
00714   300   NUMPT=NUMPT+NCPIN
00715         PRINT (6,*)"CYCLE=",NCYCLE,"FORCE UNBALANCE=",SUM
```

```
00716  305  IF(SUM-FTOLER)400,400,310
00717  310  IF(NCYCM-NCYCLE)400,400,315
00718  315  IF(NCYCLE-NUMOPT)327,320,320
00719  320  NUMOPT=NUMOPT+NOPIN
00720  400  IF (NPRINT .EQ. 1)CALL OUTPUT(NUMEL,NUMNP,T,DT)
00721        IF (SUM-FTOLER)440,440,430
00722  430  IF(NCYCM-NCYCLE)440,440,327
00723 C
00724  440  IF (NPRINT .EQ. 1)WRITE (6,9000)NCYCLE,SUM
00725  9000 FORMAT( 1HO,*PROBLEM COMPLETED, NUMBER OF CYCLES=*,I10,*FORCE UNBAL
00726      1ANCE =*,F20.10)
00727       RETURN
00728       END
00729       SUBROUTINE STRESS(NUMEL,NN,T,DT,P,TEPS,TP,TSTRESS,YIELD)
00730       COMMON /PROP/ET(382),XU(382),TH(382),PS,MAT
00731       COMMON /A/AREA(382)
00732       COMMON /DISPL/DSX(235),DSY(235)
00733       COMMON /VISCO/EVPX(382),EVPXY(382),EVPY(382),EVPZ(382),EPEFF(382),
00734      1DPEFF(382)
00735       COMMON/STOL/DSIGXX(382),DSIGXY(382),DSIGYY(382),DSIGZZ(382)
00736       COMMON /STRESS/SIGXX(382),SIGXY(382),SIGYY(382),SIGZZ(382)
00737       COMMON /BMAT/XORD(235),YORD(235),NPI(382),NPJ(382),NPK(382)
00738       COMMON /D/DX(382),DY(382),DXY(382),DZ(382)
00739       DIMENSION B(6,6),D(6,6)
00740       P=0.
00741       SY=.5*YIELD
00742       NEL=NN
00743       IF (NN .EQ. 0)GO TO 430
00744       DO 30 N=1,NUMEL
00745  10   I=NPI(N)
00746       J=NPJ(N)
00747       K=NPK(N)
00748       CALL BMATRIX(N,B)
00749       EPXX=B(1,1)*DSX(I)+B(1,3)*DSX(J)+B(1,5)*DSX(K)
00750       EPYY=B(2,2)*DSY(I)+B(2,4)*DSY(J)+B(2,6)*DSY(K)
00751       GAMM=B(3,1)*DSX(I)+B(3,2)*DSY(I)+B(3,3)*DSX(J)+B(3,4)*DSY(J)+
00752      1  B(3,5)*DSX(K)+B(3,6)*DSY(K)
00753       EPX=EPXX-EVPX(N)
00754       EPY=EPYY-EVPY(N)
00755       GAM=GAMM-  EVPXY(N)
00756       CALL DMATRIX(N,D)
00757       DSIGXX(N)=(D(1,1)*EPX+D(1,2)*EPY)/(AREA(N)*TH(N))-SIGXX(N)
00758       DSIGYY(N)=(D(2,1)*EPX+D(2,2)*EPY)/(AREA(N)*TH(N))-SIGYY(N)
00759       DSIGXY(N)=D(3,3)*GAM/(AREA(N)*TH(N))-SIGXY(N)
00760       IF (PS .EQ. 0.)DSIGZZ(N) =0.
00761       SIGX=SIGXX(N)+DSIGXX(N)
00762       SIGY=SIGYY(N)+DSIGYY(N)
00763       IF(PS.GT.0.)DSIGZZ(N)=-ET(N)*EVPZ(N)+XU(N)*(SIGX+SIGY)-SIGZZ(N)
00764     IF(PS.EQ.0.)EPZZ=-(XU(N)/(1.-XU(N)))*(EPX+EPY)+EVPZ(N)
00765       IF (PS .GT. 0.)EPZZ=0.
00766       EEFF=(EPXX**2+EPYY**2+EPZZ**2+.50*GAMM**2)**.5
00767       IF (MAT .GT. 0)GO TO 100
00768       P1=DPEFF(N)/(EEFF*TEPS)
00769       GO TO 110
00770  100  DP=.816496*(DX(N)**2+DY(N)**2+DZ(N)**2+.5*DXY(N)**2)**.5
00771       P1=DP/(EEFF*TEPS)
00772  110  IF (P1 .LT. P)GO TO 420
00773       NEL=N
00774       P=P1
00775       NTOL=2
00776  420  CONTINUE
00777       SIGEFF=(SIGXX(N)**2+SIGYY(N)**2+SIGZZ(N)**2-SIGXX(N)*SIGYY(N)
00778      1 -SIGYY(N)*SIGZZ(N)-SIGZZ(N)*SIGXX(N)+3.*SIGXY(N)**2)**.5
00779       IF (SIGEFF .LT. SY)GO TO 30
00780       DSIGEFF=(DSIGXX(N)**2+DSIGYY(N)**2+DSIGZZ(N)**2 -DSIGXX(N)*DSIGYY(
```

```
     1N)-DSIGYY(N)*DSIGZZ(N)-DSIGXX(N)*DSIGZZ(N)+3.*DSIGXY(N)**2)**.5
      P2=DSIGEFF/(SIGEFF*TSTRESS)
      IF (P2 .LT. P)GO TO 30
      NEL=N
      NTOL=1
      P=P2
30    CONTINUE
      IF (P .LT. 1.)GO TO 440
      IF(NTOL.EQ.2)PRINT(6,*)"STRAIN TOLERANCE EXCEEDED,DT=",DT,"T=",T
      IF(NTOL.EQ.1)PRINT(6,*)"STRESS TOLERANCE EXCEEDED,DT=",DT," T=",T
      PRINT(6,*)"THE CRITICAL ELEM IS ",NEL,"DZ(N)=",DZ(NEL)
      PRINT (6,*)"DX(N)=",DX(NEL),"DY(N)=",DY(NEL),"DXY(N)=",DXY(NEL)
      PRINT(6,*)"DSIGXX=",DSIGXX(NEL),"DSIGYY=",DSIGYY(NEL),"DSIGXY=",
     1DSIGXY(NEL),"DSIGZZ=",DSIGZZ(NEL)
      IF (MAT .GT. 0)PRINT (6,*)"BODNER'S PLASTIC WORK INCREMENT IS"
      PRINT (6,*)"DPEFF=",DPEFF(NEL)
      PRINT(6,*)"EVPX=",EVPX(NEL)," EVPY=",EVPY(NEL),"EVPXY=",EVPXY(NEL)
      PRINT(6,*)"SIGXX=",SIGXX(NEL),"SIGYY=",SIGYY(NEL),"SIGXY=",
     1SIGXY(NEL),"SIGZZ=",SIGZZ(NEL)
      PRINT (6,*)"P=",P
      T=T-DT
      TP=TP-DT
      DT=0.8*DT/P
      T=T+DT
      TP=TP+DT
      PRINT (6,*)"NEW TIMESTEP=",DT,"NEW TIME=",T
      DO 520 L=1,NUMEL
      EPEFF(L)=EPEFF(L)-DPEFF(L)
      EVPX(L)=EVPX(L)-DX(L)
      EVPY(L)=EVPY(L)-DY(L)
      EVPZ(L)=EVPZ(L)-DZ(L)
520   EVPXY(L)=EVPXY(L)-DXY(L)
      GO TO 440
430   CONTINUE
      DO 200 I=1,NUMEL
      SIGXX(I)=SIGXX(I)+DSIGXX(I)
      SIGXY(I)=SIGXY(I)+DSIGXY(I)
      SIGYY(I)=SIGYY(I)+DSIGYY(I)
200   SIGZZ(I)=SIGZZ(I)+DSIGZZ(I)
440   CONTINUE
      RETURN
      END
      SUBROUTINE BODNER(NUMEL,DT)
      COMMON /BODNER/DZ2,EN,Z1,ZO,ZI,EMO,RN,AC
      COMMON /STRESS/SIGXX(382),SIGXY(382),SIGYY(382),SIGZZ(382)
      COMMON /VISCO/EVPX(382),EVPXY(382),EVPY(382),EVPZ(382),EPEFF(382),
     1DPEFF(382)
      COMMON /D/DX(382),DY(382),DXY(382),DZ(382)
      DIMENSION WP(382),DWP(382)
      EQUIVALENCE (EPEFF,WP),(DPEFF,DWP)
      OM=0.
      DO 100 N=1,NUMEL
      S2=(SIGXX(N)**2+SIGYY(N)**2+SIGZZ(N)**2-SIGXX(N)*SIGYY(N)
     1 -SIGYY(N)*SIGZZ(N)-SIGZZ(N)*SIGXX(N)+3.*SIGXY(N)**2)/(8.3108E08)
      IF (S2 .EQ. 0.)GO TO 100
      Z=Z1+(ZO-Z1)*EXP(-EMO*WP(N))
      DG=(Z**2/3.)*((EN+1.)/EN)**(1./EN)
      DGS=DG/S2
      IF (DGS .GT. 150.**(1./EN))GO TO 1
      X=DGS**EN
      D2P=DZ2*EXP(-X)
      OM=SQRT(D2P/S2)
      GO TO 2
1     OM=0.
2     CONTINUE
```

```
      XDIR=(2.*SIGXX(N)-SIGYY(N)-SIGZZ(N))/43511.4
      YDIR=(-SIGXX(N)+2.*SIGYY(N)-SIGZZ(N))/43511.4
      ZDIR=(-SIGXX(N)-SIGYY(N)+2.*SIGZZ(N))/43511.4
      XYDIR=SIGXY(N)/7251.9
      DX(N)=OM*XDIR*DT
      DY(N)=OM*YDIR*DT
      DZ(N)=OM*ZDIR*DT
      DXY(N)=OM*XYDIR*DT
      EVPX(N)=EVPX(N)+DX(N)
      EVPY(N)=EVPY(N)+DY(N)
      EVPZ(N)=EVPZ(N)+DZ(N)
      EVPXY(N)=EVPXY(N)+DXY(N)
      DZZ=-AC*((Z-ZI)/Z1)**RN*DT*Z1
      ZWP=(Z1-Z)*EMO
      ZREC=DZZ/DT
      DWP(N)=(SIGXX(N)*DX(N)+SIGYY(N)*DY(N)+SIGXY(N)*DXY(N) +
     1 SIGZZ(N)*DZ(N))/14503.8+DZZ/ZWP
      WP(N)=WP(N)+DWP(N)
      IF((N.EQ.201).OR.(N.EQ.203).OR.(N.EQ.229).OR.(N.EQ.317).OR.
     1(N.EQ.325).OR.(N.EQ.333).OR.(N.EQ.341).OR.(N.EQ.343))
     1PRINT(6,*)"ELEMENT NO.",N,"  Z RECOVERY ",ZREC," Z ",Z
  100 CONTINUE
      RETURN
      END
      SUBROUTINE VISCOUS(NUMEL,VP,YIELD,HP,DT,RAM,BERG,VC,ALPHA,SLOPEA,
     1PE,VM)
      COMMON /PROP/ET(382),XU(382),TH(382),PS,MAT
      COMMON /STRESS/SIGXX(382),SIGXY(382),SIGYY(382),SIGZZ(382)
      COMMON /VISCO/EVPX(382),EVPXY(382),EVPY(382),EVPZ(382),EPEFF(382),
     1DPEFF(382)
      COMMON /D/DX(382),DY(382),DXY(382),DZ(382)
      DO 100 N=1,NUMEL
      SIGEFF=(SIGXX(N)**2+SIGYY(N)**2+SIGZZ(N)**2-SIGXX(N)*SIGYY(N)
     1 -SIGYY(N)*SIGZZ(N)-SIGZZ(N)*SIGXX(N)+3.*SIGXY(N)**2)**.5
      IF(RAM .GT. 0.) HYIELD=RAM*(EPEFF(N))**(1./BERG)
      IF(RAM .EQ. 0.) HYIELD=YIELD*(1.+ HP*EPEFF(N))
      IF(RAM.EQ.0..AND.EPEFF(N).GE..00169.AND.EPEFF(N).LT..008992)
     1HYIELD=(YIELD+8610.9)*(15.3315*EPEFF(N)+1.0)
      IF(RAM.EQ.0..AND.EPEFF(N).GE..00899) HYIELD=YIELD+16000.
      XDIR=SIGXX(N)-.5*SIGYY(N)-.5*SIGZZ(N)
      YDIR=-.5*SIGXX(N)+SIGYY(N)-.5*SIGZZ(N)
      ZDIR=-.5*SIGXX(N)-.5*SIGYY(N)+SIGZZ(N)
      XYDIR=3.*SIGXY(N)
      IF(VC .GT. 0.)VP1=VC*(SIGEFF)**(ALPHA-1.)
      IF(SIGEFF .LE. HYIELD) GO TO 200
      IF(VP.GT.0..AND.VM.EQ.-1.)VP2=VP*((SIGEFF/HYIELD)-1.)/SIGEFF
      IF(VP.GT.0..AND.VM.EQ.0.)VP2=(VP*((EXP((SIGEFF-HYIELD)/SLOPEA))-1.
     1)/SIGEFF)
  200 CONTINUE
      IF(SIGEFF .LT. YIELD) VP2=0.
      VPM=VP1+VP2
      DX(N)=VPM*XDIR*DT
      DY(N)=VPM*YDIR*DT
      DZ(N)=VPM*ZDIR*DT
      DXY(N)=VPM*XYDIR*DT
      DPEFF(N)=.816496*(DX(N)**2+DY(N)**2+DZ(N)**2+.5*DXY(N)**2)**.5
      EVPX(N)=EVPX(N)+DX(N)
      EVPY(N)=EVPY(N)+DY(N)
      EVPZ(N)=EVPZ(N)+DZ(N)
      EVPXY(N)=EVPXY(N)+DXY(N)
      EPEFF(N)=EPEFF(N)+ DPEFF(N)
      GO TO 100
C110  CONTINUE
C     DX(N)=0.
C     DY(N)=0.
```

```
00911 C       DZ(N)=0.
00912 C       DXY(N)=0.
00913 C       DPEFF(N)=0.
00914   100   CONTINUE
00915         RETURN
00916         END
00917         SUBROUTINE OUTPUT(NUMEL,NUMNP,T,DT,NN)
00918 C
00919 C       PRINT OF DISPLACEMENTS AND STRESSES
00920 C
00921         COMMON /WORK/WPP(382),WPC(382),WPE(382)
00922         COMMON /PROP/ET(382),XU(382),TH(382),PS,MAT
00923         COMMON /A/AREA(382)
00924         COMMON /DISPL/DSX(235),DSY(235)
00925         COMMON /BMAT/XORD(235),YORD(235),NPI(382),NPJ(382),NPK(382)
00926         COMMON /STRESS/SIGXX(382),SIGXY(382),SIGYY(382),SIGZZ(382)
00927         COMMON /VISCO/EVPX(382),EVPXY(382),EVPY(382),EVPZ(382),EPEFF(382),
00928        1DPEFF(382)
00929         COMMON /LOAD/XLOAD(235),YLOAD(235),FX(10),FY(10),NF,FRATE,NFA(10),
00930        1NFN(10)
00931         DIMENSION B(6,6),D(6,6)
00932         IF (NN .EQ. 0)GO TO 310
00933   400   WRITE(6,99)
00934         PRINT (6,*)"TIME = ",T,"TIMESTEP=",DT
00935         WRITE(6,121)
00936         WRITE (6,122)(M,DSX(M),DSY(M),XLOAD(M),YLOAD(M),XORD(M),YORD(M),M=
00937        1  53,63)
00938         WRITE (6,122)(M,DSX(M),DSY(M),XLOAD(M),YLOAD(M),XORD(M),YORD(M),M=
00939        1  115,200)
00940   10    CONTINUE
00941         WPPA=0.
00942         DO 300 N=1,NUMEL
00943         WPPA=WPP(N)*AREA(N)*TH(N)+WPPA
00944   300   CONTINUE
00945         PRINT (6,*)"PLASTIC EFFECTIVE STRAIN ENERGY=",WPPA
00946         WRITE(6,123)
00947         WRITE (6,224)
00948    310  CONTINUE
00949         DO 420 N=1,NUMEL
00950         I=NPI(N)
00951         J=NPJ(N)
00952         K=NPK(N)
00953         CALL BMATRIX(N,B)
00954         EPX=B(1,1)*DSX(I)+B(1,3)*DSX(J)+B(1,5)*DSX(K)
00955         EPY=B(2,2)*DSY(I)+B(2,4)*DSY(J)+B(2,6)*DSY(K)
00956         GAM=B(3,1)*DSX(I)+B(3,2)*DSY(I)+B(3,3)*DSX(J)+B(3,4)*DSY(J)+
00957        1  B(3,5)*DSX(K)+B(3,6)*DSY(K)
00958         CALL DMATRIX(N,D)
00959         EPXX=EPX-EVPX(N)
00960         EPYY=EPY-EVPY(N)
00961         GAMM=GAM-    EVPXY(N)
00962         X=(D(1,1)*EPXX+D(1,2)*EPYY)/(AREA(N)*TH(N))
00963         Y=(D(2,1)*EPXX+D(2,2)*EPYY)/(AREA(N)*TH(N))
00964         Z=0.
00965         IF(PS.GT.0.)Z=-ET(N)*EVPZ(N)+XU(N)*(X+Y)
00966         XY=D(3,3)*GAMM/(AREA(N)*TH(N))
00967         SIGXX(N)=X
00968         SIGYY(N)=Y
00969         SIGZZ(N)=Z
00970         SIGXY(N)=XY
00971         SIGEFF=(X**2+Y**2+Z**2-X*Y-Y*Z-Z*X+3.*XY**2)**.5
00972         IF (NN .EQ. 0)GO TO 420
00973         IF(N.LT.135) GO TO 420
00974         IF(N.GT.345) GO TO 420
00975         WRITE (6,124)(N,X,Y,Z,XY,EPX,EPY,GAM)
```

```
      IF(N.EQ.239.)TA=Y/1000
      IF(N.EQ.240.)TB=Y/1000
      IF(N.EQ.241.)TC=Y/1000
      IF(N.EQ.242.)TD=YZ1000
      IF(N.EQ.277.)TE=Y/1000
      IF(N.EQ.278.)TF=Y/1000
      IF(N.EQ.279.)TG=Y/1000
      IF(N.EQ.317.)TH=Y/1000
      IF(N.EQ.317.)TY=(TA+TB+TC+TD+TE+TF+TG+TH)/8
      IF(N.EQ.239.)YA=EPY*1000
      IF(N.EQ.240.)YB=EPY*1000
      IF(N.EQ.241.)YC=EPY*1000
      IF(N.EQ.242.)YD=EPY*1000
      IF(N.EQ.277.)YE=EPY*1000
      IF(N.EQ.278.)YF=EPY*1000
      IF(N.EQ.279.)YG=EPY*1000
      IF(N.EQ.317.)YH=EPY*1000
      IF(N.EQ.317.)TEPY=(YA+YB+YC+YD+YE+YF+YG+YH)/8
      IF(N.EQ.317.)WRITE(8,*)(TEPY,TY)
      WRITE(6,225)(N,EVPX(N),EVPY(N),EVPZ(N),EVPXY(N),SIGEFF,EPEFF(N),
     1  WPC(N))
  420 CONTINUE
      IF (NN .GT. 0)CALL JINTEG(NUMNP)
   99 FORMAT(1HO)
  121 FORMAT (89HONODAL POINT X-DISPLACEMENT Y-DISPLACEMENT
     1  XLOAD     YLOAD      XORD      YORD)
  122 FORMAT(I12,6E15.6)
  123 FORMAT(120HO  ELEMENT      X-STRESS          Y-STRESS          Z-STRE
     1SS      XY-STRESS          X-STRAIN       Y-STRAIN       GAM-STRAIN)
  124 FORMAT(I10,4F15.4,5X,3E15.4)
  224 FORMAT(120HO     N        EVPX            EVPY            EVPZ
     1    EVPXY           SIGEFF            WPBAR          EFFSTRAIN    )
  225 FORMAT(I8,4E15.4,F20.4,2E15.4)
  823 FORMAT(120H1  N-POINT           X-STRESS            Y-STRESS
     1       XY-STRESS          MAX-STRESS     MIN-STRESS       DIRECTION)
      RETURN
      END
      SUBROUTINE DPLOT(NUMEL,NUMNP,T,SCAL,YIELD)
      COMMON /WORK/WPP(382),WPC(382),WPE(382)
      COMMON /STRESS/SIGXX(382),SIGXY(382),SIGYY(382),SIGZZ(382)
      COMMON /VISCO/EVPX(382),EVPXY(382),EVPY(382),EVPZ(382),EPEFF(382),
     1DPEFF(382)
      COMMON /DISPL/DSX(235),DSY(235)
      COMMON /BHAT/XORD(235),YORD(235),NPI(382),NPJ(382),NPK(382)
      COMMON /LOAD/XLOAD(235),YLOAD(235)
      DIMENSION XXORD(235),YYORD(235)
      EQUIVALENCE (XLOAD,XXORD),(YLOAD,YYORD)
      CALL PLOTS(0.,0.,9)
      DO 100 I=1,NUMNP
      XXORD(I)=XORD(I)+DSX(I)*10.
      YYORD(I)=YORD(I)+DSY(I)*10.
  100  CONTINUE
      CALL FACTOR(SCAL)
      HGHT=.1/SCAL
      DO 200 I=1,NUMEL
      IF(WPC(I) .GE. .002 .AND. YIELD .GT. 0.)GO TO 200
      I1=NPI(I)
      I2=NPJ(I)
      I3=NPK(I)
      CALL PLOT (XXORD(I1),YYORD(I1),+3)
      CALL PLOT (XXORD(I2),YYORD(I2),+2)
      CALL PLOT (XXORD(I3),YYORD(I3),+2)
      CALL PLOT (XXORD(I1),YYORD(I1),+2)
      CALL PLOT(XXORD(I1),YYORD(I1),+3)
      XD1=ABS(XXORD(I1)-XXORD(I2))*SCAL
```

```
      XD2=ABS(XXORD(I1)-XXORD(I3))*SCAL
      XD3=ABS(XXORD(I2)-XXORD(I3))*SCAL
      IF (XD1 .LT. .15.AND.XD2.LT. .15 .AND.XD3.LT. .15)GO TO 10
      XCENT=(XXORD(I1)+XXORD(I2)+XXORD(I3))/3.-.1/SCAL
      YCENT=(YYORD(I1)+YYORD(I2)+YYORD(I3))/3.
      SIGEFF=(SIGXX(I)**2+SIGYY(I)**2+SIGZZ(I)**2-SIGXX(I)*SIGYY(I)
     1 -SIGYY(I)*SIGZZ(I)-SIGZZ(I)*SIGXX(I)+3.*SIGXY(I)**2)**.5
      IF (YIELD .EQ. 0.)RATIO=SIGEFF/1000.
      IF (YIELD .GT. 0.)RATIO=(SIGEFF/YIELD)*100.
      IF (RATIO .LT. 10.)XCENT=XCENT+.1/SCAL
      CALL NUMBER(XCENT,YCENT,HGHT,RATIO,0.,-1)
10    CONTINUE
200   CONTINUE
      CALL FACTOR (1.)
      CALL PLOTE(N)
      RETURN
      END
      SUBROUTINE WORK(NUMEL,T,PI)
      COMMON /D/DX(382),DY(382),DXY(382),DZ(382)
      COMMON /WORK/WPP(382),WPC(382),WPE(382)
      COMMON /DISPL/DSX(235),DSY(235)
      COMMON /BMAT/XORD(235),YORD(235),NPI(382),NPJ(382),NPK(382)
      COMMON /CSTAR/DXDT(235),DYDT(235),DDT
      DIMENSION B(6,6)
      COMMON /VISCO/EVPX(382),EVPXY(382),EVPY(382),EVPZ(382),EPEFF(382),
     1DPEFF(382)
      COMMON /STRESS/SIGXX(382),SIGXY(382),SIGYY(382),SIGZZ(382)
      DO 100 N=1,NUMEL
      WPP(N)=SIGXX(N)*DX(N)+SIGYY(N)*DY(N)+SIGZZ(N)*DZ(N)+SIGXY(N)*DXY(N
     1)+WPP(N)
      IF((N.EQ.317).OR.(N.EQ.325).OR.(N.EQ.333).OR.(N.EQ.341).OR.
     1(N.EQ.343).OR.(N.EQ.229).OR.(N.EQ.201).OR.(N.EQ.203))
     1PRINT(6,*)"ELEMENT  NO.    ",N,"   PLASTIC WORK    ",WPP(N)
      WPC(N)=.816496*(DX(N)**2+DY(N)**2+DZ(N)**2+.5*DXY(N)**2)**.5+
     1  WPC(N)
100   CONTINUE
      EFAC=.5*PI/DDT
      IF(T .GT. 0.)EFAC=1./DDT
      DO 200 N=1,NUMEL
      CALL BMATRIX(N,B)
      I=NPI(N)
      J=NPJ(N)
      K=NPK(N)
      DSXI=DSX(I)-DXDT(I)
      DSXJ=DSX(J)-DXDT(J)
      DSXK=DSX(K)-DXDT(K)
      DSYI=DSY(I)-DYDT(I)
      DSYJ=DSY(J)-DYDT(J)
      DSYK=DSY(K)-DYDT(K)
      EX=B(1,1)*DSXI+B(1,3)*DSXJ+B(1,5)*DSXK
      EY=B(2,2)*DSYI+B(2,4)*DSYJ+B(2,6)*DSYK
      GAM=B(3,1)*DSXI+B(3,2)*DSYI+B(3,3)*DSXJ+B(3,4)*DSYJ+B(3,5)*DSXK+
     1  B(3,6)*DSYK
200   WPE(N)=EFAC*(SIGXX(N)*EX+SIGYY(N)*EY+SIGXY(N)*GAM)+WPE(N)
      RETURN
      END
      SUBROUTINE JINTEQ(NUMNP)
      COMMON /STRESS/SIGXX(382),SIGXY(382),SIGYY(382),SIGZZ(382)
      COMMON /VISCO/EVPX(382),EVPXY(382),EVPY(382),EVPZ(382),EPEFF(382),
     1DPEFF(382)
      COMMON /WORK/WPP(382),WPC(382),WPE(382)
      COMMON /DISPL/DSX(235),DSY(235)
      COMMON /BMAT/XORD(235),YORD(235),NPI(382),NPJ(382),NPK(382)
      COMMON /JINT/JEL(10),JN(10,382),XN(10,382),YN(10,382),CJINT,JPATH
      COMMON /CSTAR/DXDT(235),DYDT(235),DDT
```

```
      DIMENSION B(6,6)
      IF (JPATH .EQ. 0)GO TO 200
      PRINT (6,*)"DDT=",DDT
      DO 110 I=1,NUMNP
      DXDT(I)=(DSX(I)-DXDT(I))/DDT
110   DYDT(I)=(DSY(I)-DYDT(I))/DDT
      DO 1000 I=1,JPATH
      CJINT=0.
      CSTAR=0.
      M=JEL(I)
      DO 100 L=1,M
      N=JN(I,L)
      CALL BMATRIX(N,B)
      II=NPI(N)
      JJ=NPJ(N)
      KK=NPK(N)
      EPX=B(1,1)*DSX(II)+B(1,3)*DSX(JJ)+B(1,5)*DSX(KK)
      EPXC=B(1,1)*DXDT(II)+B(1,3)*DXDT(JJ)+B(1,5)*DXDT(KK)
      EPY=B(2,2)*DSY(II)+B(2,4)*DSY(JJ)+B(2,6)*DSY(KK)
      EPYC=B(2,2)*DYDT(II)+B(2,4)*DYDT(JJ)+B(2,6)*DYDT(KK)
      DVDX=B(3,2)*DSY(II)+B(3,4)*DSY(JJ)+B(3,6)*DSY(KK)
      DVDXC=B(3,2)*DYDT(II)+B(3,4)*DYDT(JJ)+B(3,6)*DYDT(KK)
      GAM=B(3,1)*DSX(II)+B(3,3)*DSX(JJ)+B(3,5)*DSX(KK)+DVDX
      GAMC=B(3,1)*DXDT(II)+B(3,3)*DXDT(JJ)+B(3,5)*DXDT(KK)+DVDXC
      EPX=EPX-EVPX(N)
      EPY=EPY-EVPY(N)
      GAM=GAM-EVPXY(N)
      TX=SIGXX(N)*EPX
      TXC=SIGXX(N)*EPXC
      U=(.5*(TX+SIGYY(N)*EPY+SIGXY(N)*GAM)+WPP(N))*YN(I,L)
      UC=WPE(N)*YN(I,L)
      T1=-TX*YN(I,L)
      T1C=-TXC*YN(I,L)
      T2=-SIGXY(N)*DVDX*YN(I,L)
      T2C=-SIGXY(N)*DVDXC*YN(I,L)
      T3=+SIGXY(N)*EPX*XN(I,L)
      T3C=SIGXY(N)*EPXC*XN(I,L)
      T4=+SIGYY(N)*DVDX*XN(I,L)
      T4C=SIGYY(N)*DVDXC*XN(I,L)
      CJINT=CJINT+T1+T2+T3+T4+U
      CSTAR=CSTAR+T1C+T2C+T3C+T4C+UC
      PRINT*,"ELEMENT NO.",JN(I,L),"J=",CJINT,"CSTAR=",CSTAR
100   CONTINUE
      CJINT=2.*CJINT
      CSTAR=2.*CSTAR
      PRINT(6,*)"THE J INTEGRAL FOR PATH ",I," EQUALS ",CJINT
      PRINT *,"THE ELASTIC-PLASTIC CSTAR INTEGRAL IS  ",CSTAR
1000   CONTINUE
200   CONTINUE
      RETURN
      END
      SUBROUTINE NODEPOP(T,DT,DTINIT,TP,TPRINT,NUMNP,NODE,OPE,
     1CEPT,RT,CONV)
      COMMON /NPINV/SXX(235,9),SXY(235,9),SYX(235,9),SYY(235,9)
      COMMON/CRACK/ICR,ICRR,NCR(29,4),SXXC(29),SXYC(29),SYXC(29),
     1SYYC(29),TCRACK(29),YLOD(29)
      COMMON /LOAD/XLOAD(235),YLOAD(235),FX(10),FY(10),NF,FRATE,NFA(10),
     1NFN(10)
      COMMON /BMAT/XORD(235),YORD(235),NPI(382),NPJ(382),NPK(382)
      COMMON /STRESS/SIGXX(382),SIGXY(382),SIGYY(382),SIGZZ(382)
      COMMON /PROP/ET(382),XU(382),TH(382),PS,MAT
      COMMON /A/AREA(382)
      COMMON/DISPL/DSX(235),DSY(235)
      DIMENSION B(6,6)
      IF(T.LT. TCRACK(ICRR))GO TO 100
```

```
      PRINT(6,*)"IN NODEPOP SUBROUTINE NOW AT TIME =",T
      M=NCR(ICRR,1)
      PRINT(6,*)"NODE",M,"POPS AT TIME=",T
      SXX(M,1)=SXXC(ICRR)
      SXY(M,1)=SXYC(ICRR)
      SYX(M,1)=SYXC(ICRR)
      SYY(M,1)=SYYC(ICRR)
      PRINT(6,*)"SXX(",M,",1)=",SXX(M,1)
      PRINT(6,*)"SXY(",M,",1)=",SXY(M,1)
      PRINT(6,*)"SYX(",M,",1)=",SYX(M,1)
      PRINT(6,*)"SYY(",M,",1)=",SYY(M,1)
      DO 200 I=1,NUMNP
      XLOAD(I)=0.
  200 YLOAD(I)=0.
      DO 210 L=2,4
      N=NCR(ICRR,L)
      CALL BMATRIX(N,B)
      I=NPI(N)
      J=NPJ(N)
      K=NPK(N)
      YLOAD(I)=YLOAD(I)+(B(1,2)*SIGXX(N)+B(2,2)*SIGYY(N)+B(3,2)*SIGXY(N)
     1)*AREA(N)*TH(N)
      YLOAD(J)=YLOAD(J)+(B(1,4)*SIGXX(N)+B(2,4)*SIGYY(N)+B(3,4)*SIGXY(N)
     1)*AREA(N)*TH(N)
  210 YLOAD(K)=YLOAD(K)+(B(1,6)*SIGXX(N)+B(2,6)*SIGYY(N)+B(3,6)*SIGXY(N)
     1)*AREA(N)*TH(N)
      K=NCR(ICRR,1)
      YLOD(ICRR)=YLOAD(K)
      DT=DTINIT
      ICRR=ICRR+1
      TP=TPRINT
  100 CONTINUE
      RETURN
      END
      SUBROUTINE CYCLIC (T,PMAX,PO,PERIOD,PP,CYCNO)
      PRINT(6,*)"IN CYCLIC SUBROUTINE"
      PRINT(6,*)"T=      ",T,"PERIOD=     ",PERIOD
      TLOC=T-INT(T/PERIOD)*PERIOD
      IF(PO.LT.0)GO TO 100
      IF(TLOC.LE.PERIOD/2.0) PP=TLOC/(PERIOD/2.0)*(PMAX-PO)+PO
      IF(TLOC.GT.PERIOD/2.0) PP=(PERIOD-TLOC)/(PERIOD/2.0)*(PMAX-PO)+PO
   50 CONTINUE
      PRINT(6,*)"% LOAD=      ",PP,"AT TIME     ",T
      CYCNO=T/PERIOD
      PRINT(6,*)"NUMBER OF LOAD CYCLES=     ",CYCNO
      PRINT(6,*)"LEAVE CYCLIC SUBROUTINE"
      GO TO 300
  100 TTOP=PERIOD*PMAX/(2*(PMAX-PO))
      IF(TLOC.LE.TTOP)PP=TLOC/TTOP
      IF(TLOC.LE.TTOP)GO TO 200
      TBOT=-TTOP*(PO-PMAX-1)
      IF(TLOC.LE.TBOT)PP=1+PMAX-TLOC/TTOP
      IF(TLOC.LE.TBOT)GO TO 200
      PP=(TLOC/TTOP)+PO-(TBOT/TTOP)
  200 GO TO 50
  300 RETURN
      END
```

VITA

Captain Casey L. Henkel was born on 15 March 1954 in Fremont, Nebraska. He graduated from high school in Austin, Texas in 1972 and accepted a scholarship at the United States Air Force Academy from which he received a Bachelor of Science in Engineering Science in June 1976. He was commissioned in the USAF and entered pilot training, receiving his wings September 1977. He served as a KC-135 pilot in the 11th Air Refueling Squadron, Altus AFB, Oklahoma until entering the School of Engineering, Air Force Institute of Technology in May 1983.

Permanent Address: 1304 Hymen Lane
Austin, Texas 78742

Unclassified

SECURITY CLASSIFICATION OF THIS PAGE

REPORT DOCUMENTATION PAGE

1a. REPORT SECURITY CLASSIFICATION: Unclassified	1b. RESTRICTIVE MARKINGS
2a. SECURITY CLASSIFICATION AUTHORITY	3. DISTRIBUTION/AVAILABILITY OF REPORT: Approved for public release; distribution unlimited.
2b. DECLASSIFICATION/DOWNGRADING SCHEDULE	
4. PERFORMING ORGANIZATION REPORT NUMBER(S): AFIT/GAE/AA/84D-9	5. MONITORING ORGANIZATION REPORT NUMBER(S)
6a. NAME OF PERFORMING ORGANIZATION: School of Engineering; 6b. OFFICE SYMBOL (If applicable): AFIT/ENG	7a. NAME OF MONITORING ORGANIZATION
6c. ADDRESS (City, State and ZIP Code): Air Force Institute of Technology, Wright Patterson AFB, Ohio 45433	7b. ADDRESS (City, State and ZIP Code)
8a. NAME OF FUNDING/SPONSORING ORGANIZATION; 8b. OFFICE SYMBOL (If applicable)	9. PROCUREMENT INSTRUMENT IDENTIFICATION NUMBER
8c. ADDRESS (City, State and ZIP Code)	10. SOURCE OF FUNDING NOS. — PROGRAM ELEMENT NO.; PROJECT NO.; TASK NO.; WORK UNIT NO.
11. TITLE (Include Security Classification): See Box 19	
12. PERSONAL AUTHOR(S): Casey L. Henkel, B. S., Capt., USAF	
13a. TYPE OF REPORT: M.S. Thesis; 13b. TIME COVERED: FROM _____ TO _____; 14. DATE OF REPORT (Yr., Mo., Day): 1984 December; 15. PAGE COUNT: 111	
16. SUPPLEMENTARY NOTATION	

17. COSATI CODES			18. SUBJECT TERMS (Continue on reverse if necessary and identify by block number)
FIELD	GROUP	SUB. GR.	
11	06		High Temperature Fatigue; Viscoplasticity; Fracture Mechanics; Bodner-Partom Flow Law; High Temperature Superalloy; Finite Element Modeling
20	11		

19. ABSTRACT (Continue on reverse if necessary and identify by block number)

Title: Crack Closure Characteristics Considering Center Cracked and Compact TEnsion Specimens

Thesis Chairman: A. N. Palazotto, Professor, GM-15,

Approved for public release: IAW AFR 190-17.
LYNN E. WOLAVER 25 Feb 85
Dean for Research and Professional Development
Air Force Institute of Technology (AIC)
Wright-Patterson AFB OH 45433

20. DISTRIBUTION/AVAILABILITY OF ABSTRACT	21. ABSTRACT SECURITY CLASSIFICATION
UNCLASSIFIED/UNLIMITED ☒ SAME AS RPT. ☐ DTIC USERS ☐	Unclassified

22a. NAME OF RESPONSIBLE INDIVIDUAL	22b. TELEPHONE NUMBER (Include Area Code)	22c. OFFICE SYMBOL
A. N. Palazotto, Professor, GM-15	513-255-3576	AFIT/ENG

DD FORM 1473, 83 APR — EDITION OF 1 JAN 73 IS OBSOLETE.

Unclassified

SECURITY CLASSIFICATION OF THIS PAGE

Due to growing use of expensive, high performance gas turbine engines in the United States Air Force, there is a need for improved failure prediction methods for critical high temperature engine components. This new study expands current research in the area of high temperature, low cycle fatigue of IN-100 at 1350° F. the superplastic alloy used in F-100 engine turbine disks.

An in-house, 2-D, finite element program named VISCO employs the Bodner-Partom Constitutive equation to accurately model the principal features of completely reversed cyclic loading. VISCO is used to compare the effects on material behavior by considering a 2.5 Hz. compact tension specimen, a .167 Hz. compact tension specimen, and a 2.5 Hz. center cracked specimen subjected to fully reversed cyclic loading with a stress intensity factor of 35 and 45 ksi√in. The comparisons point out that the findings of Linear Elastic Fracture Mechanics must be modified under conditions of high temperature viscoplasticity.

END

FILMED

5-85

DTIC